REPLACING THERMAL SPRAYED ZINC ANODES ON CATHODICALLY PROTECTED STEEL REINFORCED CONCRETE BRIDGES

Final Report

SPR 682

RESEARCH

REPLACING THERMAL SPRAYED ZINC ANODES ON CATHODICALLY PROTECTED STEEL REINFORCED CONCRETE BRIDGES

Final Report

SPR 682

by

Xianming Shi, Ph.D., P.E.
Jon Doug Cross
Levi Ewan
Yajun Liu, Ph.D.
Keith Fortune

for

Oregon Department of Transportation
Research Section
200 Hawthorne Ave. SE, Suite B-240
Salem OR 97301-5192

and

Federal Highway Administration
400 Seventh Street, SW
Washington, DC 20590-0003

September 2011

Technical Report Documentation Page

1. Report No. FHWA-OR-RD- 12-02	2. Government Accession No.	3. Recipient's Catalog No.
4. Title and Subtitle Replacing Thermal Sprayed Zinc Anodes On Cathodically Protected Steel Reinforced Concrete Bridges		5. Report Date August 2011
		6. Performing Organization Code
7. Author(s) Xianming Shi, Jon Doug Cross, Yajun Liu, Keith Fortune, Levi Ewan		8. Performing Organization Report No.
9. Performing Organization Name and Address Corrosion and Sustainable Infrastructure Lab Western Transportation Institute P. O. Box 174250, Montana State University Bozeman, MT 59717-4250		10. Work Unit No. (TRAIS)
		11. Contract or Grant No. SPR 682
12. Sponsoring Agency Name and Address Oregon Department of Transportation Research Section and Federal Highway Administration 200 Hawthorne Ave. SE, Suite B-240 400 Seventh Street, SW Salem, OR 97301-5192 Washington, DC 20590-0003		13. Type of Report and Period Covered Final Report
		14. Sponsoring Agency Code

15. Supplementary Notes

16. Abstract

This research aimed to address questions underlying the replacement of arc-sprayed zinc anodes on cathodically protected steel reinforced concrete bridges and to develop a protocol to prepare the concrete surface for the new anode, through a combination of literature review, practitioner surveys, laboratory studies, and field investigation (Pier 9 of the Yaquina Bay Bridge, Oregon). Concrete with an equivalent electrochemical age of 5 to 45 years was found to have a reaction layer of ~1 mm. To achieve strong initial bond strength of new zinc to the profiled concrete surface, the current ODOT sandblasting operating configuration (#8 nozzle with high sand volume) is too aggressive and should be changed to #6 nozzle with low sand volume to achieve target RMS macro-roughness of 1.2-2.1 centi-inches and micro-roughness of 3.5-5 μm. It is recommended to adjust the anode removal and surface profiling based on the electrochemical age of the existing concrete. Wherever possible, large aggregates (e.g., diameters ¾ in. and bigger) should be avoided for exposure by surface profiling. For non-electrochemically aged concrete, the surface should be profiled to achieve a RMS macro-roughness of 1.1-1.8 centi-inches and 5-36% exposed aggregates. For existing concrete with relatively high electrochemical age (14 yrs), the surface should be profiled to achieve a RMS macro-roughness of 1.1-1.5 centi-inches and 44-55% exposed aggregates. The following recommendations were made for old anode removal and surface preparation before new anode application: use a reasonably low air pressure and a reasonably hard and dense abrasive material for sandblasting; have a reasonably thin coating per pass during arc-spray operations; and have a slightly thinner overall Zn coating layer (15-17 mils vs. the currently used 17 mils). It is also desirable to have concrete with good surface cohesion strength and a minimum of 150 psi initial bond strength. For existing concrete with an equivalent electrochemical age of more than 8 years, the reaction layer should be completely removed prior to profiling and arc spraying (e.g., 4 mm grinding).

17. Key Words thermal sprayed zinc, anode replacement, cathodic protection, reinforced concrete, bridge preservation, surface preparation	18. Distribution Statement Copies available from NTIS, and online at http://www.oregon.gov/ODOT/TD/TP_RES/

19. Security Classification (of this report) Unclassified	20. Security Classification (of this page) Unclassified	21. No. of Pages 201	22. Price

Technical Report Form DOT F 1700.7 (8-72)   Reproduction of completed page authorized   Printed on recycled paper

i

SI* (MODERN METRIC) CONVERSION FACTORS

APPROXIMATE CONVERSIONS TO SI UNITS

Symbol	When You Know	Multiply By	To Find	Symbol
LENGTH				
in	inches	25.4	millimeters	mm
ft	feet	0.305	meters	m
yd	yards	0.914	meters	m
mi	miles	1.61	kilometers	km
AREA				
in^2	square inches	645.2	millimeters squared	mm^2
ft^2	square feet	0.093	meters squared	m^2
yd^2	square yards	0.836	meters squared	m^2
ac	acres	0.405	hectares	ha
mi^2	square miles	2.59	kilometers squared	km^2
VOLUME				
fl oz	fluid ounces	29.57	milliliters	ml
gal	gallons	3.785	liters	L
ft^3	cubic feet	0.028	meters cubed	m^3
yd^3	cubic yards	0.765	meters cubed	m^3
NOTE: Volumes greater than 1000 L shall be shown in m^3.				
MASS				
oz	ounces	28.35	grams	g
lb	pounds	0.454	kilograms	kg
T	short tons (2000 lb)	0.907	megagrams	Mg
TEMPERATURE (exact)				
°F	Fahrenheit	(F-32)/1.8	Celsius	°C

APPROXIMATE CONVERSIONS FROM SI UNITS

Symbol	When You Know	Multiply By	To Find	Symbol
LENGTH				
mm	millimeters	0.039	inches	in
m	meters	3.28	feet	ft
m	meters	1.09	yards	yd
km	kilometers	0.621	miles	mi
AREA				
mm^2	millimeters squared	0.0016	square inches	in^2
m^2	meters squared	10.764	square feet	ft^2
m^2	meters squared	1.196	square yards	yd^2
ha	hectares	2.47	acres	ac
km^2	kilometers squared	0.386	square miles	mi^2
VOLUME				
ml	milliliters	0.034	fluid ounces	fl oz
L	liters	0.264	gallons	gal
m^3	meters cubed	35.315	cubic feet	ft^3
m^3	meters cubed	1.308	cubic yards	yd^3
MASS				
g	grams	0.035	ounces	oz
kg	kilograms	2.205	pounds	lb
Mg	megagrams	1.102	short tons (2000 lb)	T
TEMPERATURE (exact)				
°C	Celsius	1.8C+32	Fahrenheit	°F

*SI is the symbol for the International System of Measurement

ii

ACKNOWLEDGEMENTS

DISCLAIMER

REPLACING THERMAL SPRAYED ZINC ANODES ON CATHODICALLY PROTECTED STEEL REINFORCED CONCRETE BRIDGES

TABLE OF CONTENTS

LIST OF FIGURES

LIST OF TABLES

1.0   INTRODUCTION

1.1   PROBLEM STATEMENT

Corrosion of reinforced concrete structures is a major and increasing problem worldwide. The remediation of concrete bridges undertaken as a direct result of chloride-induced rebar corrosion was estimated to cost U.S. highway departments $5 billion per year *(Tang 1999)*. The Oregon Department of Transportation (ODOT) has historic reinforced concrete bridges at the coast that employ impressed current cathodic protection (CP) to greatly reduce the corrosion of the embedded steel reinforcement. The CP systems rely on passing an electric current into the concrete through zinc metal anodes that have been thermally sprayed onto the surface of the concrete. Some of these zinc anodes are nearing the end of their design lives, while others are beginning to separate from the concrete prematurely possibly due to erratic current controllers or initial contractor inexperience during installation. Anode sections that have debonded no longer protect the underlying steel reinforcement. When the natural rate of corrosion resumes, the unprotected sections are on the path to concrete spalling and steel section loss—the conditions that required ODOT to undertake expensive repairs and protection schemes. Currently, there is no procedure established by ODOT to remove old anodes, prepare the concrete surface, and install new anodes.

1.2   OBJECTIVES OF THE STUDY

The objectives of the research were to 1) determine the most cost-effective method to remove existing zinc anodes, and 2) develop a protocol to prepare the concrete surface for the new anode.

1.3   THERMAL SPRAYED ZINC AND ODOT EXPERIENCE

Chloride-induced corrosion of the reinforcing steel is the primary contributor to the deterioration of Oregon's coastal bridges, and CP has been the main technology applied to protect these bridges (e.g., Cape Creek Bridge, Yaquina Bay Bridge, Depoe Bay Bridge) and to preserve the economic and cultural resources invested in them *(McGill and Shike 1997)*. In 1992, ODOT installed the world's first impressed current cathodic protection (ICCP) system featuring arc-sprayed zinc coating as the anode to protect the steel rebar in concrete on the 10,000-m^2 substructure of the Yaquina Bay Bridge, which is still one of the largest single substructure CP projects ever undertaken in the United States. According to McGill and Shike *(1997)*, the "arc-spray process was selected as it provided a coating that could be easily applied to the complex shapes found on substructure surfaces… The gray color of zinc has the advantage of appearing very much like concrete—another important feature for historic bridges. Also, the low electrical resistivity of zinc allows uniform distribution of cathodic protection current, and the zinc system minimizes the dead load added to the structure, which is an important feature for older coastal bridges."

The Oregon Department of Transportation implemented stringent surface preparation and initial adhesion-strength requirements, including: brushing and blowing down the concrete surface to remove dust, having the concrete surface at 70°F (21°C) or higher to keep it dry, and applying supplemental surface heating immediately prior to zinc application to bring the concrete surface temperature to about 250°F (120°C). All of this added to the cost of the ICCP system installation *(Holcomb et al. 1996)*.

To obtain improved understanding of the performance and service life of thermally sprayed zinc (TS-Zn) anode, the National Energy Technology Laboratory in Albany, Oregon (formerly the Albany Research Center) conducted accelerated electrochemical aging in the laboratory using a current density of 3 mA/ft^2 (0.032 A/m^2, a factor of 15 higher than the approximately 0.2 mA/ft^2 used by ODOT on coastal bridges), which was found to cause chemical and physical changes at the zinc–concrete interface *(Holcomb et al. 1996)*. As shown in Figure 1.1, two reaction zones formed between the TS-Zn coating and the cement paste. Zone 1 was zinc that had oxidized to form mostly zincite (ZnO), mixed with wulfingite (Zn(OH)$_2$), simonkolleite (Zn$_5$(OH)$_8$Cl$_2 \cdot$H$_2$O), and hydrated zinc hydroxide sulfates (Zn$_4$SO$_4$(OH)$_6 \cdot$xH$_2$O), whereas Zone 2 was cement paste that had went through secondary mineralization in which Zn had replaced Ca. These zones were also found on the Cape Creek Bridge in Oregon *(Holcomb et al. 1996)*. The anode–concrete interfacial pH was found to drop quickly to the order of 6-8 during the middle stage of periodically wetted anode service under ICCP, and such acidification of the interface led to a reaction zone featuring calcium depletion where calcium and zinc aluminum silicates form in the cement paste *(Covino et al. 2002)*.
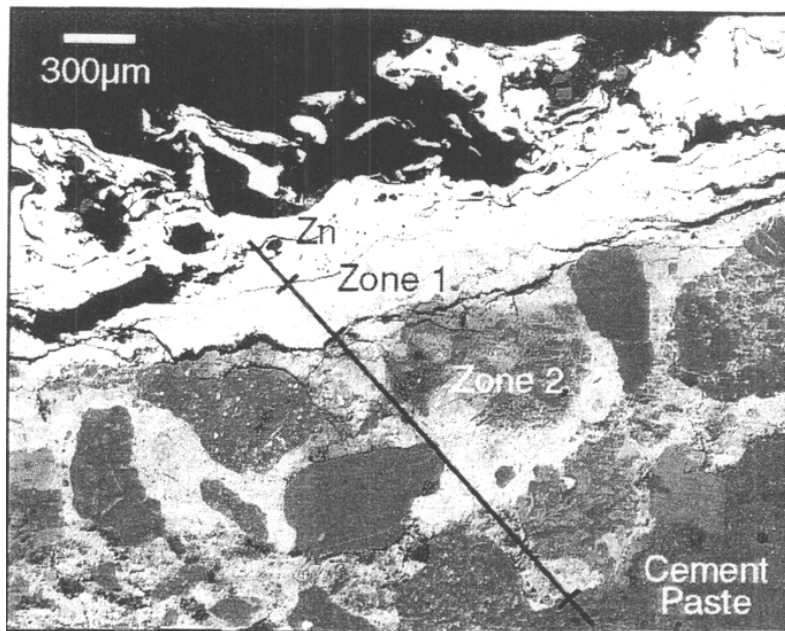
Figure 1.1: Back-scattered SEM micrograph of an electrochemically aged zinc–concrete interface showing voids in the coating and failures along the interface. The concrete sample was preheated, arc sprayed with Zn, and electrochemically aged to simulate 13.2 years of ODOT ICCP operations (Holcomb et al. 1996).

While preheating the concrete significantly improved the initial TS-Zn adhesion strength to concrete, the beneficial effects of preheating disappeared after electrochemical aging of more

than 200 KC/m^2 (5.2 A-h/ft^2, equivalent to three years of typical ODOT ICCP operations) *(Holcomb et al. 1996)*. The service life of TS-Zn was estimated to be approximately 27 years based on the adhesion strength measurements in accelerated ICCP tests. It was recommended to eliminate the supplemental heating of concrete surface and to reduce the thickness of the TS-Zn from 20 to 10 mils (500 to 250 μm) since only 3.4 mils were expected to be consumed from electrochemical reactions in 27 years of ODOT ICCP operations *(Holcomb et al. 1996)*.

Holcomb et al. *(1996)* proposed a four-parameter empirical model to account for the evolution of anode adhesion strength over the electrochemical age, as shown in Figure 1.2. They also proposed the following strengthening and weakening mechanisms for the TS-Zn adhesion on concrete: "The initial zinc coating had a purely mechanical bond to the concrete. The preheated concrete allowed for a tighter bond and thus a higher initial adhesion strength. Upon electrochemical aging, the ZnO that formed decreased the mechanical bonding due to a volume expansion. With additional aging, secondary mineralization locally strengthened the bond at the coating–concrete interface and led to an increase in adhesion strength. With increased electrochemical aging, inhomogeneities in the ZnO thickness (from "hot spots") created stresses and cracking within zone 1 and at the zone 1–zone 2 interface. The cracking eventually decreased the adhesion strength of the zinc coating to zero." Therefore, in addition to anode bond strength, ICCP system *circuit resistance* is another important operating characteristic that can be used to effectively monitor the TS-anode condition as it ages *(Covino et al. 2002)*. Moisture at the anode–concrete interface thus has a strong effect on anode performance *(Covino et al. 2002)*. ODOT research indicated that humectants (lithium bromide for galvanic CP and lithium nitrate for ICCP) could improve the electrical operating characteristics of the anode and increase the service life by up to three years *(Holcomb et al. 2002)*.
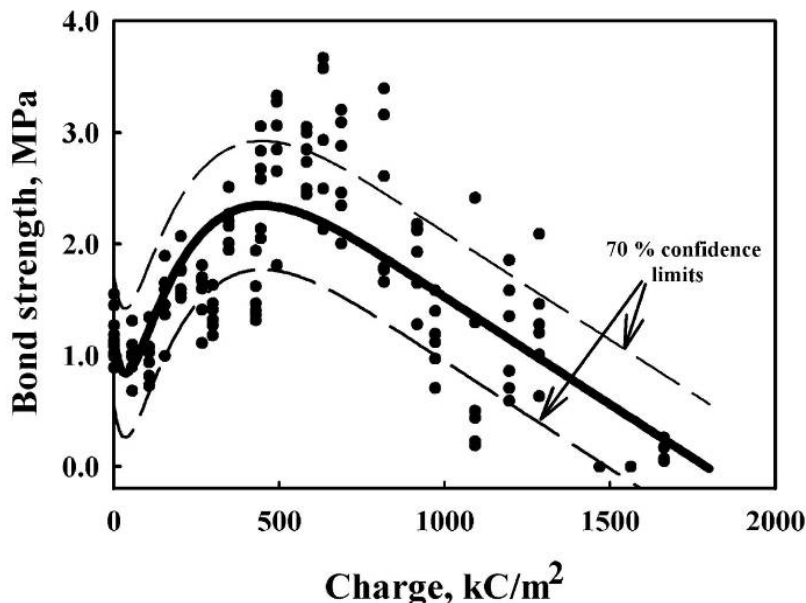
Figure 1.2: Bond strength of periodically wetted TS-Zn anodes on concrete as a function of electrochemical age in accelerated ICCP tests *(Cramer et al. 2002)*.

In practice, the ODOT-approved procedures use the initial zinc-to-concrete bond strength as an important parameter for quality assurance of TS-Zn operations. The concrete surfaces are generally not wet or damp since they tend to be kept above 80°F due to the use of a heated main closure to contain the zinc-spray operations. A weed burner is typically used to achieve appropriately low moisture levels for isolated concrete areas. The target thickness of sprayed zinc falls in the range of 15 to 20 mils (375–500 μm) to ensure that the entire concrete surface (despite its roughness) is fully coated with TS-Zn, which takes at least six passes of zinc spraying. Additional passes are needed for rough and irregular concrete surfaces.

1.4   SCOPE OF WORK AND REPORT ORGANIZATION

To accomplish the proposed objectives, this project consisted of a comprehensive literature review, practitioner surveys, and laboratory and field investigations. The Yaquina Bay Bridge, an arch bridge spanning Yaquina Bay south of Newport, Oregon, (see Figure 1.3) had a CP system installed in 1994, and several sections had prematurely failed. One of these sections was the entire surface of Pier 9 on the south end of the bridge, which was used for the field evaluations detailed in Chapter 4.

Figure 1.3: Yaquina Bay Bridge: geographic location (left); main span and base views (right).

The following chapter will present a comprehensive review of CP technologies for reinforced concrete. Chapter 3 presents the key findings from the surveys of current practice related to CP technologies and thermally sprayed zinc. Chapter 4 presents the methodology, results and discussion pertinent to methods of zinc anode removal and concrete surface preparation from both laboratory and field evaluations. Finally, Chapter 5 summarizes the key findings from this work followed by recommendations for implementation by ODOT. Appendices conclude this report.

2.0   CP TECHNOLOGIES FOR REINFORCED CONCRETE: INTRODUCTION AND RECENT DEVELOPMENTS

The research team conducted a comprehensive literature review to gather information relevant to this project. A detailed Internet-based search was conducted, using online databases including NACE, TRIS online, Google Scholar, SciFinder Scholar, and Scirus. The following sections present a synthesis of the available literature in order to document the state of the practice and the state of the art pertinent to cathodic protection (CP) technologies, with particular emphasis on new materials, innovative methods, and recent advancements used by other states and other countries to protect bridge substructures in coastal environments. It should be of value and interest to engineers involved in bridge design, bridge management, and structural maintenance, rehabilitation and preservation.

CP is an electrochemical technique to mitigate rebar corrosion in concrete structures regardless of their chloride content. This synthesis includes knowledge of two types of CP technologies (impressed current CP (ICCP) and sacrificial anode CP (SACP)), anode materials, methods of predicting anode service life and testing CP performance, monitoring techniques, thermally sprayed zinc anode installation and replacement, and recent advancements in CP technologies. In addition, this synthesis covers the computational models to treat the transport of ions in concrete and of electrons within rebars of CP systems. Various boundary conditions necessary for CP prediction are systematically classified, which, in combination with the conservation laws of mass and electricity, can predict CP performance under various external conditions.

2.1   INTRODUCTION

Reinforced concrete structures play a vital role in the infrastructure systems around the world. The highly alkaline pore solution in concrete normally protects embedded steel rebars from corrosion by forming a passive film on their surface. The dense protective film can be an oxide or a hydroxide that is coherent with the underlying rebar, thereby reducing the oxidation rate *(Enevoldsen et al. 1994)*. In addition, concrete can act as a physical barrier to the species that are aggressive to steel. However, there are two mechanisms by which the protective environment in concrete and the accompanying passivation effect for rebar can be undermined. Firstly, the local alkalinity can be reduced by losing alkaline substances through water leaching or reacting with CO_2. Secondly, the protective film on reinforcing steel can be broken down by electrochemical interactions with chloride and oxygen.

Chloride, often originating from salt-laden environments in coastal areas or from deicer salt applications on highways, can initiate rebar corrosion once its concentration has reached a threshold level on the rebar surface *(Glass and Buenfeld 1997)*. For reinforced concrete structures such as highway bridges, chloride-induced degradation is the most important environmental attack to reinforced concrete *(Gjørv and Vennesland 1979; Alonso et al. 2000; Sergi and Glass 2000; Zornoza et al. 2008)*. The corrosion products (rust) can occupy more

volume of the original steel, thereby causing tensile forces and cracking to develop in concrete, which subsequently facilitates the ingress of deleterious species (e.g., moisture, oxygen and chlorides) to the embedded rebar. The rate of corrosion directly affects the remaining service life of a concrete structure, which not only causes structural disfigurement but also leads to premature structural failure.

CP is a proven electrochemical technique that can effectively mitigate rebar corrosion in concrete *(Bertolini et al. 1998; Whiting et al. 1996; Hartt 2002; Polland and Page 1988; Page and Sergi 2000)*. The rationale behind CP is to make rebar more cathodic relative to anodes so as to reduce its corrosion to a much lower level. The current flows between rebar and the anode through the surrounding medium as an ionic current. In practice, such retention of steel electrons is achieved with an anode to supply a higher counter current to the original corrosion circuit. Accordingly, CP can be realized either by an impressed current (ICCP) or by the use of sacrificial anodes (SACP). In ICCP, an anode is attached to the concrete surface, and an external current is imposed between the anode and the rebar in concrete. In contrast, SACP is based on the relative position of specific metals in the galvanic series so that the consumption of anode materials can produce the electrons that the steel would otherwise release. The fundamentals and operations of ICCP and SACP have been recently reviewed by Szabó and Bakos *(2006a; 2006b)*.

While CP can be adopted as a repair strategy to address reinforcement corrosion, it is most cost-effective and labor-saving for structures in chloride-contaminated environment by eliminating the need to remove contaminated concrete. In addition to mitigating corrosion, the cathodic current has been known to extract deleterious chloride ions away from the rebar surface, which effectively lowers the chloride content below the critical level *(Parthiban et al. 2008a)*. The growth trend of cathodic protection in North America from 1973 to 1989 was recorded in a Strategic Highway Research Program (SHRP) document *(Broomfield and Tinnea 1992)*, which showed 283 cathodic protection systems were installed on 200 bridges, as shown in Figure 2.1. In 1994, there were 350 operational CP systems in the United States and Canada (*Sohanghpurwala 2009*). To update such information for recent years, the National Bridge Inspection Standards (NBIS) database was queried and a survey among public agencies was conducted for North America, the results of which reveal that 573 bridges possess CP systems. Of those, 376 bridges are in the United States and 197 bridges are situated in Canada. The Oregon Department of Transportation (ODOT) has pioneered CP for preservation of existing major historic coastal bridges *(Bottenberg 2008)*, with nine CP systems on decks, 11 on superstructures, nine on caps, and seven on columns (*Sohanghpurwala 2009*). Over recent decades, CP of concrete structures has evolved to a mature technique with its own protection criteria, anode types and power supplies, thereby allowing for effective and economical long-term protection of chloride-contaminated infrastructures.
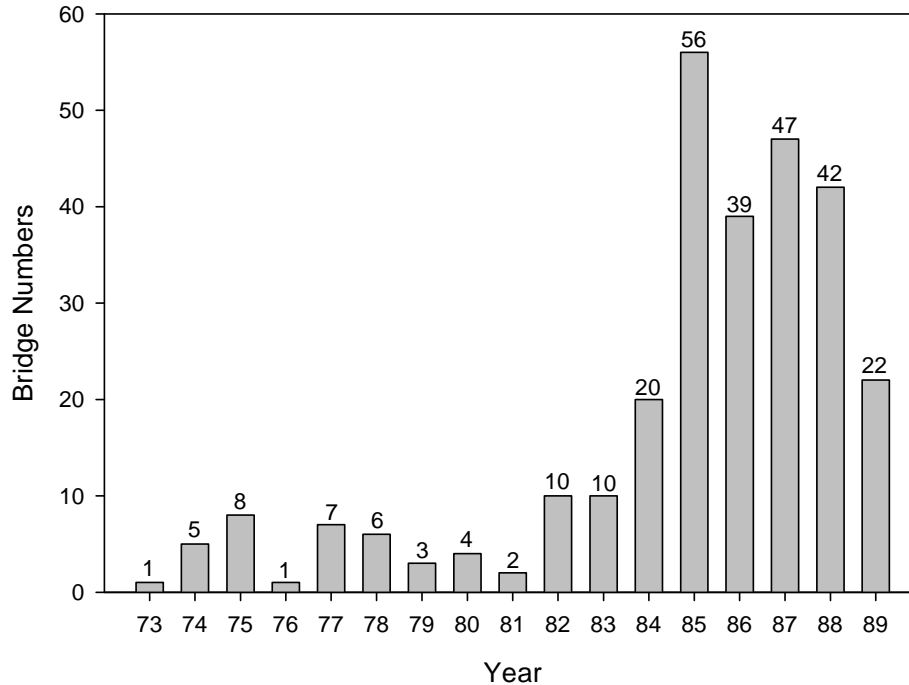
Figure 2.1 Cathodic protection systems installed per year in North America *(Sohanghpurwala 2009)*.

In addition to controlling the steel corrosion, CP has been found to have other interesting effects on the structures being protected. While measured chloride profiles indicated that little chloride migration occurred at low current densities of 0.01 A/m^2, migration away from the rebar and general chloride depletion in its vicinity were observed at current densities of 0.05 A/m^2 or higher *(Mussinelli et al. 1987; Polland and Page 1988)*. CP was demonstrated to induce microstructure alterations and some micro-cracking, while effectively retarding corrosion-induced crack initiation and propagation *(Hu et al. 2005)*. The cathodic current was also found capable of accelerating the alkali-silica reaction in concrete containing potentially reactive aggregates and changing its mechanical properties *(Chang et al. 2005)*. For high-strength prestressing steels, CP also poses a risk of hydrogen embrittlement especially if overprotection is applied *(Isecke and Mietz 1993)*.

Two other electrochemical applications exist in addition to CP - desalinization and realkalization. For carbonated concrete, realkalization is a technique to increase the pH value of pore solutions to be above 10.5 to regain passivity for rebar. The underlying principle is electro-osmosis, in which alkaline solutions are propelled by an externally applied electric current towards negative electrodes. Desalination, also known as electrochemical chloride removal (ECE), is a similar technique to CP but characterized by a much higher applied current density to drive chloride ions out of the chloride-contaminated concrete structures. Such deleterious ions migrate towards externally positioned electrodes, where they are collected and carried away. Meanwhile, hydroxyl ions are generated in the vicinity of the rebar surface, which is beneficial

for rebar repassivation. Unlike CP, desalination and realkalization are short-term applications to revitalize concrete structures.

CP requires that to protect the cathode, it should be immersed in an environment with continuous and conductive electrolyte. Steel structures in seawater belong to such a scenario, where the electrolyte is nearly neutral with relatively high conductivity. For buried metal structures, soil possesses a relatively low conductivity in an almost neutral environment, which entails well-positioned anodes for a satisfactory protection behavior. The situation of rebar in concrete is similar to the scenario in soil, where the resistivity of the electrolyte is of major importance. In cement-based materials, the electrolyte is the aqueous pore solution constrained within the finite pore geometry. Such a unique feature makes the electrical criteria used to judge CP performance in concrete structures to be different from those utilized in seawater and soil. In recent years, the CP technique for reinforced concrete structures has evolved into a well-established discipline with its own criteria, anode types, and power supplies.

For ICCP, the impressed current can be tuned so as to have a large driving voltage for structures in environments with high resistivity. In addition, ICCP needs comparatively fewer anodes, and can maintain an effective protection even when surface applied anodes have mechanical damage. For atmospherically exposed reinforced concrete structures, ICCP is usually the most appropriate corrosion mitigation technique. In 1972, the California Department of Transportation (Caltrans) first implemented ICCP for the protection of reinforced concrete bridge decks from deicing salt attack, using a corrosion-resistant silicon iron primary anode in a backfill of conductive carbon coke breeze added to asphalt. Since the 1980s, ICCP systems have also been installed on bridge substructures by highway agencies and others, followed by a SHRP report on the state of the art and a SHRP manual of practice for ICCP *(Bennett et al. 1993)*.

SACP systems have the advantage of no auxiliary power supplies. Due to their minimal requirements for installation, maintenance and monitoring, they are less costly than ICCP systems. While driving voltages up to 100 V can be available in ICCP systems, the maximum driving voltage for SACP systems is controlled by the open circuit potential (OCP) difference between the anode and steel, which cannot exceed 1 V. SACP systems are less prone to erroneous operations, which would otherwise lead to hydrogen embrittlement of the steel, unexpected anode aging, and/or deterioration of the anode–concrete and steel–concrete interfaces. On the other hand, SACP systems are less adjustable once installed and proper distribution of sufficient protective current is dependent on the anode zoning, the resistances of the concrete matrix and interfaces, as well as the anode passivation and longevity. The electrical resistance of concrete structures is crucial to judge whether the SACP system is viable. In cases where the concrete resistance is too high, the effective potential difference between the steel and the anode may not be sufficient to protect the structure. Thus, SACP has been successfully used on substructures of reinforced concrete bridges and bridge decks in marine environments within the United States *(Broomfield et al. 1990)*.

2.2   ANODE MATERIALS

The selection of anode material and its application are known to be critical to the effectiveness and durability of any CP system. To protect vertical and soffit surfaces of bridge substructures in

a coastal environment, the selection of anode material should take into account factors different from those considered for horizontal bridge deck surfaces. For instance, a concrete pile can be divided into atmospheric zone, splash zone, tidal zone, and submerged zone, each featuring different levels of chloride, moisture, and oxygen availability and thus significantly different corrosion risks to the reinforcing steel. An interesting solution is to employ a suite of CP technologies together, e.g., the combined use of thermally sprayed zinc for the atmospherically exposed concrete, zinc jackets for the splash zone, and bulk aluminum-zinc-indium (Al-Zn-In) anodes for the lower tidal zone and fully submerged piling *(Tinnea et al. 2004)*.

2.2.1 Impressed Current Cathodic Protection Systems

For ICCP systems, various anode materials have been used, including mainly: *inert anodes* (activated titanium anode mesh, titanium ribbon mesh, thermally sprayed titanium coatings, discrete titanium or conductive ceramic anodes), *carbon-based anodes* (conductive polymers, carbon-based paste as a backfill around discrete anodes, surface applied conductive coatings, carbon fibers dispersed in overlay), and *consumable anodes* (thermally sprayed zinc coatings) *(Virmani and Clemena 1998; Sohanghpurwala 2004b; Callon et al. 2004)*. NACE International has published a recommended practice standard on ICCP of atmospherically exposed steel-reinforced concrete *(2000)*, a standard test method for embeddable anodes *(2007)*, and a standard test method for organic coating anodes on a concrete slab *(2005)*.

2.2.1.1 *Non-Metallic Conductive Anodes*

To obtain uniform current distribution over the deck surface and protect the primary anode and instrumentation from traffic flow, a conductive coke-asphalt overlay anode system with commercially available high silicon cast iron primary anodes was developed for the Sly Park Road Overcrossing bridge deck of U.S. Route 50 in California by Caltrans *(Stratfull 1974; Wyatt 1993)*. As a secondary anode, the coke-asphalt overlay functioned, but suffered from structural degradations such as freeze–thaw deterioration of improperly air-entrained concrete beneath the overlay. Recognizing the disadvantages of the coke-asphalt system, the Ontario Ministry of Transportation and Communications modified the original design and added some conventional aggregate to the coke-asphalt mix. Although the electrical resistivity is slightly increased, such a modification produced an overlay with higher stability in terms of traffic loading *(Mailvaganam 1991)*.

Despite the inherent advantages of coke-asphalt overlays, their increase in weight, height, and freeze–thaw deterioration spurred the development of slotted systems. The primary anode was commercial platinized wires, which must be well-spaced to efficiently distribute current over the deck surface. With platinized wire anodes placed in slots, a backfill conductive material is needed to withstand traffic loadings and environmental attack. Slotted systems using polymer-modified mortar as backfill materials were initially tested *(Manning and Ryell 1979)*. Unfortunately, the gases and acid generated on the anode surface failed such systems. A conductive cementitious grout, although having advantages in strength and freeze–thaw resistance, experienced attack from the acid generated on the anode surface in a field trial on a Toronto bridge deck in Canada *(Nicholson 1980; Fromm and Pianca 1981)*. To achieve a backfill material with desired

acid resistance and excellent freeze–thaw durability, research was undertaken by the Federal Highway Administration (FHWA) to pursue a conductive polymer grout material with a vinyl ester resin, appropriate additives and coke breeze as the conductive filler *(Virmani 1982)*. Later, FHWA focused on a mounded grid anode system, which employed latex modified concrete overlays to allow completion of the overlay installation without damage to the anode grid. With its top covered by a conventional rigid overlay, a mesh anode made of copper and polymeric materials was constructed in Canada and the United States *(Swiat and Bushman 1989)* that required no electronically conductive backfill. Mixed metal oxide mesh anodes utilized titanium mesh as a base material, on which the mixed metal oxide coatings were formed through thermal decomposition. Such anodes are characterized by long service life and uniform current distribution, and have been successfully applied in both decks and substructures *(Burke and Bushman 1998; Manning and Schell 1987)*. According to Broomfield and Wyatt (2002), titanium-based anodes with mixed metal oxide coatings are the most ideal deck anodes as ribbon in slots or as mesh under an overlay.

The development of new anodes for CP of concrete structures has caught great research attention. In order to ensure continuous electrical conductivity, DePeuter and Lazzari *(1993)* applied carbon fibers coated by a thin corrosion-resistant metal to a cementitious conductive overlay, on which a layer of polymer-modified mortar can be conveniently sprayed. Bertolini et al. *(2004)* studied the behavior of a cementitious conductive overlay anode containing nickel-coated carbon fibers, the results of which confirmed its validity as an effective anode. Based on the results, a maximum current density of 10–15 mA/m^2 and a distance of 1 m between primary anodes were suggested for a safe design. Surface applied anodes, such as conductive coatings or carbon-loaded paints, are commonly used as secondary anodes on concrete members without traffic loadings, and feature the advantages of being applied easily to irregular surfaces such as deck soffits and bridge piers. Their effectiveness in protecting rebar in humid environments has been confirmed by well-designed systems *(Sohanghpurwala 2004b)*. To evaluate the suitability as anodes in concrete structures, Orlikowski *et al. (2004)* performed electrochemical measurements on conductive coatings made of pigmentary graphite and polymer matrix. Electrochemical parameters were determined for coatings under long-term anodic polarization on reinforced concrete, from which the optimum graphite content in coatings fell in the range of 40% to 45%.

2.2.1.2   *Metallic Anodes*

Inert anodes are generally recommended for an ICCP system when the remaining or designed service life of a concrete structure is long, as those anodes require no periodic replacement *(Bullard et al. 2000)*. Among the few noble elements in the periodic table, platinum and palladium-platinum alloys are most frequently utilized as anode materials. Traditionally, the wide application of platinum-coated anodes has been hampered by the lack of pore-free claddings on silver- or copper-based materials. This problem has now been overcome by the use of tantalum or titanium as rectifier materials, thereby not necessarily demanding pore-free claddings or coatings *(Preiser 1959)*. Titanium and tantalum feature a useful property to form an insulating oxide on their surface, which is

stable below puncture voltage. Although a consensus on minimum thickness of platinum from direct operational evidence for CP of concrete is still lacking, platinum coatings with a 50-micron thickness were successfully applied for seawater and brackish environments *(Preiser 1959; Cotton 1958)*. Innovative ways of applying platinum thin coatings on titanium and tantalum thus make those inert anodes commercially available, the cost of which depends on the target thickness of platinum coatings and the complexity of anode geometry. Such inert anodes are useful for submerged structures and land groundbeds for buried substructures.

Thermally sprayed zinc (TS-Zn) anodes for concrete application were developed by Caltrans researchers as secondary anodes *(Carello et al. 1989; Apostolos et al.1987)*. Brousseau, Arnott and Baldock *(1995)* evaluated three different types of zinc anodes for ICCP on reinforced concrete by monitoring the circuit resistance and anode bond strength with polarization time and concluded that TS-Zn performed well while TS 85%Zn-15%Al and mortar-enhanced zinc sheets performed poorly. Later, Brousseau *et al. (1996b)* showed that sprayed Zn anodes manifested good protective properties, while Al coatings did not result in expected behaviors.

Reaction products on Zn anodes can accumulate around the anode–concrete interface during electrochemical aging. To obtain improved understanding of the performance of TS-Zn anode, accelerated electrochemical aging was conducted using a current density of 3 mA/ft^2 (0.032 A/m^2, a factor of 45 higher than the approximately 0.2 mA/ft^2 used on coastal bridges by ODOT), which was found to cause chemical and physical changes at the anode–concrete interface, as shown in Figure 1.1 *(Holcomb et al. 1996)*. Two reaction zones were formed between the TS-Zn coating and the cement paste. Zone 1 was zinc that had oxidized to form mostly zincite (ZnO), mixed with wulfingite ($Zn(OH)_2$), simonkolleite ($Zn_5(OH)_8Cl_2 \cdot H_2O$), and hydrated zinc hydroxide sulfates ($Zn_4SO_4(OH)_6 \cdot xH_2O$), whereas Zone 2 was cement paste that had gone through secondary mineralization in which Zn had replaced Ca. The anode–concrete interfacial pH was found to drop quickly to the order of 6-8 during the middle stage of periodically wetted anode service under ICCP, and such acidification of the interface led to a reaction zone featuring calcium depletion where calcium and zinc aluminum silicates form in the cement paste *(Covino et al. 2002)*. While preheating the concrete significantly improved the initial TS-Zn adhesion strength to concrete, the beneficial effects of preheating disappeared after electrochemical aging of more than 200 KC/m^2 (5.2 A-h/ft^2, equivalent to three years of typical ODOT ICCP operations). Holcomb et al. *(2002)* proposed a four-parameter empirical model to account for the evolution of anode adhesion strength over the electrochemical aging. They also proposed the following strengthening and weakening mechanisms for the TS-Zn adhesion on concrete: "The initial zinc coating had a purely mechanical bond to the concrete. The preheated concrete allowed for a tighter bond and thus a higher initial adhesion strength. Upon electrochemical aging, the ZnO that formed decreased the mechanical bonding due to a volume expansion. With additional aging, secondary mineralization locally strengthened the bond at the coating–concrete interface and led to an increase in adhesion strength. The cracking eventually decreased the adhesion strength of the zinc coating to zero."

Ti and their alloys are prone to passivation by forming an adherent thin protective oxide film. While such a film is beneficial in terms of corrosion resistance, it undermines the ability to perform as anodes in ICCP systems until the breakdown potential is exceeded *(Shreir 1986)*. Bennett *et al. (1995a)* developed a thermally sprayed (TS) Ti-based anode for ICCP of reinforced concrete featuring inherently high bond strengths and minimal safety and environmental concerns.[1] TS-Ti-based coatings can be catalyzed *(Bennett et al. 1995b)* for service at low anodic potentials, which is beneficial if long operational life is desired. Because of good mechanical properties, sprayed Ti anodes can extend the failure-free time of ICCP systems *(Bennett et al. 1995c)*. The protection effectiveness of TS coatings, according to Covino et al. *(1999)*, is dependent on such parameters as spraying pressure, atomizing gases, bond strength, coating resistivity, water penetration, and interfacial chemistry. Because of very good electrochemical properties, the current densities for such materials can be very high *(Ali and Al-Ghannam 1998)*. Brousseau et al. *(1998)* systematically investigated TS-Ti anodes with three catalysts, Pt-Ir, Ru-Ti and Co oxide, in reinforced concrete that was powered at constant current density, where cobalt oxide was found to be the best catalyst. Composite anodes, such as platinized Ti and Nb are the most commonly used primary anodes to overcome shortcomings of anodes made of a single material. The base metals provide desired shapes and mechanical strength, while coatings act as inert materials for current transfer and enhance the resistance to corrosion.

2.2.2 Sacrificial Anode Cathodic Protection Systems

Since the 1990s, significant advancements have been made in adapting SACP systems to bridges, especially substructures in marine environments *(Kessler and Powers 1993)*. For SACP systems, anode materials used mainly include: thermally sprayed zinc, mortar enhanced zinc anodes, zinc mesh, aluminum alloys, and magnesium alloy*s (Hu et al. 2005; Isecke and Mietz 1993; Sohanghpurwala 2004a)*.

Al, Mg, Zn and their alloys are more electronegative than steel, thereby acting as anodes when electrically coupled to steel. Due to its high electrical resistivity, concrete demands sacrificial anodes with a high driving voltage. The use of Mg anodes is therefore favorable. However, studies on Mg-based sacrificial anodes for CP in concrete are very limited *(Kessler et al. 1998b; Yunovich 2004)*, and the finite findings indicate that longer durations are required for CP to stabilize. Parthiban et al. *(2008b)* evaluated the long-term performance of Mg-based anodes in chloride-contaminated reinforced concrete slabs, where the potential of embedded steel and the ionic current were measured. The potential of steel was initially shifted to more negative values, followed by less negative results. Removal of chloride ions from the vicinity of steel was also found, which is attributed to the electrical field generated by the sacrificial anodes.

Moisture at the anode–concrete interface is vital to anode performance *(Covino et al. 1999; Rothman et al. 2004)*. Using hydrogel to improve moisture content on the zinc–concrete interface, Bennett and Firlotte *(1997)* demonstrated that protective current distribution in

---

[1] The deposit efficiency and Ti consumption were improved by *low standoff distance*, *high carrier gas pressure*, and *fast gun speed*.

concrete structures could be greatly improved. ODOT has experience with the use of zinc/hydrogel anodes and TS Al-12Zn-0.2In anodes for SACP systems *(Cramer et al. 2002*; *Bullard et al. 1999)*. When used in an ODOT SACP system *(Cramer et al. 2002)*, the Al-12Zn-0.2In anode produced less current than either the zinc/hydrogel anode or the TS-Zn anode. A different TS Al-Zn-In anode, however, was reported to provide sufficient current densities (1.1 mA/m^2 and above) and exceed the 100 mV polarization decay criterion for CP on a Texas coastal bridge *(Burns and Daily 2004)*. Yet another study in New York suggested that the TS Al-Zn-In anode performed better than the TS-Zn anode in the dry zone due to its relatively higher driving potential. Al-Zn-In was reported to have good performance as an anode, but it is now off the market.[2] The zinc/hydrogel anode is relatively simple to install (see Figure 2.2), but has been reported to have durability problems especially in wet conditions where adhesion of the hydrogel can be a serious issue *(Rothman et al. 2004*; *Bullard et al. 1999)*.

Figure 2.2: Arc spray application of galvanic Al-Zn-In to a bridge pier in Texas (left); and application of zinc/hydrogel anode to a bridge pier in Florida (right) *(Daily 1999)*.

A recent development in alternative anodes for SACP systems is a liquid coating that can be brushed or sprayed to a concrete substrate at room temperature, featuring a mixture of fine particles of 75% zinc and 25% magnesium in an ethyl silicate binder applied over titanium or stainless steel mesh *(MacDowell and Curran 2003)*. A field study by the Texas DOT suggested that "durability of the CP systems was challenged much more by the harsh marine environment than by the normally anticipated electrical consumption of the anode" *(Whitney et al. 2003)*. By investigating the performance behaviors of thermal sprayed Zn and catalyzed thermal sprayed Ti, Covino *et al. (1999)* concluded that "anodes generally fail due to loss of bond strength rather than Zn consumption." These two studies reach a consensus that anode consumption is not the mode of failure.

---

[2] Personal communications with Rob Reis, Senior Corrosion Specialist, Caltrans Corrosion Technology Branch, June 2008.

2.3   CP PERFORMANCE CRITERIA AND MONITORING TECHNIQUES

The two most important factors for a CP system are the current density on steel cathodes and the current distribution path *(Hassanein et al. 2002; Bertolini et al. 1993; Polder 1990)*. Although CP requires a supply of sufficient protective current to concrete structures, such designed values are not an assurance of adequate protection. The development of acceptable monitoring techniques and criteria has still been a practical concern. Realizing the improbability of arriving at a universal criterion for all concrete structures under all exposure conditions, various criteria are now employed to assess protection status. The current density required for sufficient cathodic protection is dependent on the rebar corrosion status in concrete structures *(Stockert et al. 2005)*, which varies with respect to moisture, chloride content, aeration, cover depth, and component geometry. The magnitude of the driving voltage required from the direct current source depends on a number of factors, including the electrolytic conductivity of the environment, the area of structure to be protected, the nature of the electrode reaction at the auxiliary electrode, and the resistance of the auxiliary electrode *(Hassanein et al. 2002; Harriott et al. 1993)*.

2.3.1 CP Performance Criteria

2.3.1.1   *Half-cell Potential*

Based on thermodynamic considerations, half-cell potential mapping is the simplest technique to evaluate reinforcement corrosion. However, potential criteria are mainly developed through empirical knowledge that is gained through successful CP practice, which provides no quantitative information on corrosion. The corrosion situation can be estimated with potential values according to ASTM C876-91 standards, e.g., there is a 95% probability of corrosion for regions where potential values are more negative than -350 mV CSE (Copper Sulfate Electrode, $Cu/CuSO_4$) and a 5% probability of corrosion where potential values are less negative than -200 mV CSE. If the oxygen diffusion is limited, potential values can be more negative than -350 mV CSE without appreciable corrosion. Potential values can be affected by highly resistive concrete layers, as measurements are conducted at places away from reinforcement. Such an effect can lead to a deviation of 200~300 mV from real values, making the obtained results less negative. Some other factors that can affect conductivity should also be taken into consideration, such as corrosion product, age of concrete, reference electrode position, concrete constituents, and cracks. Full CP protection can be achieved when the local cathodes are polarized to the open circuit potential (OCP) of the most active local anode *(Jones 1987)*. The anodes are thus not able to discharge current and corrosion can cease. Corrosion of steel in concrete with a high chloride level can be prevented when sufficient cathodic current is applied to reduce the potential to -600 mV CSE *(Montemor et al. 2003)*. More negative potentials from -710 mV CSE to -770 mV CSE are also reported for chloride-contaminated concrete *(Naish and McKenzie 1998)*. For carbonated or damaged concrete, potentials more negative than -900 mV CSE need to be shifted for corrosion control *(Holcomb et al. 2002)*. A criterion of -850 mV CSE is frequently used for bare steel in various environments *(Montemor et al. 2003)*. If the concrete structure

14

contains high-strength steels, a low limit value of -1000 mV CSE is ensured to avoid severe reactions on electrodes and to reduce the risk of hydrogen embrittlement *(Ahmad 2003)*.

Another performance criterion based on depolarization is the instant-off potential between the anode and the protected steel, which is a widely adopted means of evaluating CP levels. This is done in practice by adjusting the protection current with a subsequent sudden current interrupt so that a potential difference of 100 mV can be achieved in about four hours *(Page and Sergi 2000; Bullard et al. 2004; Presuel et al. 2002a; NACE International 2008)*. Such a value should be measured at the most anodic location in each 50 m^2 area, according to the NACE SP0408-2008 (Standard Practice – Cathodic Protection of Reinforced Steel in Buried or Submerged Concrete Structures). If the decayed off-potential is less than -200 mV CSE, no CP is necessary as the steel structure is passivated. Potential shift upon removal of protection current stems from the relative amounts of oxidizing and reducing species to exert potential evolution on the system. If the driving force toward corrosion is significant, the potential will shift to the corrosion potential that is well defined from the availability of anodic sites and the local supply of oxygen. One factor governing the potential shift and the time required for that change after current interrupt is oxygen depletion around the protected steel. The rate of oxygen depletion can feature large variations as a result of slow diffusion in concrete. Due to the complex chemical and physical interactions between species and their environments, the application of CP may alter local chemistry, thus making originally anodic areas less anodic. Environmental conditions, such as temperature and moisture, have direct impact on the rate at which potential decays. When the CP has been applied on a concrete structure for a prolonged period, a great amount of alkaline species are generated at the corrosion site and a significant amount of chloride ions have been transported away from steel rebar. Thus, a strong redox couple characterized by a strong corrosion potential will be absent, with the local potential determined by oxygen level.

When an excessive current density is applied on cathodes, hydrogen atoms generated can migrate within the steel lattice and get trapped around defects like second-phase particles and gliding dislocations, thereby leading to decohesion and void formation. Cracking of steel can occur either through a strain-controlled mechanism at the macro-scale with transgranular cracking or a stress-controlled decohesion on the micro-scale with intergranular cracking *(McMahon 2001)*. This phenomenon is known as hydrogen embrittlement, which results in a reduction in ductility of rebar even in the absence of external load. Hydrogen embrittlement is characterized by various mechanisms such as high-pressure bubble formation, reduction in surface energy, interaction with defect structures, and hydride formation *(Nagumo et al. 2001; Eliaz 2002; Nagumo 2001)*. The most classical one is with the internal pressure mechanism from hydrogen precipitation around second-phase particles, thereby pinning their movement. Other mechanisms may also be operational, depending on materials type, hydrogen concentration and loading types. It is generally accepted that a small amount of hydrogen can lead to dramatic changes in material properties, and the increase in rebar strength enhances the susceptibility of hydrogen embrittlement with serious in-service implications. For low-strength steel, the introduction of hydrogen may adversely affect fatigue properties. For

high-strength steel, hydrogen ingress can be more detrimental to its durability and performance. The extent to which hydrogen can migrate and thus get trapped within steel depends upon many internal and external factors. To reduce the possibility of overprotection and the subsequent hydrogen embrittlement, SACP has been utilized for prestressed concrete pipelines. For above-ground prestressed structures that are not highly susceptible to hydrogen embrittlement, suitability assessment can be performed based on the criteria proposed by Klisowski and Hartt *(1996)*. For concrete structures on which corrosion-related cracking and spalling are present, cathodic protection is qualified, if the remaining cross-sections of reinforcement are at least 85% and 90% in areas of uniform corrosion and localized attack, respectively.

Corrosion potential is only a measure of whether the anode and cathode can undergo electrochemical reactions. Corrosion current density, on the other hand, presents a quantitative kinetic indication of corrosion attack in reinforced concrete *(Pedeferri 1996)*. As such, polarization curve and electrochemical impedance spectroscopy (EIS) measurements can be used to assess the performance of CP systems.

2.3.1.2   Polarization Curves

The linear polarization method is a simple and non-destructive method to acquire corrosion current density *(Andrade 1986; Andrade et al. 2001; Rodriguez et al. 1994)*. However, several challenges are imposed on this technique, such as the high Ohmic drop of concrete between rebar and the reference electrode. For concrete structures, irregular distribution of electrical signal on counter electrodes has hindered the use of this technique, as the electrical signal decays with increasing distance from the counter electrode. In addition, the corrosion current density is inherently related to the Tafel constant that must be accurately known. Based on a relationship between concrete resistivity and ohmic resistance and considering the non-uniform distribution of the applied current, Feliu et al. *(1988)* developed a method to acquire the true polarization resistance from the apparent polarization resistance, where an analytical solution is proposed. Although this technique allows the validity of the solution to be verified by experimental measurement of polarization resistance obtained with a uniform distribution of the applied signal, it tends to underestimate polarization resistance for passive reinforced structures. Gonzalez et al. *(1991)* proposed a transmission line model to account for the uniform distribution of electrical signal on counter electrodes, where both counter electrodes are maintained at the same electrical potential with respect to the working electrode. The success relies on the use of a central auxiliary electrode to locally polarize rebar, with another electrode concentrical to the former one so as to provide polarization to the rest of the rebar around the area affected by the central one. Mansfeld *(1973)* and Bandy *(1980)* reported some methods to estimate Tafel slopes from polarization data. However, there are some inherent shortcomings in these techniques according to LeRoy *(1975)*. For example, the non-linearity of polarization data must be appropriate to avoid mathematically infinite solutions for Tafel slopes.

With guard ring electrodes, Sehgal et al. *(1992)* studied the quality of polarization resistance, where various variables such as wetting and surface morphology were taken

into consideration. A planar concrete surface and decreased contact resistance between probe and concrete surface were found to be beneficial for data accuracy. However, the guard ring technique still suffers from such limitations as dependence on concrete resistivity, thus leading to an underestimate of corrosion rates. To eliminate the effect of concrete ohmic drop on the polarization data for error-free estimation of corrosion current density, Ahmad and Bhattacharjee *(1995)* suggested an arrangement based on a linear polarization technique for the in-situ measurement of the corrosion current density of embedded rebar. Using the experimental observations, such an apparatus (shown in Figure 2.3) allows the Ohmic resistance of concrete, the polarization resistance of rebar, the Tafel slopes, and the corrosion current density to be simultaneously determined.
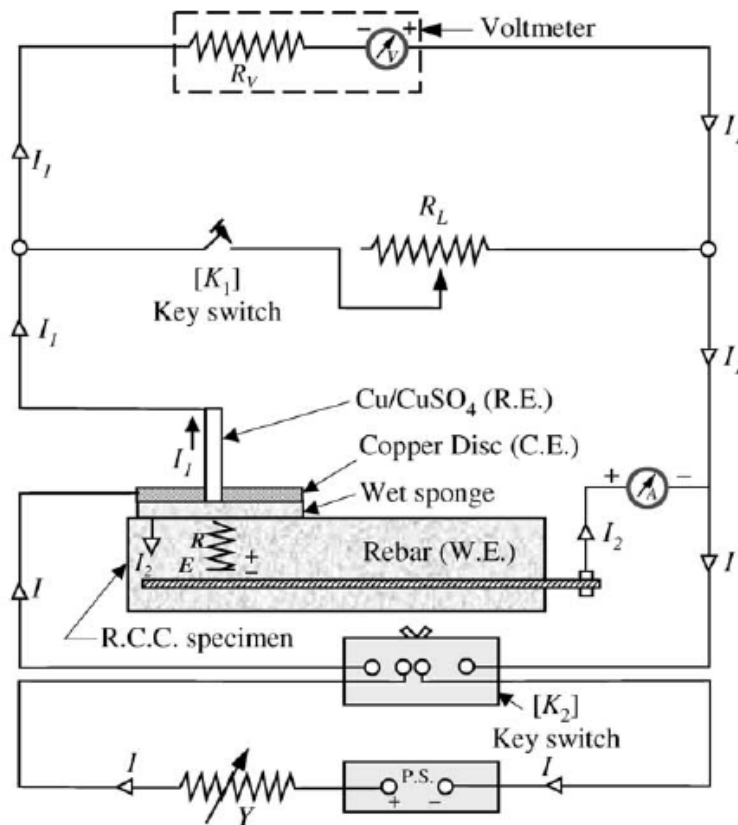
Figure 2.3: Arrangement for the determination of corrosion potential, Ohmic resistance and polarization resistance *(Ahmad and Bhattacharjee 1995)*.

Unfortunately, there are some aspects that constrain the effectiveness of the polarization curves. The high resistivity of concrete necessitates a long time to track the response from an applied signal. As such, the measured polarization curve can be strongly dependent on the scanning rate. Corrosion rate can be significantly influenced by the estimation of the polarization area of the reinforcement. In addition, the surface condition of rebar may be displaced from the real one by the high polarization current density, thereby resulting in biased corrosion rate.

2.3.1.3   *Electrochemical Impedance Spectroscopy*

The CP performance can be evaluated by electrochemical impedance spectroscopy (EIS), especially when a non-destructive technique is desired for high impedance and multiphase materials like reinforced concrete *(Song and Saraswathy 2007; Schechirlian et al. 1993; Genesca and Juarez 2000; Qiao and Ou 2007; Koleva et al. 2007)*. From the dynamic behavior between impedance and frequency, an equivalent electrical circuit can be established to provide information on the rebar–concrete interface, the concrete matrix, and the anode–concrete interface. EIS does not require switching off the CP current. Instead, it only superimposes a small alternating current or potential to the original DC signal on the polarized electrode *(Jankowski 2002)*. The response signal in terms of time or frequency can be analyzed to gather electrochemical information of reinforced concrete. Parameters of interest, such as charge transfer resistance, corrosion current density and Tafel slopes, can be mathematically extracted based on equivalent electrical circuits. Such knowledge can help the quality control of CP and on-line adjustment of CP parameters so as to maintain effective and efficient corrosion protection of the rebar.

John et al. *(1981)* applied EIS to monitor corrosion in concrete structures exposed to seawater. The impedance responses in both the low and high frequency ranges were analyzed, with the former correlated with charge transfer and the later with surface film. Gonzalez et al. *(1985)* concluded that EIS can provide similar or smaller polarization resistance relative to that obtained from the linear polarization technique. Assuming steel and concrete are purely resistive and their interface is reactive, MacDonald et al. *(1988)* proposed a transmission line model to account for the steel/concrete system, which allows corrosion to be identified with the real and imaginary parts of the impedance response and phase angle at low frequencies. For small structures, the circuit model proposed by Wenger and Galland *(1989)* can be used to interpret impedance response, with the response at high frequencies to characterize the presence of a lime-rich film on the steel surface. Dhouibi-Hachani et al. *(1996)* adopted another circuit configuration to account for reaction products, the results of which can satisfactorily represent the Nyquist diagram from experimental data, and the response from the high-frequency range allows concrete resistivity to be assessed. Using a perturbation signal on steel in concrete, Thompson et al. *(1988)* analyzed the impedance spectra obtained at different polarization levels. Significant differences between spectra determined from naturally corroding and polarized electrodes were observed. The degradation mechanism for a freely corroding electrode is the diffusion controlled state, and the mechanism switches to the activation-controlled process when the protection potential is reached. Pruckner et al. *(1996)* used EIS to study rebar status in chloride-contaminated concrete under CP, where a simple method using two selected AC frequencies was employed. The corrosion rates in concrete samples with different chloride levels were determined. Such a fast and efficient technique allows the characterization and monitoring of CP in large structures. However, there are still concerns on whether this technique has been sufficiently developed to correctly assess the CP protection level, as the data are difficult to interpret for many concrete structures subjected to corrosion. EIS measurements necessitate complicated

equipment and are time-consuming as well. In addition, the measured surface area of rebar in concrete depends on the utilized frequency.

2.3.2 Monitoring of CP Performance

2.3.2.1 *Continuous Monitoring*

Corrosion rates vary significantly in marine structures between the atmospheric, splash and tidal zones. The protective current density used to arrive at a particular cathode potential is prone to environmental variations which can modify the cathode polarization. Cathodic current may thus be a dynamic measure that needs to be incorporated into CP design. Sensors that are permanently embedded in concrete can reach equilibrium with the surroundings, thereby providing a means of in-situ monitoring without any destructive operation. To facilitate current assessment and future enhancement, it is very important to establish performance trends from measurement over a representative period. Parameters for automatic monitoring include corrosion rate, chloride penetration rate, carbonation rate, electrical resistivity, oxygen supply, relative humidity, and temperature. In response to the corrosion rate of rebar, the driving voltage and protection current can be simultaneously adjusted to optimize cathodic protection and increase anode service life.

Sun *(2004)* evaluated the performance of coupled multi-electrode sensors under CP conditions. The sensor response to rebar corrosion at different potentials confirmed the validity of such sensors for real-time monitoring of localized rebar corrosion.

Bazzoni and Lazzari *(1992)* presented a new approach to monitoring and automatic control of cathodically protected reinforced concrete structures based on the idea of measuring the potential of the anode rather than the cathode that is normally investigated. One electrode was reported to be sufficient. This approach has striking advantages in that it is safe against overprotection and also requires a limited number of reference electrodes to monitor CP. The anode potential is acquired in-situ and the feeding voltage is subsequently calculated based on the criterion with prefixed overprotection limit, which eliminates the occurrence of overprotection in the system. The test was performed on a post-tensioned new bridge deck and a conventional concrete structure that had been in CP service for a few years, the results of which verified the capability of this design for variable feeding conditions.

2.3.2.2 *Remote Monitoring*

Remote monitoring units for CP systems have been commercially available and allow measurements to be conducted on several systems from a remote central location so that problems can be detected and solved in a timely manner *(Van Blaricum and Norris 1997; Bennett and Schue 1998)*. In addition, remote monitoring systems can acquire measurements at periodic intervals for later analysis. The use of remote monitoring systems by the Florida Department of Transportation (FDOT) dates back to 1993 *(Kessler et al. 2002)*, when such units could acquire signals at predefined intervals and interrupt protection current for instant-off parameter measurement. Around 1996, remote

monitoring units evolved to have the ability to automatically interact with rectifiers to modify circuit output. In 2000, new units adopted by FDOT were able to fax in-situ output signals to the central office and keep track of on-site conditions at predefined intervals, which is useful for quick response in accordance with physical conditions at substructure sites. The units also had built-in modules that enabled on-site repairs, which eliminated the need to remove the entire unit from the enclosure. Implanting remote monitoring units for CP incurs additional expense. In addition, electronic equipment is prone to environmental attack, which necessitates special care for their protection.

2.4   ANODE SERVICE LIFE PREDICTION

Anodes can be consumable over time under service conditions, and they need to be replenished or replaced before depletion. Estimating anode service life is therefore of practical importance to gain information on long-term performance. Although consumption rate can be determined from anode weight loss or volume change, such measurement is not convenient or practical for submerged anodes. When anode current is monitored in real time, environmental change can be reflected in anode consumption rate. The service life of anodes depends on their weight and current output. Anode weight determines the average current supplied over a given service period, which is in fact affected by the prevailing operating conditions, such as locations, humidity and temperature.

The current output of a CP system is governed mainly by electric resistivity, anode/electrolyte resistance and anode potential. An anode configuration that can provide the desired current output is not sufficient. The long-term performance of anodes depends on installation variables, and can be hampered by inadequate or improper factors in the design, installation and monitoring of the CP system. Estimation of anode service life must be undertaken to ensure the design can provide protection for a reasonable period. For non-metallic anodes such as conductive polymer backfill, conductive paint and mixed metal oxide, their service life may be extrapolated from measured weight change over a specified period. As to metallic anodes, service life can be given by Eqn. (2-1) *(Gurrappa 2005; Miyata et al. 2008)*:

$$L = \frac{W \times u}{E \times I}$$

(2-1)

where L is the anode service life (yr); W is the anode weight (kg); E is the consumption rate of the anode (kg/(A·yr)); u is an efficiency factor to account for a reduction in output as anode surface area decreases with time; I is the mean current output over a specified period for sacrificial anodes (A). For ICCP anodes, I may be characterized by the difference between the input current from the rectifier and the output of the anode, which features the rate of self-consumption.

Spriestersbach et al. *(1999)* suggested that the service life of a TS-Zn anode could last up to 20 years or more, which can be considerably enhanced with an organic topcoat. According to Rothman et al. *(2004)*, the use of a supplemental topcoat would decrease the oxidation of the TS-Zn anode from its exposed side and reduce its self-consumption. ODOT research indicated that humectants (lithium bromide for SACP and lithium nitrate for ICCP) improved the electrical

operating characteristics of the anode and increased service life by up to three years *(Brousseau et al.1996b).*

Life expectancy of sacrificial anodes is typically less than that of ICCP anodes. For instance, the life expectancy of thermally sprayed Al-Zn-In was estimated to be 10–15 years in a sub-tropical marine environment and possibly 15–20 years in northern deicing salt environment, whereas inert anodes for ICCP were expected to last between 25 and 100 years depending on the type of anode and catalytic coating used *(Callon et al. 2004).* In addition to its weathering in the marine environment, a TS-Zn anode is expected to passivate with time, and its service life in SACP systems was thus estimated to be only seven to ten years *(Clemena and Jackson 1998).* Similarly, based on the performance of ICCP systems in the field, TS-Zn anodes in such systems were estimated to last only 10 to 15 years *(Clemena and Jackson 1998),* which was considerably shorter than the 27 years estimated from bond strength measurements in accelerated ICCP tests sponsored by ODOT *(Holcomb et al. 1997).* In moisture-lean environments, Zn reaction products cannot be sufficiently transported into the cement paste, thereby leading to a significantly shortened service life. Field evaluation of a water-based conductive paint indicated that it could last for at least 15 years when used as the secondary anode in ICCP systems for inland concrete piers using platinized niobium copper (Pt-Nb-Cu) wires as the primary anode *(Isecke and Mietz 1993).*

Efforts were initiated by FHWA to evaluate the service life of different anodes on highway structures *(Sohanghpurwala and Scannell 2000)* where various anode materials were used for ICCP or SACP systems to determine their effectiveness and long-term performance. Cathodic protection was tested in 19 bridges and one tunnel in the United States and Canada on which 19 ICCP systems and five SACP systems were installed. Some protection systems were still operational when the research was ended, while others functioned improperly as summarized in Table 2.1.

Table 2.1: Summary of anode performance and service life *(Sohanghpurwala and Scannell 2000).*

Anode Material & Configuration	Environment	No. of Systems	Age of Systems (years)	Protection Provided	Estimated Service Life (years)
Impressed-current Cathodic Protection Systems					
Arc-sprayed zinc	Semi-marine & deicing	2	2	Poor[1]	10 to 15
Arc-sprayed zinc	Marine	1	1	Excellent	7 to 12
Arc-sprayed zinc	Deicing	1	8	Not determined[2]	10 to 15
Titanium mesh	Deicing	3	6 to 12	Excellent	>25
Titanium mesh	Marine	1	1	Excellent	>25
Titanium ribbon	Deicing	1	9	Excellent	15 to 25
Arc-sprayed titanium	Semi-marine & deicing	1	1	Poor[1]	Not determined[3]
Arc-sprayed titanium	Marine	1	1	Poor	Failed in 1 year
Conductive paint	Deicing	2	4 to 9	Good	5 to 10
Conductive polymer slotted	Deicing	1	12	Fair	5 to 10
Conductive polymer mounded	Deicing	1	15	Poor	5 to 10
Coke breeze	Deicing	3	5 to 9	Excellent	10 to 15
Galvanic Cathodic Protection Systems					
Arc-sprayed zinc	Marine	3		Excellent	7 to 10
Zinc foil with adhesive	Deicing	1	1	Excellent	7 to 10
Expanded zinc mesh & bulk	Marine	1	3	Good	15 to 20

Research conducted by the Albany Research Center for ODOT compared the TS-Zn anode with other conductive coating anodes and concluded that the TS-Zn was preferred in terms of application cost, performance and service life *(Covino et al. 2002)*, as shown in Table 2.2.

Table 2.2: Comparison of TS-Zn anode with other conductive coating anodes *(Covino et al. 2002)*.

Property	TS Zn [1]	Co-catalyzed TS Ti	Solvent-based acrylic C paint
Anode reactant	Zn	H_2O	C, Cl, H_2O
Consumable anode	yes	no	partly
Sensitive to moisture content of concrete	very	moderate	moderate
Fifteen year bond strength, MPa (psi)	1.2-1.6 (130-170)	0.26-0.35 (38-50)	0.39-0.62 (57-90)
Fifteen year anode-concrete interfacial pH	6.5-8	5.7-7.7	5.4-7.8
Circuit resistance, ohm-m^2	200→5,000 to 35,000	~600	~1000
Cost of CP installation including environmental enclosure, but not including concrete repairs, 1997 $US per m^2	$184.70- $114.70	$104.84	$218.40 ($37.70 based on parking garages)
Service life, years	~27	23 ++	15 ++

It should be noted that there are NACE standard test methods for evaluating anodes used for CP systems such as the NACE Standard TM0190-2006 (Impressed Current Laboratory Testing of Aluminum Alloy Anodes) and the NACE Standard TM0294-2007 (Testing of Embeddable Impressed Current Anodes for Use in Cathodic Protection of Atmospherically Exposed Steel-Reinforced Concrete). The former method determines the potential and current capacity characteristics of anodes, whereas the latter involves accelerated life testing of anodes.

2.5 THERMALLY SPRAYED ZINC ANODE INSTALLATION AND REPLACEMENT

2.5.1 Concrete Surface Preparation

For aging concrete structures, an on-site evaluation is needed to assess corrosion status and the possibility of using CP as a rehabilitation technique *(Harriott et al. 1993)*. This evaluation includes visual inspection, delamination survey, concrete cover evaluation, half-cell potential mapping, and total chloride content determination. Provided that corrosion of the steel reinforcement has not impaired structural integrity, all delaminated areas need to be repaired before anodes are installed because protection current cannot pass through an air gap. Removal of delaminated areas should be sufficiently below the top reinforcing steel so that it can be encapsulated within new concrete, which should have a similar resistivity to that of the parent concrete to guarantee a uniform current distribution.

Some of the ODOT TS-Zn anodes are nearing the end of their design lives, while others are beginning to separate from the concrete prematurely possibly due to erratic current controllers or initial contractor inexperience during installation. When the natural rate of corrosion resumes, the unprotected sections are on the path to concrete spalling and steel section loss. Aged TS-Zn anodes that have a poor bond with concrete can be easily removed by scraping or sand blasting, while those with a strong bond require sand blasting. If TS-Zn anodes are still operating with a sufficient Zn thickness, then the surface oxides and debris can be removed, the surface metalized, and the bond strength checked.

The NACE No. 6/SSPC-SP 13 includes preparation procedures of concrete surfaces, inspection procedures and acceptance criteria prior to the application of protective coating or lining systems. Removal of surface contaminants (including loose zinc anode and its byproducts) allows the new anode material to have direct contact with the substrate, increasing the surface area and roughness of the surface and providing increased anchorage of the applied material.

Surface preparation is a critical factor in the performance of coatings and repair materials applied to concrete. The various methods used to remove existing thermally sprayed zinc anodes and to prepare the concrete surface for the new anode application should minimize damaging the concrete surface. Concrete damage characterized by various degrees of micro-cracks and fractures will affect the bonding of the new anode to the concrete substrate. Factors that influence the depth of blast and the resulting surface profile include quality of concrete; hardness of the concrete surface; condition of the old anode; type, hardness, size, shape, and amount of the abrasive; speed of the machine; air pressure; standoff distance, etc.

For conductive coating anodes, a surface profile with appropriate anchor pattern, minimum moisture content, minimum bond-inhibiting substances such as dust and oils, and adequate bond strength to the concrete substrate are the key to achieving desired performance of the CP system and long service life of the new anode. Profile is important because an irregular surface allows the coating to grip and affects the bond strength of the new anode to the concrete. The profile is also expected to affect the evolution of the anode–concrete interfacial chemistry over the duration of electrochemical aging. It should be noted that too deep a profile may expose too much aggregates, which can weaken the coating adhesion and increase the electrical resistance of the anode–concrete interface.

In the case of thermal spray (TS) coatings, "a high degree of surface preparation is essential," which can "only be achieved by abrasive blasting with a good quality, properly sized angular blast media" *(USACE 1999b)*. Abrasive blasting typically uses compressed air to propel a high-speed stream of solid media (e.g., sand, steel shot, aluminum oxide grit, plastic beads) from a nozzle in order to remove surface layers of concrete. The selection of an abrasive should consider hazards associated with its use. Sufficient blasting must be done to get a desired surface condition, but it shall not be so excessive as to expose aggregates on which thermally sprayed Zn tends to have poor bonding ability.

According to the ACI Committee 364, "replacing the commonly used sand in abrasive blasting with alternative materials such as sintered slag, flint silicon carbide, or aluminum oxide can reduce damage" *(American Concrete Institute 2006)*. It also suggests that "where the more damaging methods must be used to increase production or reduce costs, the damage can be

mitigated somewhat by abrasive shot- or water-blasting as a final preparation step for the final 0.10 in." In addition, the use of abrasive blasting or shotblasting to remove the existing zinc anodes will produce zinc-contaminated materials. A potentially cost-effective alternative to disposing of the spent blasting materials and concrete waste is to recycle them in an environmentally sound application, such as non-structural mortar or concrete *(Webster and Loehr 1996; Salt et al. 1995)*. The use of chemical strippers or high-pressure water blasting to remove the old coating is not desirable as they will generate liquid waste that is hard to collect, dispose of, or recycle.

2.5.2 Anode Installation and Replacement

Thermal spray is a process in which molten metals or alloys are spread onto the target surface to form uniform protective coatings. The technique can be dated back to early 1900s when metal particles were melted by an oxygen-acetylene flame and then propelled by compressed air. On metallic substrates, adhesion strength ranged from 3000 psi to 5000 psi and porosity was as high as 10%. The arc-spray method shares a similarity to the flame spray technique, but features its own advantages in that arc-sprayed coatings possess superior adhesion strength and lower porosity to maximize corrosion resistance.

For the ODOT concrete structures, according to McGill and Shike *(1997)*, "the arc-spray process was selected as it provided a coating that could be easily applied to the complex shapes found on substructure surfaces. The gray color of zinc has the advantage of appearing very much like concrete—another important feature for historic bridges. Also, the low electrical resistivity of zinc allows uniform distribution of cathodic protection current, and the zinc system minimizes the dead load added to the structure, which is an important feature for older coastal bridges."

Spray factors that affect the bond strength include current control from the equipment, spray distance from the concrete, angle of spray incidence, etc. ODOT implemented stringent surface preparation and initial adhesion strength requirements, including brushing and blowing down the concrete surface to remove dust, having the concrete surface at 70°F (21°C) or higher to keep it dry, and applying supplemental surface heating immediately prior to zinc application to bring the concrete surface temperature to about $120^{\circ}C$, all of which add to the cost of the ICCP system installation *(Whitney et al. 2003)*. Recent ODOT studies have shown that preheating is of no practical value. Brousseau et al. *(1993)* performed some earlier research on TS-Zn bond strength, which revealed that in order to achieve good TS-Zn bond strength, it is desirable to have concrete with good surface cohesion strength, minimal moisture content, and higher surface temperature; to use harder and denser grit material and a lower air pressure for abrasive blasting; to avoid the exposure of too much aggregate phase; to have a thinner coating per pass during arc-spray operations; and to have a thinner overall Zn coating layer (less than 20 mils, 12 mils recommended by ODOT). While the adhesion of metalized zinc on concrete does not appear to be influenced by severe freeze–thaw cycling, the loss of adhesion was observed with high current densities and long polarization times, likely due to the oxidation of "anchors" that usually provide the mechanical bonding *(Brousseau et al. 1996a)*. The adhesion of zinc on a concrete surface was found to be mainly governed by the mechanical interaction of molten zinc droplets with the surface; the root mean square (RMS) roughness obtained from a depth profile was the main parameter that can be related to the TS-Zn bond strength *(Legoux and Dallaire*

1995). For the Single Wire Arc Plasma process, a short standoff distance (7 cm) was found to be most preferred for spraying large structures as it led to a reasonably high deposition efficiency (> 60%) and adequate bond strength (>2.07 MPa) *(Berndt et al. 1995)*. After spraying, moist-cured polyurethane can be applied to the surface of anode coatings as a protective topcoat *(Cramer et al. 1999; Cramer et al. 2002)*. Upon completion of anode installation, the ICCP system needs to be powered with a temporary rectifier for a preliminary evaluation.

For ICCP systems, short circuits between anodes and rebar are most commonly encountered during anode installation, and therefore systematic testing should be performed *(Stratfull 1974)*. Systems should also consider interaction with surroundings. For example, rectifier cards on a bridge CP system in Virginia failed within weeks of installation *(Sharp and Brown 2007)*. Although the reason was not clear, interference between the rectifiers and nearby electrical systems was suspected. Cramer and Anderson *(2009)* investigated the cause of anode delamination in ICCP regions on the arches and south approach sections of the Yaquina Bay Bridge, where the thermally sprayed Zn anodes were installed in 1994 and 1997, respectively. Using microanalysis techniques such as scanning electron microscopy, energy-dispersive X-ray analysis, image analysis and X-ray diffraction, anode bond failures were not attributed to the original coating configuration. Despite having been operated with the same current density, Zn anodes were consumed at much higher rates in some regions. Recommendations were therefore given on reduced anode current density, improved zone configurations for better current density distribution, and current interruption during drought seasons.

2.6   CATHODIC PROTECTION MODELING

CP design should address amounts and arrangement of sacrificial or impressed current anodes for concrete structures to be protected. From modeling aspects, concrete can be treated as an external domain within which rebar and anodes are embedded as internal regions. All the operational zones are linked by suitable boundary conditions that interplay between current density and local potential. Due to complex geometries of concrete structures and non-linear boundary conditions, the finite element method (FEM) and boundary element method (BEM) are anticipated to be effective numerical techniques for CP modeling. For an improved computational efficiency, CP models can be solved using a hybrid method where FEM and BEM are employed for external and internal zones, respectively. To describe the evolution of a system mathematically, it is necessary that all the underlying principles be understood to the extent that the governing equations are well established to guarantee a unique solution. The quality of simulation results depends on the degree of accuracy to which each individual process has been modeled, depth of physical insights, and reliability of model parameters.

2.6.1 The Concrete Domain

The spatial and temporal evolution of concentrations and potential within concrete requires a solution of coupled partial differential equations expressed in the conserved form by Eqn. (2-2) *(Song and Sridhar 2008; Toumi et al. 2007)*:

$$(1-p)\frac{\partial C_{mb}}{\partial t} + p\frac{\partial C_{mf}}{\partial t} + \nabla \cdot (\vec{J}_m) = R_m \qquad (2\text{-}2)$$

where C_{mb} and C_{mf} are the bound and free concentrations for species m, respectively; t is time; p is porosity; R_m is the source rate at which species m is created or annihilated; $\vec{J}_m$ is the flux of the species m expressed by Eqn. (2-3) *(Wrobel and Miltiadou 2004)*:

$$\vec{J}_m = -D_m \nabla C_{mf} - \frac{z_m F C_{mf} D_m}{RT} \nabla \phi \qquad (2\text{-}3)$$

where z_m and D_m are the charge and diffusion coefficient for species m, respectively; ϕ is the electric potential.

The CP model for concrete must account for the current flow, which, in the absence of capillary force, can be expressed in terms of ionic fluxes *(Sun and Liu 2000)*:

$$i = F\sum_m z_m D_m \nabla C_m - F^2 \sum_m \frac{z_m^2 C_m D_m}{RT} \nabla \phi \qquad (2\text{-}4)$$

where i is the current density vector; F is Faraday constant; the summation is taken over all the species present in the concrete electrolyte. ϕ is defined relative to rebar and has an inverse sign against the potential relative to a reference electrode, such as saturated calomel electrode.

If the conductivity of the electrolyte can be defined by:

$$k = F^2 \sum_m \frac{z_m^2 C_m D_m}{RT} \qquad (2\text{-}5)$$

Substituting Eqn. (2-5) into Eqn. (2-4) leads to:

$$i = F\sum_m z_m D_m \nabla C_m - k\nabla \phi \qquad (2\text{-}6)$$

The first term corresponds to the current density contributed by concentration gradients, which can be neglected in large-scale problems since concentration gradients only exist in the thin diffusion layers *(Amaya 2005)*. Such concentration information can be incorporated in polarization curves that are generally used as boundary conditions. For simplicity, the current density in the concrete electrolyte can be given by:

$$i = -k\nabla \phi \qquad (2\text{-}7)$$

Assuming no accumulation or loss of ions in the concrete electrolyte, conservation of electrons reads *(Martinez and Stern 2000)*:

$$\nabla \cdot i = -\nabla \cdot (k\nabla \phi) = 0 \qquad (2\text{-}8)$$

2.6.2 The Rebar Domain

In some cases, the potential of steel framework can be assumed to be uniform. However, the potential drop in rebar can be significant when rebar is long or the current level is high, which entails accurate numerical solution for current and potential distribution. The current flow within rebar is strictly governed by the Laplace equation (Rabiot et al. 1999):

$$\nabla \cdot (k'\nabla V) = 0 \qquad (2\text{-}9)$$

where V is rebar potential; k' is rebar conductivity.

2.6.3 Boundary Conditions

The surface potentials of sacrificial anodes can be treated as constants over a wide current density range. However, the large current drain in impressed current anodes can cause significant potential variation across anodes, which must be taken into account in practice. The boundary conditions include the Neumann boundary condition on which the current density is defined, and the Dirichlet boundary on which the potential value is imposed. Current density and potential are not independent, and their relation manifests the interaction between electrodes and surroundings. Such information can be obtained from polarization curves through experiments.

The mathematical forms of various boundary conditions can be expressed as below:

$$i = i_0 \qquad (2\text{-}10)$$

$$\phi = \phi_0 \qquad (2\text{-}11)$$

$$\phi = f_A(i) \qquad (2\text{-}12)$$

$$\phi = f_C(i) \qquad (2\text{-}13)$$

where i_0 and ϕ_0 are the predefined values for current density and potential, respectively; $f_A(i)$ and $f_C(i)$ stand for the nonlinear polarization curves for anodes and cathodes, respectively.

The current density boundary condition is defined by:

$$i \cdot (-n) = k \frac{\partial \phi}{\partial n} \qquad (2\text{-}14)$$

where n is outward normal vector; $\partial / \partial n$ is the outward normal derivative. i is thus positive when the current flows into the domain of interest across the boundary.

When the boundary is insulated, the current flux is equal to zero:

$$\frac{\partial \phi}{\partial n} = 0 \tag{2-15}$$

2.6.3.1   Bare Steel Cathode

Based on the electrochemical reactions and the Butler–Volmer kinetics, boundary conditions on steel cathodes can be established to represent actual polarization behaviors. Three principal reactions, including iron oxidation, oxygen evolution and hydrogen evolution, are frequently assumed to prevail at the steel–concrete interface, but proceed at different rates in active and passive regions. Reverse reactions involved on electrodes are trivial in practical problems.

1) Metal Oxidation *(Riemer and Orazem 2005):*

$$\text{Fe} \rightarrow \text{Fe}^{2+} + 2\text{e}^- \tag{2-16}$$

$$i_a = i_{0a} e^{(E_{0a} - \phi_s)/\beta_a} \tag{2-17}$$

where i_a is the partial current density due to iron dissolution; i_{0a} is the exchange current density; E_{0a} is the equilibrium potential; ϕ_s is the potential at a point in the electrolyte adjacent to the metal surface; β_a is the anodic Tafel slope.

2) Oxygen Reduction *(Yan et al. 1992):*

$$\text{O}_2 + 2\text{H}_2\text{O} + 4\text{e}^- \rightarrow 4\text{OH}^- \tag{2-18}$$

$$i_c = i_{0c} \frac{C_O}{C_O^*} e^{(\phi_s - E_{0c})/\beta_c} \tag{2-19}$$

where i_c is the partial current density due to oxygen reduction; i_{0c} is the exchange current density; E_{0C} is the equilibrium potential; C_O and C_O^* are the in-site and equilibrium oxygen concentration, respectively; β_c is the cathodic Tafel slope.

3) Hydrogen Evolution *(Riemer and Orazem 2005):*

$$2\text{H}_2\text{O} + 2\text{e}^- \rightarrow \text{H}_2 + 2\text{OH}^- \tag{2-20}$$

$$i_h = i_{0h} e^{(\phi_s - E_{0h})/\beta_h}$$

(2-21)

where i_h is the partial current density due to hydrogen formation; i_{0h} is the exchange current density; E_{0h} is the equilibrium potential; β_h is the Tafel slop for hydrogen formation.

The total current density on steel cathodes is thus the summation of the above three partial current densities, which takes the following form *(Yan et al. 1992)*:

$$i = i_{0a} e^{(E_{0a} - \phi_s)/\beta_a} - i_{0c} \frac{C_O}{C_O^*} e^{(\phi_s - E_{0c})/\beta_c} - i_{0h} e^{(\phi_s - E_{0h})/\beta_h}$$

(2-22)

2.6.3.2   Coated Steel Cathode

For CP systems in which bare steel can be characterized by polarization curves, the above formulation is sufficient to describe dynamic response between current density and potential on cathodes under consideration. However, some regions of cathode surfaces are occupied by insulators or less conductive products, such as paints and scales, which diminish effective areas for charge transfer and impose challenges in related mathematical treatment. For coating, a small current can flow across such layers once the pores are filled with a sufficient amount of water. Scale formation is a dynamic process that depends on local current density and the related polarization peculiar to that location. At a specific time step, if the polarization curve is known, the current density can then be estimated. Scale formation is then prone to this new current density, which further modifies the polarization curve. The boundary condition that features its own polarization characteristics is therefore time-dependent and spatially evolving.

When anodes are covered by insulating coatings with pores through which ionic species can travel, the effective electrical resistivity of such coatings will depend on the number and configuration of pores per unit area. The current density can be related with the potential drop and effective resistivity as follows *(Orazem et al. 1997)*:

$$i = \frac{\Phi - \Phi_{in}}{\rho \delta}$$

(2-23)

where Φ is the potential at the coating–electrolyte interface; Φ_{in} is potential at the coating–steel interface; ρ is the coating effective resistivity; δ is the coating thickness. In combination with Eqn. (2-23), the current density can also be expressed as *(Orazem et al. 1997)*:

$$i = \frac{A_{pore}}{A} [i_{0a} e^{(E_{0a} - \phi_s)/\beta_a} - i_{0c} \frac{C_O}{C_O^*} e^{(\phi_s - E_{0c})/\beta_c} - i_{0h} e^{(\phi_s - E_{0h})/\beta_h}]$$

(2-24)

where A_{pore}/A is the effective surface fraction available for electrochemical reactions. Eliminating the current density in Eqns. (2-23) and (2-24) leads to *(Riemer and Orazem 2005)*:

$$\frac{A(\Phi - \Phi_{in})}{A_{pore}\rho\delta} = \left[i_{0a}e^{(E_{0a}-\phi_s)/\beta_a} - i_{0c}\frac{C_O}{C_O^*}e^{(\phi_s-E_{0c})/\beta_c} - i_{0h}e^{(\phi_s-E_{0h})/\beta_h} \right] \qquad \textbf{(2-25)}$$

In a numeric step, Φ_{in} can be evaluated from Eqn. 25 with given values of ϕ_s and Φ, which can then be employed to update the current density with Eqn. 24 in a subsequent step.

2.6.3.3   *Galvanic Anode*

Anode materials are more anodic than rebar cathodes so as to provide electrons by self-consumption. Provided that anode consumption is rate-limited by oxygen supply, the anode boundary condition in accordance with oxygen consumption can be given by *(Riemer and Orazem 2005)*:

$$\frac{i}{4F} = D_{O_2}\frac{\partial C_{O_2}}{\partial n} \qquad \textbf{(2-26)}$$

where the factor 4 arises from the number of electrons in the reduction reaction with one mole of O_2, i.e. $O_2 + 2H_2O + 4e \rightarrow 4OH$. Presuel *et al. (2002b)* constructed one-dimensional and three-dimensional models to predict galvanic cathodic prevention with sacrificial Zn anodes on partially submerged piles, where the oxygen flow is described with Eqn. (2-26). The results obtained from computational studies were in reasonable agreement with experimental observations. Such computational practices demonstrate that even with conservative assumptions, the predictions can shed light on cathodic prevention on field-scale structures, with a final target of field applications. In addition, cathodic prevention can be more effective at higher elevations with a favorable combination of system dimensions and electrochemical properties.

According to Riemer and Orazem *(2005)*, with hydrogen evolution neglected and anode reaction balanced by oxygen diffusion, the total current density on anodes can be represented as:

$$i = i_0 \exp(\frac{\alpha_M F}{RT}(V - \Phi - E_M)) - i_{O_2} \qquad \textbf{(2-27)}$$

where i_0 is the exchange current density for oxidation; α_M is a transfer coefficient; E_M is the equilibrium potential for oxidation; V is anode potential; Φ is the electrolyte potential near the anode; i_{O_2} is the oxygen diffusion-controlled current density. Hydrogen evolution on galvanic anodes is negligible by virtue of its small fraction in the net

current. Eqn. (2-27) can be further modified with corrosion potential as *(Riemer and Orazem 2005)*:

$$i = i_{O_2}(10^{(V-\Phi-E_{corr})/\beta_{anode}} - 1)$$

(2-28)

where β_{anode} is the Tafel slope for anode oxidation. Kranc et al. *(1997)* modeled corrosion distribution in reinforced concrete to predict the efficiency of CP on partially submerged piles with a zinc sacrificial anode below water and surface anodes above water. The concrete was treated with variable electric resistivity and oxygen diffusivity. Boundary conditions at the reinforcing steel were based on the electrochemical reactions, which is characterized by Butler–Volmer kinetics. Local variations of oxygen concentration, potentials and currents in concrete were thus predicted, which were in agreement with experimental investigations in a CP study with both surface anodes and bulk anodes.

2.6.3.4   *Impressed Current Anode*

ICCP anodes and rebar cathodes are connected to the positive and negative terminals of rectifiers, respectively. Rectifier output can be adjusted so as to shift cathode potential sufficiently. Consequently, ICCP protective current is usually one order of magnitude larger than that from galvanic anodes, and can therefore protect larger areas with greater effect in highly resistive concrete. Water oxidation dominates at ICCP anodes. Thus the polarization behavior resembles that of galvanic anodes, except that the potential contribution from rectifiers should be taken into account, which leads to *(Riemer and Orazem 2005)*:

$$i = i_{O_2}(10^{(V-\Phi-\Delta V_{rect}-E_{O2})/\beta_{O2}} - 1)$$

(2-29)

where ΔV_{rect} is the potential contribution from rectifiers; E_{O_2} and β_{O_2} are the equilibrium potential and the Tafel slope for the water oxidation, respectively. If chloride ions are present near anodes, Eqn. (2-29) must be modified in accordance to the contribution from chloride evolution.

2.7   RECENT DEVELOPMENTS IN CP TECHNOLOGIES

Technological advances accompany new developments in materials and equipment, providing enhanced CP performance. Although incorporating new technologies into systems incurs additional cost, such expense can be offset by long-term savings such as reduced routine maintenance.

2.7.1 Solar Power

ICCP systems require a sufficient power supply for corrosion mitigation. For concrete structures in remote and difficult-to-access locations, power must be supplied by autonomous systems. For remote and hilly areas where external current is not available, solar-powered systems can be

used to polarize CP systems during the day and recharge storage batteries to provide current at night and for cloudy occasions *(Mishra et al. 2000)*. Kessler et al. *(1998a)* evaluated an intermittent ICCP technique using photovoltaic energy on bridge concrete piles where polarization and depolarization of rebar as well as the protection current were monitored. With solar power and mortar samples exposed to tap water, Bin Ismail and Bin Yusoff *(2002)* applied intermittent CP to investigate whether cathodic protection can be achieved with intermittent solar power supplied during the day. Measurements were performed during power interrupt to impede depolarization of the reinforcement. Although the protective current was only imposed during the day, laboratory experiments provided direct evidence that intermittent solar-powered CP can be effectively applied to concrete structures. Glass et al. *(2001)* demonstrated that an integrated protection current of 6 mA/cm^2 induced the passivation of steel exhibiting an initial corrosion rate of 60 mA/cm^2 and the protective effects were mainly attributed to the changes in the environment at the cathode, instead of the negative potential shift, in the case of an intermittent current applied to reinforced concrete.

2.7.2 Galvanic Batteries

Galvanic batteries are another type of power supply for ICCP system, which makes cathodic protection of finite systems in remote locations possible by saving the high cost of providing AC power source. In addition, the cost on wiring required for operation can be eliminated. When needed, several batteries can be combined to accommodate higher current requirements. Kessler et al. *(2000)* applied galvanic batteries on bridge pilings, which consist of zinc anodes, aerated cathodes and gel electrodes housed in cast black polyvinyl chloride. Those batteries can provide an initial current of 100 mA for 30 to 60 days and a subsequent steady-state current of 30 mA for about five years. Field tests were conducted on three bridges, two of which featured Ti mesh pile jacket systems and the rest of which possessed a conductive rubber anode system. The installed batteries functioned properly for about two and a half years.

2.7.3 New Galvanic Anodes

Development of new Zn sacrificial anodes is the major achievement for bridge components in the past 10 years. Ideal sacrificial anodes are capable of providing sufficient current, require no specialized installation knowledge and demand minimum maintenance service. Pianca and Schell *(2004)* evaluated three types of new Zn sacrificial anode for bridge deck applications. The first anode system, Galvashield mesh anode, was characterized by a zinc mesh top capped with a glass fiber mesh. To ensure good contact between anodes and the concrete surface, a cementitious backfill containing lithium hydroxide was used. The glass fiber mesh provided not only mechanical strength but also shrinkage resistance for the cementitious backfill. The second anode system, Galvostrip anode, was made of zinc chains covered by a polymer backfill with a depth of about 8 mm. The third anode system, Galvashield strip anode, featured precast strips placed at 300 mm intervals. Each strip anode had two zinc rods that were embedded in a cementitious backfill containing lithium hydroxide. To minimize shrinkage cracks in cementitious overlay and obtain a better bonding surface, a carbon fiber mesh was installed on the strips. Field trials demonstrated that such novel anodes supplied sufficient current to meet the 100 mV criterion for cathodic protection. These anode systems are applicable on structures with minimal delamination and high corrosion potentials.

2.8 CONCLUSION

Cathodic protection is a proven technique that can effectively mitigate rebar corrosion in concrete, thereby extending the service life of reinforced concrete structures exposed to marine environment and deicing applications. Technological advances have made CP more attractive by providing new alternatives to engineers, which is manifested by improvements in new electronic equipment that facilitates the effective monitoring and control of the operational system. This review incorporates important aspects of cathodic protection on concrete structures, such as anode materials, anode performance testing, anode service life prediction, CP performance monitoring, thermally-sprayed zinc anode installation and replacement, and related numeric treatments. Such knowledge will benefit the development of best practices of selecting, installing, maintaining and replacing CP systems.

CP has become so mature that in the near future revolutionary changes may not emerge. However, continuous and incremental improvements to existing materials, equipment, and characterization techniques are anticipated. Novel conductive paint anodes may be developed that feature self-healing capability to minimize the risk of mechanical damage and thus maximize the system performance. From the industrial point of view, novel metallic anode materials less prone to the acidity derived from the electrochemical aging may be developed to meet the high-current requirement of CP systems in regions where the electrical resistivity of the concrete is high (e.g., dry-climate states). More research is also needed to enhance the electrical properties of concrete, overlay and backfill materials so as to enable a conductive circuit in dry-climate areas, which can be achieved by using novel additives like carbon fibers. While improvements of this kind are likely from the technology perspective, it is still subject to economic considerations, and user acceptance can be a barrier to implementation until the benefits and reliability of new technologies are proven or demonstrated. The development of universal monitoring and control systems is highly desirable but technically challenging.

Many existing CP systems with thermally sprayed Zn anodes will reach or exceed their design life in the near future and thus may function improperly or insufficiently, making it necessary to replace the aged anodes. In this context, there is an urgent need to research the most cost-effective method to remove existing Zn anodes and to develop a protocol for the preparation of the concrete surface for new anodes.

Fundamental research should be devoted to advancing the knowledge base needed for better CP performance and reliability, including the exploration of electrochemical aging behavior of thermally-sprayed anodes and their detachment from underlying concrete. Such a dynamic process is complex under the polarized conditions, but the results would provide a better basis for estimating anode service life and better prediction of when failing and end-of-life CP anodes should be replaced.

3.0 SURVEY OF THE CURRENT PRACTICE

On the basis of the literature review (as detailed in Chapter 2), the research team designed and distributed two online surveys to document the current practice related to CP technologies and thermal sprayed zinc and to capture the field experience of ODOT and other identified agencies/practitioners. The two surveys were published online at: https://www.surveymonkey.com/s/NSQ9C6J and https://www.surveymonkey.com/s/FM7VBRP and distributed to various professional forums and groups (including NACE Corrosion Network, Corrosion Forum, Corrosion Discussion Forum, Corrosion Engineering Forum, Materials Forum, Concrete Forum, Thermal Spray Society Forum, ODOT bridge engineers, TRB Corrosion Committee members, Corrosion Prevention Association members, and other targeted experts). The following sections present the main results from these two surveys.

3.1 SURVEY OF CP TECHNOLOGIES

Survey of Cathodic Protection Technologies — SurveyMonkey

1. Which of the following best describes the type of organization you work for?

	Response Percent	Response Count
Federal Agency	0.0%	0
State Agency	9.1%	2
City or County Agency	4.5%	1
Private Agency	36.4%	8
University and/or Research Organization	18.2%	4
Other	31.8%	7
	please specify if other Show Responses	6
	answered question	22
	skipped question	0

2. Which of the following best describes your responsibilities?

🍰 Create Chart ⬇ Download

		Response Percent	Response Count
Operations and Maintenance		13.6%	3
Production		4.5%	1
Management		22.7%	5
Consulting		**27.3%**	**6**
Research		13.6%	3
Development		0.0%	0
Other		18.2%	4
	please specify if other Show Responses		4
		answered question	22
		skipped question	0

3. Which of the followings corrosive environments are of concern to you? (check all that apply)

🍰 Create Chart ⬇ Download

		Response Percent	Response Count
Sour and alkaline solutions		36.4%	8
Salt and brackish solutions		**77.3%**	**17**
Other		22.7%	5
	please specify if other Show Responses		3
		answered question	22
		skipped question	0

4. Which of the following technologies have you used for corrosion protection? (check all that apply)

🥧 Create Chart ⬇ Download

		Response Percent	Response Count
Cathodic protection		95.5%	21
Anodic protection		4.5%	1
Coatings		68.2%	15
Inhibitors and additives		36.4%	8
Other		4.5%	1
		please specify if other Show Responses	2
		answered question	22
		skipped question	0

5. Please indicate your experience with the cathodic protection (CP) technologies.

🥧 Create Chart ⬇ Download

		Response Percent	Response Count
0 year		4.5%	1
1-2 years		18.2%	4
3-4 years		9.1%	2
5-8 years		13.6%	3
over 8 years		54.5%	12
		answered question	22
		skipped question	0

6. On what objects have you applied the cathodic protection method? (check all that apply)

 Create Chart   Download

		Response Percent	Response Count
Metals embedded in concrete		56.3%	9
Metal or alloys immersed in aqueous solutions		62.5%	10
Metal or alloys exposed in the air		12.5%	2
Pipes buried in soils		**81.3%**	**13**
Naval facility		18.8%	3
Parking structure		6.3%	1
Reinforced concrete bridge		50.0%	8
Other		18.8%	3
	please specify if other Show Responses		4
	answered question		16
	skipped question		6

7. What kind of cathodic protection technologies have you used?

 Create Chart   Download

		Response Percent	Response Count
Impressed current CP		12.5%	2
Sacrificial anode CP		12.5%	2
Both		75.0%	12
	And why? (please comment:) Hide Responses		7

3/17/09: Depending on the asset and requirements. I would use impressed for above ground & anodic for buried preferentially.

2/2/09: We are manufacturer of Titanium Mixed Metal Oxide Anodes

1/15/09: Depends on applicability and economics decision

12/10/08: Depended on the type of installation. Reinforced concrete used an impressed current CP system. Steel swings(?) in salt water used a galvanic CP system. Steel sheet piling used an impressed current anode system. Bridge deck system used a conductive polymer system - also tried metallized zinc.

12/5/08: Because it was the most cost effective solution

12/3/08: Depending the project requirements

12/3/08: Thermal spray to provide the current distribution on odd shaped structures or concrete structures not in an electrolyte.

8. What types of anode systems have you used? (check all that apply)	Create Chart ▼ Download	Response Percent	Response Count
Thermally-sprayed Zinc		62.5%	10
Coated Ti mesh		43.8%	7
Conductive coating		31.3%	5
Conductive overlay		18.8%	3
Discrete anode		68.8%	11
Other		18.8%	3
(Please specify if other). Are you satisfied with their performance? (Please share your success story and/or lessons learned) Hide Responses			5

3/17/09: As long as the system is properly set up and all the initial data is error free, then once the CP system becomes active I have found that there are usually no major concerns. CP needs to be regularly monitored by logging devices to assure protection continuity. I found that knowledge transfer and defective low-quality logging equipment usually bring problems not the actual systems.

2/2/09: We have a 20 years track record on installations with expanded mesh and ribbon mesh anodes. Our materials are successfully applied in Cathodic Protection and Cathodic Prevention for new structures worldwide.

1/15/09: Mixed metal oxide, magnesium anode

12/5/08: Generally yes. I had one major delamination of a shotcrete overlay on a MMO mesh system. I have tried thermally spayed titanium.

12/3/08: Magnesium sacrificial anodes.

	Response Count
Hide Responses	16

10/13/09: Close interval potential survey and direct current voltage gradient.

3/17/09: Recommend Borgtech's CPL2 Data Loggers and Digital Voltage Buffer (DVB) for Data Loggers reading a V not ground referenced. www.borgtech.com.au

2/9/09: Low Signature Cathodic Protection for Naval Ships and Submarines. Long life, no-maintenance/replacement for sacrificial anodes.

2/2/09: Recently we patented Stargard discrete anodes that are bumpy-shape anodes that deliver the higher current output within the boundaries of Current Density indicated by NACE Standard Practice SP0290-2007 "Impressed Current Cathodic Protection of Reinforcing Steel in Atmospherically Exposed Concrete Structures."

1/15/09: Continuous impressed current anode along the pipeline

12/11/08: Bulk Mg anodes on marine substructures

12/10/08: Have tried conductive polyester concrete, but not sure of the long-term ability for the material to bond to the deck.

12/3/08: Zinc or magnesium ribbon used in freshwater immersion, 200' or longer anodes

12/3/08: Metal oxides anodes for impressed current CP

12/3/08: Close interval potential survey and direct current voltage gradient.

10. Do you have experience with the application or removal of thermal- 🔵 Create Chart ⬇ Download
sprayed metallic coatings (e.g., zinc), or with the preparation of concrete surface for such coating application?

		Response Percent	Response Count
Yes		42.9%	6
No		57.1%	8
If not, please provide name and contact information of any other agency or individual who might have such research or user experience. Show Responses			1
		answered question	14
		skipped question	8

11. May we follow up with you through email or phone for more details? 🔵 Create Chart ⬇ Download

		Response Percent	Response Count
Yes, email me		71.4%	10
Yes, phone me		7.1%	1
No		21.4%	3
	answered question		14
	skipped question		8

12. (The following information will be kept confidential) ⬇ Download

		Response Percent	Response Count
Name: Show Responses		100.0%	14
Company: Show Responses		100.0%	14
Address: Show Responses		100.0%	14
Address 2: Show Responses		50.0%	7
City/Town: Show Responses		85.7%	12
State: Show Responses		42.9%	6
ZIP/Postal Code: Show Responses		92.9%	13
Country: Show Responses		92.9%	13
Email Address: Show Responses		100.0%	14
Phone Number: Show Responses		85.7%	12
	answered question		14
	skipped question		8

Some countries from where responses were obtained (with the specific response date in each bracket): Egypt (10/13/09), Austria (3/17/09), UK (2/9/09), Italy (2/2/09), USA (1/15/09), USA

(12/11/08), USA (12/10/08), UK (12/5/08), Kuwait (12/3/08), USA (12/3/08), Mexico (12/3/08), Egypt (12/3/08).

3.2 ADVANCED SURVEY OF THERMAL-SPRAYED ANODE CP TECHNOLOGY

1. Zinc and other alloys can be thermally sprayed onto concrete to act as the anode for a cathodic protection (CP) system. Do you have research or user experience with the preparation of concrete surface for such coating application? ⓒ Create Chart ⬇ Download	Response Percent	Response Count
Yes	38.2%	21
No	61.8%	34
If no, skip the next two questions and press Next. If yes, please describe what type of anode you used and how was the performance: Hide Responses		7

12/29/08: 99.9% zinc applied to grit-blasted concrete surface or to pressure washed concrete surface.

12/24/08: Work with the Florida Department of Transportation and we use thermally applied zinc on concrete structures.

12/19/08: Our company was a pioneer in this type of application. We have completed over one million square feet of thermal spray applications using a variety of metal compositions both on concrete and steel structures. We typically use a very pure zinc (low iron) for concrete applications and have very good success. In drier applications, we may use *Corrspray*® or *Asset Guard*® which is an alloy consisting of Al/Zn/In. This type of alloy is more active and can facilitate effective corrosion control in drier regions such as the underside of bridge decks, beams and girders. We also have used aluminum alloys, which are typically used on steel structures, pipelines and other metal substrates. All of these had great success and provided effective cathodic protection/corrosion control for 10-15 years.

12/18/08: Worked on behalf of client for *Asset Guard*® application. System less than 6 months old, but looks ok so far.

12/18/08: We used an Aluminum-Zinc-Indium arc-sprayed galvanic system on a demonstration project on two bridges on the superstructure and substructure reinforced concrete. The contractor patched various areas with a rapid set concrete patching material and then applied a curing compound as suggested by the patch material supplier. The contractor brush blasted the surface and then applied the anode. The first time all the anode either wouldn't bond or bonded and flaked off within 24 hrs. The contractor sand blasted these off and still had similar problems. Finally, he grit blasted (with *Black Beauty*®, ground slag, aggregate) and the Al-Zn-In stuck to the concrete surface.

12/10/08: We have worked with the Oregon, Washington & Alaska DOT's on several cathodic protection projects, including zinc, a zinc-aluminum-indium alloy, and titanium. We have also applied 3M's zinc hydrogel product, but that is adhesive and not thermally sprayed. The 99% pure zinc is by far the most effective anode that we have used, and it has proven to have excellent performance in preventing future corrosion of the rebar if the CP system is monitored adequately. Our experience with the other anodes was on an experimental basis, and none proved to be as cost effective or useful as the pure zinc.

12/9/08: Zinc works good. Titanium works good. Aluminum-Zinc-Indium never worked.

2. The bond strength between the anode and the concrete may affect the service life of ⬇ Download the anode as well as the CP system. Based on your experience or knowledge, what are the key factors during the steps of preparing the concrete surface that lead to good or poor anode/concrete bonding?	
	Response Count
Show Responses	16
answered question	16
skipped question	39

3/9/09: Proper pH, moisture content and chloride levels.

1/23/09: Key factors include: proper profile of concrete surface, substrate temperature and moisture content, any bond inhibiting substances such as dust on the concrete surface. Aggressive preparation of the surface can lead to exposure of the aggregate which can also affect bond strength. Also, thickness of the applied anode has shown to affect the bond strength, areas where the anode has been sprayed on too thick tend to debond easily.

12/29/08: Preparation technique - excessive grit-blasting causes excessive dust and laitance that inhibits bond. Pressure washing avoids dust and provides better bond development.

12/23/08: 1) Remove any oil, debris, or any curing compound left on the surface of the concrete; 2) Level of blasting should be just enough to remove the above; 3) Air blast and dust residue from surface prior to application.

12/19/08: Clean concrete surface.

12/19/08: Surface preparation is key to facilitating a good bond, but there are also other control factors that contribute to bond strength such as current control on the metalizing equipment, distance from the object to be metallized, angle of incidence for applying the metalizing, etc. Any residual grease, marine growth, surface prep grit, moisture, etc. all can affect bond strength.

12/19/08: Proper and adequate surface prep before spraying... removal of loose material, spraying onto a dry substrate.

12/18/08: The usual - cleanliness and moisture.

12/18/08: Don't use any curing compounds on patches, wet cure if possible. A good grit blasting and blowing-off of laitance on the surface is needed. This left a somewhat porous rough surface to which the arc-sprayed anode stuck very well.

12/18/08: We use AWS C2.20/C2.20M:2000. (Note by the authors: The American Welding Society Standard C2-20-C2-20M-2002: THERMAL SPRAYING ZINC ANODES ON STEEL REINFORCED CONCRETE, which explains metalized zinc CP systems for corrosion protection of concrete structures with steel reinforcing and includes information on job safety, pass/fail reference standards, feedstock materials, needed equipment, and instructions for surface preparation, thermal spraying, and quality control).

12/10/08: The concrete surface must be properly prepared by sand blasting. The blast must be hard enough to remove any paint, chalk, efflorescence, slurry coat, or other contaminants, but must not be hard enough to expose excessive aggregate as thermally sprayed zinc will not bond well to rocks. After the blast is performed, it is important to keep hands and other body parts off the surface so as not to re-contaminate as the oils from skin can negatively affect bond strength. Additionally, after zincing one pass area, it is important to blow down the surface of the next area to be sprayed to remove any zinc dust prior to applying the thermally sprayed zinc there.

12/9/08: A good bond requires the surface to be clean and dry, free from all contaminates such as dust and oils. Any contamination will cause the anode-concrete bond to be poor. A good bond also requires the concrete surface to have a good profile for the anode to "grab" onto.

3. How did you ensure the quality of the prepared concrete surface for anode application? What tools or methods did you use to measure such quality?	⬇ Download
	Response Count
Show Responses	16
answered question	16
skipped question	39

3/9/09: Full time inspection of contractor work. Verify/measure moisture content, surface profile and level of contaminants.

1/23/09: Zinc is applied as soon as possible after surface prep to limit possibilities of surface contaminants. Surface is inspected for profile and moisture content, surface is blown clean with air immediately prior to application, heat is applied if drying or temperature increase is required. Bond strength of anode to the substrate is tested with a pull tester on regular intervals to confirm quality of application. Thickness of the anode applied to the concrete is tested on regular intervals by means of tape tests and a micrometer.

12/29/08: Pull-off tests - ASTM D4541 - testing performed by independent CP specialist.

12/24/08: 1) Understanding that not all concretes require the same level of blast cleaning, for each bridge, we metalize test windows prior to commencing production metalizing. The test areas are metalized with different levels of blasting and a target bond is established for the project. 2) Metalizer is responsible for achieving that min target bond for the final product to be accepted.

12/19/08: Not yet, but on my opinion - sand blasting.

12/19/08: Utilized proper control and QC with equipment and proper training of personnel applying the coating.

12/19/08: The term "Quality" is utterly meaningless... there is no such material property. This needs to be evaluated in terms of properties which can be measured - density/porosity, adhesion strength, level of oxidation, coating thickness and so on.

12/18/08: Contractor's responsibility, insurance backed warranty means they come out and fix it if it fails.

12/18/08: We had no specifications requiring any tests. A rough porous appearing surface would be a good visual test. A good laser surface texture meter could be specified or sand patch test as used on pavement, if a horizontal surface is available. (A researcher at Missouri S&T developed a laser texture meter that worked well for testing texture to apply Fiber Reinforced Polymer-FRP to concrete. His contact information is Dr. Norman Maers - norbert@mst.edu). A pull-off test of the anode after applied would also seem a logical step, however I don't know what a good number would be (150-200 psi?).

12/17/08: All areas to receive cathodic protection including repairs shall be prepared by grit blasting to achieve a suitable surface profile CSP number (International Concrete Repair Institute Guideline 037320). Removal of all contaminants, old coatings, curing membranes, surface laitance, loosely adherent object detrimental to cathodic performance, is required to achieve a sound, clean, dust free surface and to provide a suitable base for a good physical bond for the thermal sprayed metal to be used. Where wet grit blasting is used or the concrete surface is washed down after abrasive blasting, the surface shall be protected from the weather and sufficient time shall be allowed for the concrete surface to dry out before the application of the thermal sprayed metal. After metalizing the Contractor shall perform pull-off adhesion test at a minimum of four locations for each zone on each structure to demonstrate compliance with the minimum adhesion values.

12/10/08: We use clean, dry, oil-free air through an appropriate sized blast nozzle, had extensive class-room and on-hands training for all personnel involved in quality critical processes, including preparing the surface. After spraying of the zinc, "pucks" or "dollies" were glued onto the zinc surface and were pull tested using a Proceq unit to ensure that we were achieving adequate bond strength.

12/9/08: The concrete surface was blasted clean and then visually inspected to ensure a good surface profile.

4. When the thermally sprayed coating system is out of service, there is a necessity to replace the old and damaged coating with new ones. Do you have research or user experience with the removal of thermal-sprayed zinc anode or other metallic coatings?		Response Percent	Response Count
Yes		22.2%	10
No		77.8%	35
If no, skip the next two questions and press Next. If yes, please describe the intended application and how the old materials are removed and how the surface condition can be improved to accommodate the new coatings. Show Responses			7
		answered question	45
		skipped question	10

12/24/08: Normally the residual zinc and zinc products are removed with a brush blast.

12/19/08: Surface preparation is key and must be performed to a proper QC plan.

12/10/08: We have worked with the Oregon DOT on 4 bridges to perform surveys to determine if CP systems were working properly and to make repairs as necessary. The old coating was scraped off and contained. We found that most of the failed areas had a lot of loose dust build-up behind the coating, suggesting that there may have been quality control issues when the original surface was sprayed. When new coating is installed over repaired areas, depending on the size of the repair areas, small repairs could be accomplished by scraping off damaged zinc, using a needle-gun or small sand-blaster (if containment is possible), the area blown down with clean compressed air, and zinc spray touched-up to adequate millage using a portable flame-spray system. If large areas need to be replaced, a containment enclosure would most likely need to be installed to allow for sand-blasting and zinc application using the usual Thermion thermal spray system.

12/9/08: Portions of the old coating was delaminated and were removed by scraping the zinc off with putty knives.

5. How did you ensure the quality of the coating removal? What tools or methods did you use to measure such quality?	Response Count
Show Responses	7
answered question	7
skipped question	48

12/24/08: 1) We do not require 100% removal. If any good zinc is present, this is left in place and metalized over. 2) All zinc oxides and other surface debris are removed and verified by visual inspection. 3) If zinc is left behind to be metalized over, bond strength is performed (100 psi min is required).

12/19/08: This is an art and the techniques involve skills, and not procedures.

12/10/08: Coating removal was inspected visually to ensure it was all removed.

12/9/08: No measures were taken to ensure quality.

6. Based on your experience or knowledge, what are the key factors that affect the successful and efficient removal of thermal-sprayed zinc anode or other metallic coatings?	⬇ Download
	Response Count
Show Responses	8
answered question	8
skipped question	47

12/24/08: 1) Most important factor is the experience and skills of the metalizer executing surface prep. 2) Also important is the angle of the blast. This may differ by bridge.

12/19/08: Using the right equipment and hiring the right personnel.

12/19/08: Characterization.

12/10/08: Zinc that has inadequate bond is fairly easily to remove by scraping or sand blasting. Anode with a strong bond requires a complete sand blast to remove.

12/9/08: Unknown.

7. Do you have research or user experience with the application of thermal-sprayed zinc anode or other metallic coatings?		ⓒ Create Chart ⬇ Download
	Response Percent	Response Count
Yes	47.6%	20
No	52.4%	22
If no, skip the next two questions and press Next. If yes, please describe the intended application and how was the performance: Show Responses		13
answered question		42
skipped question		13

1/23/09: Applications include thermal sprayed zinc applied to reinforced concrete surface to act as an anode for both galvanic and impressed current cathodic protection system. Performance was very good.

12/24/08: Continuously use zinc metalizing to protect concrete structures. Use of this method has been very successful in FL. We have been metalizing concrete since 1989. We use the metalizing as a galvanic system.

12/18/08: Experience with depositing virtually all other metallic coatings for tribological, corrosion, electrical, and other applications by plasma spray, HVOF, and detonation gun deposition.

12/18/08: Have two bridges with Al-Zn-In galvanic anode. System only in place 3 years but appears to be providing adequate current and protection. One of the two test locations wired to test the current and electrical potential shorted out so we have limited data on this bridge.

12/17/08: I have experience by painting.

12/17/08: The first project was a demonstration project involving three different CP systems for an 80 years old carbonated concrete structure. The duration of the project was 12 months. The CP performance by the arc-sprayed zinc system was intermediate in terms of CP current density. We had to spray a humectant chemical to boost the CP performance 2-3 months after it was applied.

12/17/08: Thermal spayed zinc was applied to one face of a set of "leaf piers" (supporting walls) on a highway interchange in the north of England. The anode went on well with a few minor areas of flaking and has performed well for the past four years.

12/17/08: The application was field metalizing on steel, not concrete.

12/10/08: We have installed zinc anode and other metallic coatings as part of a cathodic protection system on over a dozen concrete bridges. As a whole, the zinc coating performance has been excellent.

12/9/08: Cathodic protection of reinforced concrete bridges. The performance is good.

8. Based on your experience or knowledge, what are the key factors that affect the successful and efficient application of thermal-sprayed zinc anode or other metallic coatings?	⬇ Download
	Response Count
Show Responses	16
answered question	16
skipped question	39

1/23/09: Surface prep and condition and training/skill/experience of applicator are key factors.

12/29/08: surface preparation, applicator training and experience.

12/24/08: 1) Use only of proper components. 2) For galvanic use, there should be sufficient humidity present to keep the zinc active. 3) Do not use too close to the water as it would deplete quickly. 4) Use a topcoat to reduce self-consumption.

12/19/08: Process selection, process parameters, metallographic characterization and analysis.

12/18/08: Surface preparation and adherence to properly developed deposition parameters.

12/18/08: A clean rough concrete surface.

12/17/08: I had no problems of bond in normal atmosphere The coating stays after more than 10 years.

12/17/08: Environment should be the first consideration. If the service climate is too dry, it will gradually decease to operate. The second factor would be concrete surface condition prior to coating application. The third factor is quality of top (seal) coat.

12/17/08: Experienced spray operative. Good surface preparation. Adequate climate control (enclosure against wind and water spray). Control of water rundown during application.

12/17/08: Surface prep, surface prep, surface prep; followed by temp control during application.

12/10/08 Adequate surface preparation is key to successful thermally zinc application. Other than that, operators must be thoroughly trained to apply the zinc correctly. A quick and light first pass is important in order to avoid thermal shock, which would reduce bond. Adequate surface dryness and air cleanliness and ventilation are also necessary to provide successful application.

12/9/08: Operator skill, moisture (surface and ambient), equipment quality, surface preparation, temperature.

9. How did you ensure the quality of the coating application? What tools or methods did you use to measure such quality?	Download	
		Response Count
	Show Responses	15
	answered question	15
	skipped question	40

1/23/09: Quality is ensured through: visual inspection for consistency, tape tests for thickness of anode on regular intervals, and bond strength testing on regular intervals.

12/29/08: Thickness tests and pull-off tests - independent CP specialist.

12/24/08: 1) Strict requirements on thickness measurements and bond strength. 2) Require previous experience from the Contractor. 3) Always require that the Contractor hires a NACE certified CP Specialist to conduct and report quality assurance.

12/19/08: Dolly tests, pull-off tests, thickness measurement, potential reading after activated, etc.

12/18/08: Primarily metallographic examination of witness samples.

12/18/08: We have not on this CP application but we have used texture testing before and pull-off testing after to determine bond of epoxy on FRP strengthening projects.

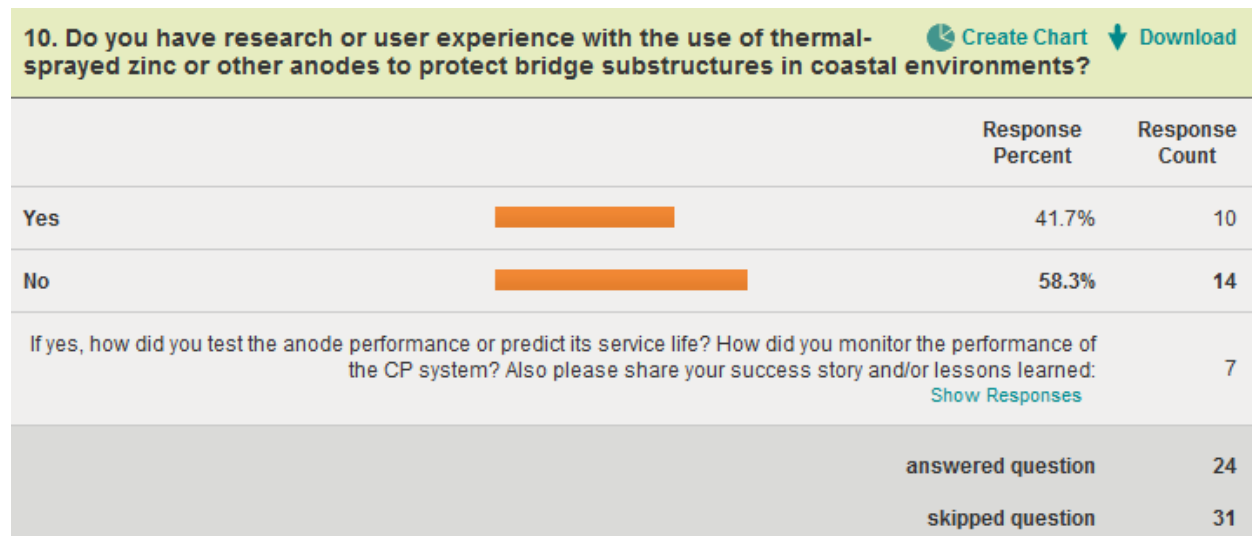12/17/08: I did nothing special. Simply I painted.

12/17/08: We relied on skill of the coating applicator with occasional coating thickness check using duct tape pieces that were placed prior to spraying.

12/17/08: Application trials and pull off testing.

12/17/08: Indirect film thickness measurement, finish quality.

12/10/08: Applicators were thoroughly trained. We used a full containment enclosure to achieve adequately low humidity and adequately high surface temperatures to ensure the surface was dry. Zinc thickness was measured using micrometers and bond strength was measured using a Proceq unit.

12/9/08: Operator training, temperature and humidity controlled enclosure.

10. Do you have research or user experience with the use of thermal-sprayed zinc or other anodes to protect bridge substructures in coastal environments?		Response Percent	Response Count
Yes		41.7%	10
No		58.3%	14
If yes, how did you test the anode performance or predict its service life? How did you monitor the performance of the CP system? Also please share your success story and/or lessons learned: Show Responses			7
		answered question	24
		skipped question	31

1/23/09: Anode performance is generally measured through the polarization effect on the reinforcing steel. This is done with reference cells and either manually or with data logging equipment. Service life can be predicted by monitoring the amount of current output over time, this current can be used to calculate anode life using Faraday's law. CP system performance can be monitored manually with periodic site inspections and testing or through remote access and

data logging equipment. A hands-on physical inspection of any system is always the best alternative.

12/24/08: As mentioned before, all our applications are in marine environments. Service life prediction is an estimation based on experience and the location of the components to be metalized on the bridge. Also depends on the location of the bridge. In most aggressive environments such as the FL Keys, the measured service life ranges from 5 to 8 years. On less aggressive such as Central FL, the service life has been from 10 to 12 years. Lessons learned: (a) always require an experienced Contractor, (b) always require that the metalizer is also the one conducting surface preparation, (c) require daily inspection of equipment (to avoid moisture during application), and (d) do not use metalizing for components in the splash area.

12/19/08: Service life is based on anode current density requirements, available anode mass, bond strength, concrete cover, etc., anode life can be calculated using Fick's Law and applying the Nernst Equation. Must measure current output and back-calculate anode life.

12/18/08: Six months old system, so long-term performance not yet known. The structure was a series of prestressed concrete beams on in-situ RC support structure. The longevity is based on a mass of zinc applied to the surface, no real detailed calculations done, but then these would be based on an assumed current density which may or may not have been realistic anyway so it would have been math for the sake of math and not realistic.

12/10/08: We worked with the Oregon DOT to survey several bridges that had formerly had CP systems installed. We tested the readings of the implanted reference cells vs. the reading of the portable cells placed in the test-wells. We also tested the voltage of the zinc surface to the system negative stud to see if the CP zone was shorted out or still operational. After it was discovered that it was difficult to open J-boxes after they had set out in the coastal air for over 10 years, ODOT instructed us to install external test studs on the J-boxes so that tests could be performed without opening the boxes themselves.

12/9/08: Accelerated testing in a lab environment. CP systems are monitored by reference cells in the bridges and data loggers collecting reference cell readings, power supply voltages, power supply current (voltages across shunts), ambient temperature and humidity.

11. The following information will be kept confidential   ⬇ Download

		Response Percent	Response Count
Name: Show Responses		100.0%	24
Company: Show Responses		100.0%	24
Address: Show Responses		91.7%	22
Address 2: Show Responses		41.7%	10
City/Town: Show Responses		95.8%	23
State: Show Responses		70.8%	17
ZIP/Postal Code: Show Responses		91.7%	22
Country: Show Responses		79.2%	19
Email Address: Show Responses		100.0%	24
Phone Number: Show Responses		87.5%	21
		answered question	24
		skipped question	31

Some companies/agencies from which responses were obtained (with the specific response date in each bracket):

> PT. Samator Gas Industry (1/25/10), ASFD (4/10/09), Actco (3/12/09), PVE (3/10/09), V&A (3/9/09), CAS Composite Anode Systems GmbH (2/19/09), Vector Corrosion Technologies (1/23/09), Virginia Transportation Research Council (12/29/08), FL Department of Transportation (12/24/08), Corrosion Service Co. (12/20/08), Electro Tech CP, LLC (12/19/08), Drexel University, MSE Dept. (12/19/08), The Tucker Group LLC (12/18/08), Mott Macdonald (12/18/08), Missouri DOT (12/18/08), Politecnico di Milano - Dip CMIC (12/18/08), Institute of Construction sciences (12/17/08), FHWA (12/17/08), MDT (12/17/08), Broomfield Consultants (12/17/08).

Some countries from where responses were obtained (with the specific response date in each bracket):

52

QWE (4/10/09), UAE (3/12/09), Austria (2/19/09), Canada (1/23/09), USA (12/29/08), Canada (12/20/08), USA (12/19/08), USA (12/19/08), USA (12/18/08), UK (12/18/08), USA (12/18/08), Italy (12/18/08), USA (12/17/08), UK (12/17/08), USA (12/17/08), USA (12/10/08), USA (12/9/08)

Some states from where responses were obtained (with the specific response date in each bracket):

MN (5/25/11), CA (1/25/10), IL (4/10/09), UT (3/12/09), IA (3/10/09), CA (3/9/09), VA (12/29/08), FL (12/24/08), FL (12/19/08), PA (12/19/08), FL (12/18/08), MO (12/18/08), VA (12/17/08), MT (12/17/08), VT (12/17/08), OR (12/10/08), OR (12/9/08)

3.3   KEY FINDINGS FROM THE SURVEYS

3.3.1 Anodes to protect bridge substructures in coastal environments

- One respondent's experience: We have worked with the Oregon, Washington and Alaska DOTs on several CP projects, including zinc, a zinc-aluminum-indium alloy, and titanium. We have also applied 3M's zinc hydrogel product, but that is adhesive and not thermally sprayed. The 99% pure zinc is by far the most effective anode that we have used, and it has proven to have excellent performance in preventing future corrosion of the rebar if the CP system is monitored adequately. Our experience with the other anodes was on an experimental basis, and none proved to be as cost-effective or useful as the pure zinc.

- Anode performance is generally measured through the polarization effect on the reinforcing steel. This is done with reference cells and either manually or with data logging equipment. Service life can be predicted by monitoring the amount of current output over time, this current can be used to calculate anode life using Faraday's law. CP system performance can be monitored manually with periodic site inspections and testing or through remote access and data logging equipment. A hands-on physical inspection of any system is always the best alternative.

- Service life prediction is an estimation based on experience, the location of the bridge, and the location of the components to be metalized on the bridge. In most aggressive environments such as the FL Keys, the measured service life ranges from 5 to 8 years. On less aggressive environments such as Central FL, the service life has been from 10 to 12 years. Lessons learned: (a) always require an experienced Contractor, (b) always require that the metalizer is also the one conducting surface preparation, (c) require daily inspection of equipment (to avoid moisture during application), and (d) do not use metalizing for components in the splash area.

- Service life is based on anode current density requirements, available anode mass, bond strength, concrete cover, etc., anode life can be calculated using Fick's Law and applying the Nernst Equation. Must measure current output and back-calculate anode life.

- CP needs to be regularly monitored by logging devices to assure protection continuity. Knowledge transfer and defective low-quality logging equipment usually bring problems, not the actual systems.

3.3.2 Key factors affecting anode-concrete bonding

- A good bond requires the concrete surface to be clean and dry and to have a good profile for the anode to "grab" onto. Key factors affecting the bonding of anode to concrete may include: *proper profile of concrete surface*, *substrate temperature and moisture content*, any *bond inhibiting substances* (e.g., residual grease/oil, paint, chalk, efflorescence, slurry coat, curing compound, marine growth, debris, surface prep grit and dust on the concrete surface), and proper *pH and chloride* levels. Also, thickness of the applied anode has shown to affect the bond strength; areas where the anode has been sprayed on too thick tend to debond easily.

- *Preparation technique*: Excessive grit-blasting causes excessive dust and laitance that inhibits bond. Pressure washing avoids dust and provides better bond development. Aggressive preparation of the surface can lead to exposure of excessive aggregates. Sandblasting should not be hard enough to expose excessive aggregates as thermally sprayed zinc will not bond well to rocks. After the blast is performed, it is important to keep hands and other body parts off the surface so as not to re-contaminate as the oils from skin can negatively affect bond strength. Additionally, after zincing one pass area, it is important to blow down the surface of the next area to be sprayed to remove any zinc dust prior to applying the thermally sprayed zinc there.

- Surface preparation is key to facilitating a good bond, but there are also other control factors that contribute to bond strength such as current control on the metalizing equipment, distance from the object to be metallized, angle of incidence for applying the metalizing, etc.

- Do not use any curing compounds on patches, wet cure if possible. A good grit blasting and blowing-off of laitance on the surface is needed. This left a somewhat porous rough surface to which the arc-sprayed anode stuck very well.

3.3.3 How to best ensure the quality of prepared concrete surface

- The concrete surface is blasted clean and then visually inspected to ensure a good surface profile. All areas to receive cathodic protection (including repairs) shall be prepared by grit blasting to achieve a suitable surface profile CSP number (International Concrete Repair Institute Guideline 037320).

- Zinc is applied as soon as possible after surface prep to limit possibilities of surface contaminants. Surface is inspected for profile and moisture content, surface is blown clean with air immediately prior to application, heat is applied if drying or temperature increase is required. Bond strength of anode to the substrate is tested with a pull tester on

regular intervals to confirm quality of application. Thickness of the anode applied to the concrete is tested on regular intervals by means of tape tests and a micrometer.

- Understanding that not all concretes require the same level of blast cleaning. For each bridge, we metalize test windows prior to commencing production metalizing. The test areas are metalized with different levels of blasting and a target bond is established for the project. Metalizer is responsible for achieving that minimum target bond for the final product to be accepted.

- Utilized proper control and QC with equipment and proper training of personnel applying the coating. Quality can be assessed in terms of measurable properties such as: density/porosity, adhesion strength, level of oxidation, and coating thickness. A good QC tool is the (ASTM D4541) pull-off test of the applied anode performed by an independent CP specialist. Pull-off adhesion test should be conducted at a minimum of four locations for each zone on each structure to demonstrate compliance with the minimum adhesion values.

3.3.4 Quality of anode coating application

- 1) Use only of proper components and equipment. 2) For galvanic use, there should be sufficient humidity present to keep the zinc active. 3) Do not use too close to the water as it would deplete quickly. 4) Use a topcoat to reduce self-consumption.

- Surface prep and condition are key to the quality of applied anode coating, so are the training, skills, and experience of the applicator. In addition to a clean rough concrete surface, also important are adequate climate control (adequately low humidity and adequately high surface temperature to ensure dry concrete surfaces, air cleanliness and ventilation, ambient temperature and humidity control, and enclosure against wind and water spray), appropriate selection of process and associated parameters, and adherence to properly developed deposition parameters.

- Quality of the applied anode coating is typically ensured through: visual inspection for consistency, tape tests for thickness of anode on regular intervals, and bond strength testing on regular intervals. Or it could be ensured through: metallographic characterization and analysis, or potential reading of the anode after being activated.

- 1) A quick and light first pass is important in order to avoid thermal shock, which would reduce bond. 2) Strict requirements on thickness measurements and bond strength. 3) Require previous experience from the Contractor. 4) Always require that the Contractor hires a NACE certified CP Specialist to conduct and report quality assurance.

3.3.5 Removal of old anode coating

- Zinc that has inadequate bond is fairly easily to remove by scraping or sand blasting. Anode with a strong bond requires a complete sand blast to remove. Where portions of the old coating are delaminated, they are removed by scraping the zinc off with putty

knives. It may be unnecessary to require 100% removal of old anode coating. If any good zinc is present, this is left in place and metalized over (a minimum of 100 psi bond strength is required).

- One respondent's experience: We have worked with the Oregon DOT on 4 bridges to perform surveys to determine if CP systems were working properly and to make repairs as necessary. The old coating was scraped off and contained. We found that most of the failed areas had a lot of loose dust build-up behind the coating, suggesting that there may have been quality control issues when the original surface was sprayed. When new coating is installed over repaired areas, depending on the size of the repair areas, small repairs could be accomplished by scraping off damaged zinc, using a needle-gun or small sand-blaster (if containment is possible), the area blown down with clean compressed air, and zinc spray touched-up to adequate millage using a portable flame-spray system. If large areas need to be replaced, a containment enclosure would most likely need to be installed to allow for sand-blasting and zinc application using the usual Thermion thermal spray system.

- Quality of coating removal is typically verified by visual inspection and sometimes by characterization. The most important factor is the experience and skills of the metalizer executing surface preparation. Also important is the angle of the blast, which may differ by bridge and by bridge section.

4.0 INVESTIGATING METHODS OF ZINC ANODE REMOVAL AND CONCRETE SURFACE PREPARATION

4.1 INTRODUCTION

In light of the findings from the literature review and practitioner surveys, the research team proceeded to identify, investigate and compare the various methods used to remove existing thermally sprayed zinc anodes and to further treat the concrete surface prior to the new anode application. Without significantly increasing the costs, the methods used should minimize the "bruising" of concrete surface (characterized by various degrees of microcracks and fractures), which will affect the bonding of the new metallic anode to the concrete substrate. According to the ACI Committee 364, "replacing the commonly used sand in abrasive blasting with alternative materials such as sintered slag, flint silicon carbide, or aluminum oxide can reduce damage" *(American Concrete Institute 2006)*. It also suggests that "where the more damaging methods must be used to increase production or reduce costs, the damage can be mitigated somewhat by abrasive shot- or water-blasting as a final preparation step for the final 0.10 inch" (2.5 mm). Note that the use of abrasive blasting or shotblasting to remove the existing zinc anodes will produce zinc-contaminated materials that may be classified as hazardous by the Environmental Protection Agency. The use of chemical strippers or high-pressure water blasting to remove the old coating is not desirable as they will generate liquid waste that is hard to collect, dispose of, or recycle. For this project, sandblasting (vs. shotblasting, flame cleaning, or pressure washing) was chosen as the main method for in-depth investigation, considering the ODOT current practice, costs of labor and equipment needed as well as the applicable environmental regulations.

The NACE No. 6/SSPC-SP 13 includes preparation procedures of concrete surfaces, inspection procedures and acceptance criteria prior to the application of protective coating or lining systems.

Factors that influence the depth of blast and the resulting surface profile include the following: quality of concrete (level of cracking and air void characteristics); hardness of the concrete surface; condition of the old anode; type, hardness, size, shape, and amount of the abrasive; speed of the machine; air pressure; standoff distance, etc. For instance, grit is irregular in shape with jagged edges and provides better cutting action than shot and creates a deeper anchor pattern, which promotes adhesion for the coating. Profile is important because an irregular surface allows the coating to grip and affects the bond strength of the new anode to the concrete; it is also expected to affect the evolution of the anode–concrete interfacial chemistry over the duration of electrochemical aging.

4.2 A PRELIMINARY INVESTIGATION INTO THE ZINC–CONCRETE INTERFACE

It was known that removal of surface contaminants (including loose zinc anode and its byproducts) allows the new anode material to have direct contact with the substrate, increasing the surface area and roughness of the surface and providing increased anchorage of the applied material. Nonetheless, one fundamental question to be answered during this "method screening" process was how much of the TS-Zn coated surface needed to be removed in order to get rid of the TS-Zn coating as well as zone 1 and zone 2 affected by acidification of the interface (as shown in Figure 1.1).

To this end, the National Energy Technology Laboratory (NETL) provided the WTI research team with dozens of concrete slabs from previous research projects. NETL, formerly known as the DOE Albany Research Center, had electrochemically aged the TS-Zn anode of these concrete slabs to various degrees (as shown in Appendix A). Before experimenting with various methods of anode removal and concrete surface preparation, the WTI team examined the history and other relevant information of the NETL concrete slabs as well as their surface condition.

The focus for this preliminary study centered on the interface between the concrete and thermally sprayed zinc anodes. Based on theoretical calculations, this interface bond should last more than 20 years with minimal de-bonding caused by the acidification at the interface (a result of electrochemical reactions). As it turned out, the longevity of this system in the field fell short of the predicted life span primarily due to the zinc–concrete interface bond failure.

Based on comments from metalizing spray contractors, the zinc–concrete bond is inherently weak and the bond strength and interface longevity is directly influenced by the concrete surface profile and the concentration of exposed aggregates. To provide mechanical anchors for the molten zinc to attach, the substrate is profiled by sandblasting prior to applying the zinc. This profiling process removes a fine layer of cement paste from the surface, exposing both coarse and fine aggregates. For first-time applications, the profiling process only removes the outer most paste layer so larger aggregates are less of a problem and the bond strengths tend to be higher. Subsequent surface profiling increases the exposure of aggregate and reduces the overall bonding capacity of the thermally sprayed zinc system. If a zinc system is to be removed and replaced, the interface bonding becomes a much greater concern because of the larger concentration of exposed aggregates.

The laboratory work started by selecting six samples from the NETL inventory shipped to WTI in early 2009. Table 4.1 presents the relevant information about the NETL samples selected for in-depth investigation.

Table 4.1: Information about the select NETL samples

NETL Sample No.	Initial Chloride Content (lbs/yd^3)	Equivalent Electrochemical Age (yrs)	Nominal Current Density for Aging (mA/ft^2)	Average Bond Strength of New TS-Zn to Concrete
204	5	5	1	272
235	5	8.6	3	252
214	5	22.4	3	169
906	5	37.6	2.5	268
905	5	45.4	2.5	202
1003	10	45.4	2.5	163

These concrete samples were approximately 10 years old. Once fully cured, a total quantity of 342-3085 KC/m^2 was applied between the embedded rebar and the thermally sprayed zinc anode on the concrete surface, using a nominal current density of 1-3 mA/ft^2 for accelerated aging. In other words, they had an equivalent electrochemical age of 5–45 years, assuming a normal ICCP current density of 0.2 mA/ft^2. Once these source samples were selected, small cubes (1″×1″) and thin discs (0.5″ thick, 4″ in diameter) were cut from them for various tests. Cross-sectional slices were cut from the small cubes and subjected to examination by the scanning electron microscope (SEM) in combination with energy-dispersive X-ray spectroscopy (EDX), to determine the approximate thickness of the reaction layer (i.e., zone 1 and zone 2 shown in Figure 1.1). The cube samples were subsequently placed in a humidity-controlled chamber for 48 hours before starting the DC resistivity and EIS measurements. The moisture content of the cube samples ranged between 5 to 6 percent during testing. The thin discs, used for gas permeability measurements, were oven-dried for 18 hours prior to each test.

For the select electrochemically aged concrete specimens, their thickness of Zn-rich reaction layer measured using SEM/EDX was in the range of 1 mm. Figure 4.1 illustrates the approach taken to estimate the Zn-rich reaction layer thickness, which was defined as the distance from the zinc–concrete interface to the zone where zinc signal was no longer detectable by EDX. Note the samples 1003 and 906 were both wetted daily during the accelerated electrochemical aging by a nominal current density of 2.5 mA/ft^2. Sample 1003 featured an initial chloride content of 10 lbs/yard^3 and equivalent electrochemical age of 45.4 years, whereas sample 906 featured an initial chloride content of 5 lbs/yard^3 and equivalent electrochemical age of 37.6 years. Figure 4.1 indicates that sample 906 featured a higher level of Zn penetration into the reaction layer relative to sample 1003, likely due to its lower chloride content in concrete. Furthermore, Figure 4.2 presents the representative EDX spectra of Zn-rich and low-Zn zones of the Zn–concrete interface of sample 1003. The Zn-rich zone of the Zn–concrete interface featured: Ca=7.45%; Zn=32.33%; Zn/Ca=4.3; Na/Ca=0.27; K/Ca=0.05; Si/Ca=0.9; Al/Ca=0.23; S/Al=0.2; Fe/Ca=0.4; Mg/Ca=0.06. The low-Zn reaction layer: Ca=14.33%; Zn=0.00%; Zn/Ca=0.0; Na/Ca=0.11; K/Ca=0.03; Si/Ca=0.6; Al/Ca=0.22; S/Al=0.0; Fe/Ca=0.2; Mg/Ca=0.03. Relative to the inner zone, the Zn-rich top concrete zone featured higher Na/Ca, K/Ca, Si/Ca, S/Al, Fe/Ca, and Mg/Ca ratios but similar Al/Ca ratio, confirming the replacement of Ca and Al in cement hydrates by Zn (i.e., secondary mineralization) due to electrochemical aging.
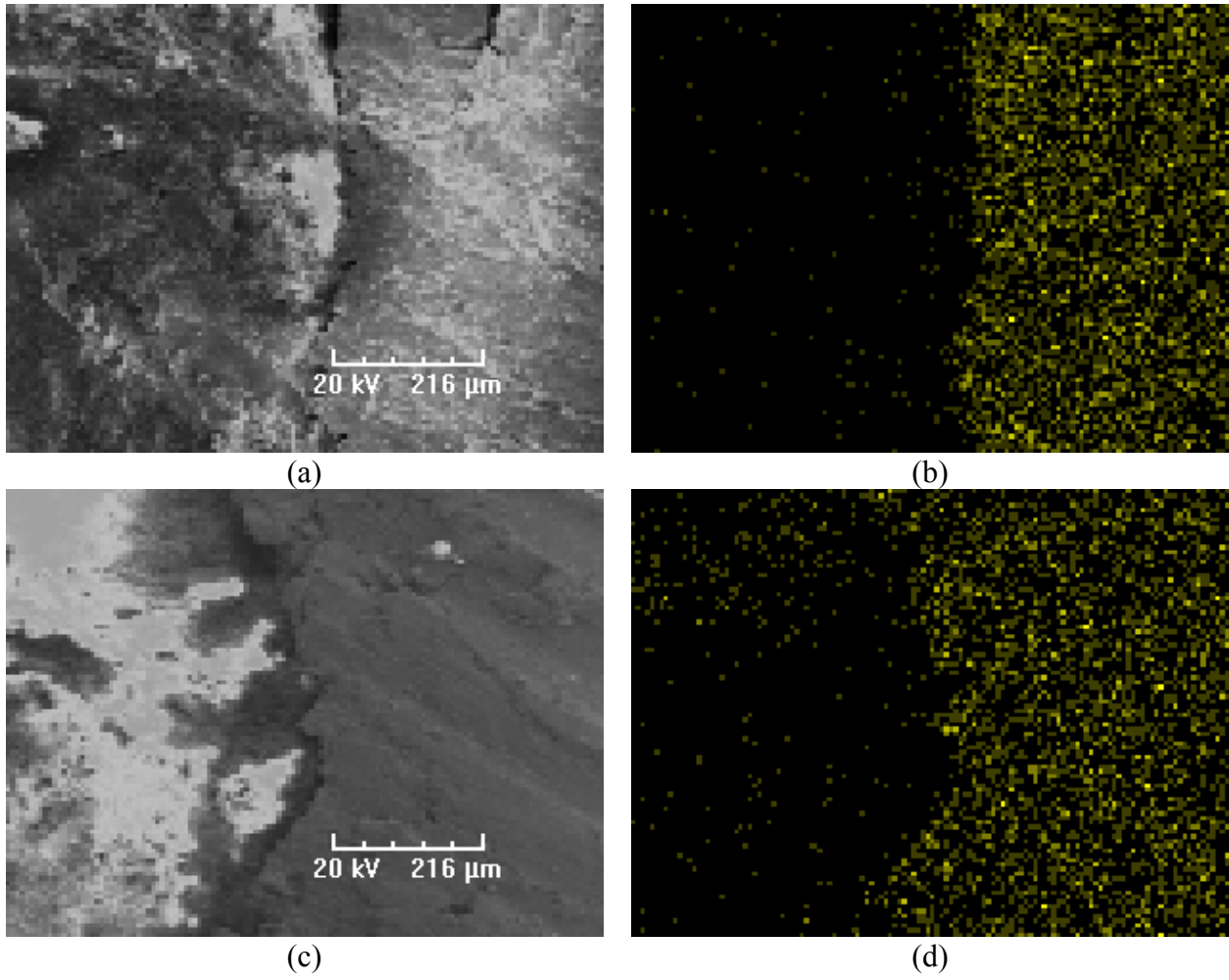
(a)

(b)

(c)

(d)

Figure 4.1: Typical zinc–concrete interface: (a) SEM micrograph and (b) Zn element map for NETL sample 1003; and (c) SEM micrograph and (d) Zn element map for NETL sample 906.
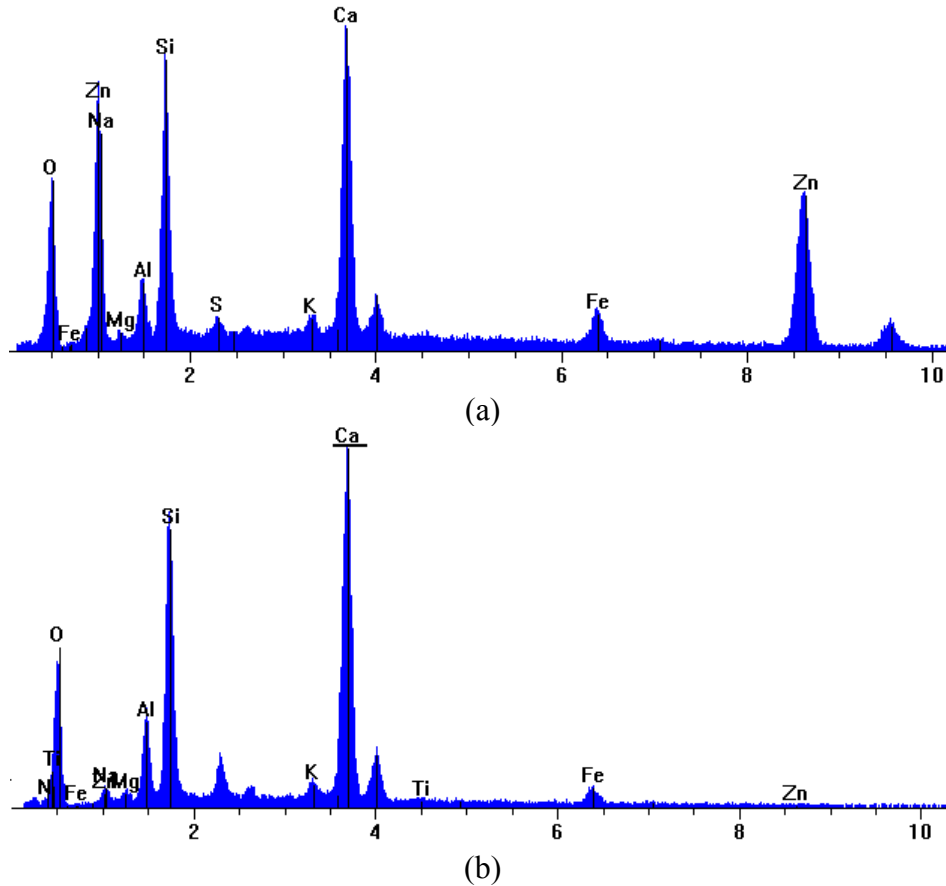
Figure 4.2: Representative EDX spectrum of (a) Zn-rich zone of the Zn–concrete interface corresponding to the area shown in Figure 4-2a; and (b) low-Zn reaction layer. Data collected from areas of 864×648 μm, with magnification of 125 times.

In addition to environmental stresses, there are two main areas of focus with respect to the zinc–concrete bond failure mechanisms. They are 1) physical, and 2) chemical. While the various mechanisms may interact with each other and create synergism on the performance and service life of zinc anode, it is desirable to examine each one individually to shed light on the relevant cause-and-effect relationships and when in the life cycle each mechanism occurs. It is proposed that the ultimate failure of the zinc–concrete interfacial bond starts with a physical failure at the time of application and is propagated by both chemical and environmental stresses throughout the remaining reduced life span of the system.

EIS has been used traditionally for life prediction of organic coatings on metals *(Kendig and Scully 1990)*, for monitoring a coated metal undergoing loss of adhesion *(Kendig et al. 1993)*, and recently for evaluating the bond between external carbon fiber reinforced polymer (CFRP) reinforcement and concrete in beams *(Hong and Harichandran 2004)*. For instance, the impedance typically increases in magnitude as the crack propagates *(Davis et al. 1999)*. EIS is considered one of the most powerful electrochemical techniques, especially when investigating high impedance corrosion systems and multiphase materials such as reinforced concrete.

EIS provides information on interfaces and thus sheds light on the active/passive behavior of the rebar and the properties of the concrete matrix *(Shi et al. 2009)*, and on the condition of the anode–concrete interface. EIS and a passivation verification technique derived from EIS have been used to monitor the CP performance and efficiency, respectively *(Talavera et al. 2000; Martinez et al. 2007)*. An equivalent circuit presenting the impedance elements between a conductive coating anode and the rebar in a reinforced concrete CP system is shown in Figure 4.3, and details are available in the literature *(Scully et al. 1993; Zhang 1996)*.
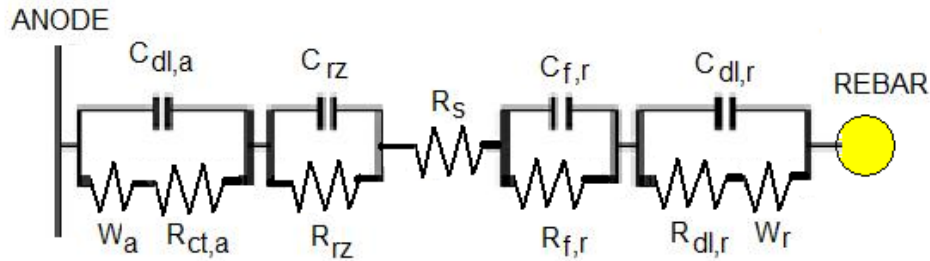
Figure 4.3: Equivalent circuit for ICCP between TS-Zn anode and rebar *(Davis, Dacres and Krebs 1999)*.

4.2.1 Physical Considerations

The following section describes the effect of incremental removal of reaction layer on the gas permeability, electrical resistivity, and electrochemical impedance spectroscopy (EIS) from concrete specimens cut from the select NETL slabs (see Table 4.1). The standard operating procedures of testing the gas permeability, DC electrical resistivity, and EIS of concrete specimens are provided in Appendices B through D, respectively. Note that for all the following discussions, the Zn-rich reaction layer thickness was assumed to be 1 mm in light of SEM/EDX measurements.

4.2.1.1 *Electrical Properties as a Function of Reaction Layer Removal*

With a few exceptions, the electrical resistivity and capacitance of the electrochemically aged concrete specimen tended to increase once 100% of the Zn-rich reaction layer was removed (see Figure 4.4). When the Zn-rich reaction layer was only partially removed, however, there was no consistent trend observed among the six NETL samples. For instance, samples 204 and 235 exhibited higher electrical resistivity and higher equivalent capacitance once the Zn-rich reaction layer was partially removed (up to 50%). Once more of the reaction layer was removed, these trends showed a reversal. Once the Zn-rich reaction layer was fully removed, however, these trends reversed again. The other samples exhibited much different trends with partial removal of Zn-rich reaction layer.
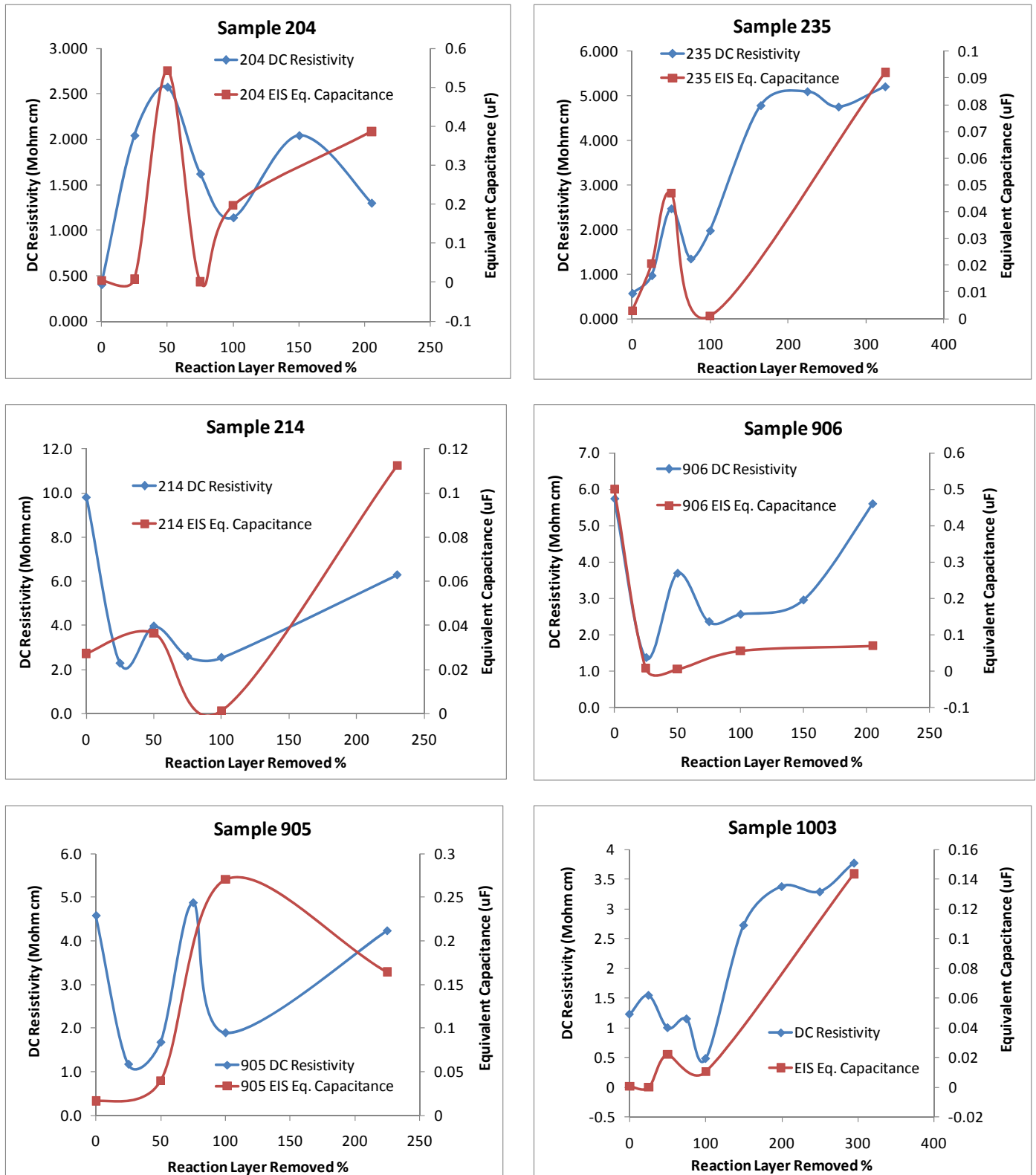
Figure 4.4: Electrical properties of select NETL samples as a function of reaction layer removal.

4.2.1.2 Gas Permeability as a Function of Reaction Layer Removal

With a few exceptions, the gas permeability of the electrochemically aged concrete specimen tended to increase once 100% of the Zn-rich reaction layer was removed (see Figure 4.5). When the Zn-rich reaction layer was only partially removed, however, there was no consistent trend observed among the six NETL samples. For instance, samples 235, 906, and 905 exhibited higher gas permeability once the Zn-rich reaction layer was partially removed (up to 25%). Once more of the reaction layer was removed, these trends showed a reversal. Once 50-80% of the Zn-rich reaction layer was removed, however, these trends reversed again. The other samples exhibited much different trends with partial removal of Zn-rich reaction layer.

These non-linear relationships between reaction layer removal and the resulting electrical and permeability properties can be attributed to the complex physical and chemical parameters defining the chemistry and microstructure of the heterogeneous concrete matrix near the Zn–concrete interface. For instance, for sample 204, the increase in the electrical resistivity along with the decrease in the gas permeability, suggests that the partial removal of reaction layer led to finer pore structure (lower porosity, smaller pores, or less pore connectivity) *(Alshamsi and Imran 2002)*. The increase in the equivalent capacitance corresponded to a decrease in the EIS-measured impedance, which is not likely attributable to the coarsening of the concrete pore structure *(Liu and Beaudoin 1999)*, but rather to changes in the chemical composition. For sample 906, the decrease in the equivalent capacitance along with the decrease in the gas permeability, suggests that the partial removal of reaction layer led to finer pore structure. The decrease in the electrical resistivity, thus is unlikely attributable to the coarsening of the concrete pore structure, but to changes in the chemical composition.

It should be cautioned that the raw resistivity samples were cut using a diamond blade wet saw from a larger concrete slab on all sides except on the reaction layer surface. This led to smooth edges on all sides except the reaction layer surface which can be quite rough. It is reasonable to conclude that this roughness can lead to a reduction in contact area between the rigid stainless steel electrode and the jagged raw reaction layer surface. This reduction in contact area would lead to an increase in measured resistivity.

For sample 1003, the relationships between reaction layer removal and the resulting electrical or permeability properties are significantly different from those seen in sample 905, likely attributable to their difference in initial chloride content (5 and 10 lbs/yd^3 for samples 905 and 1003 respectively).
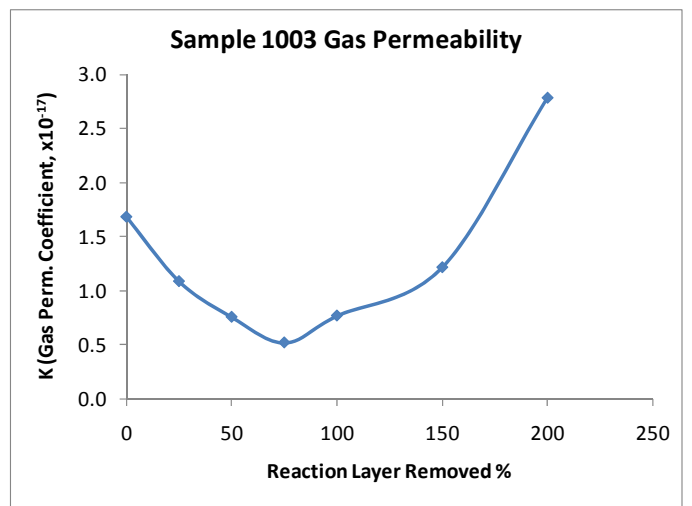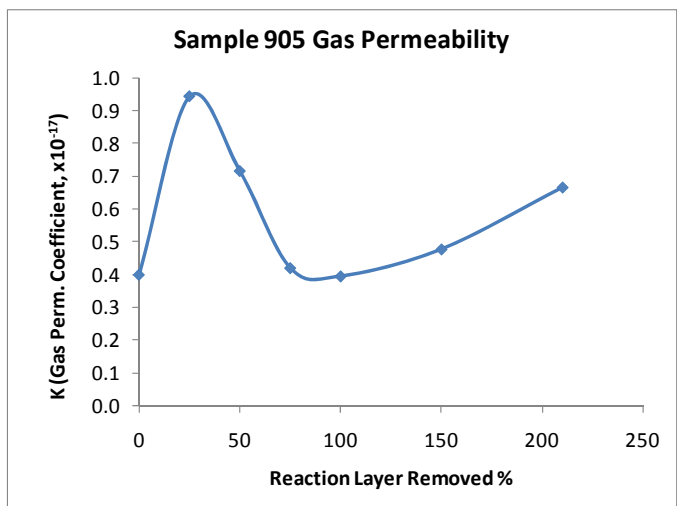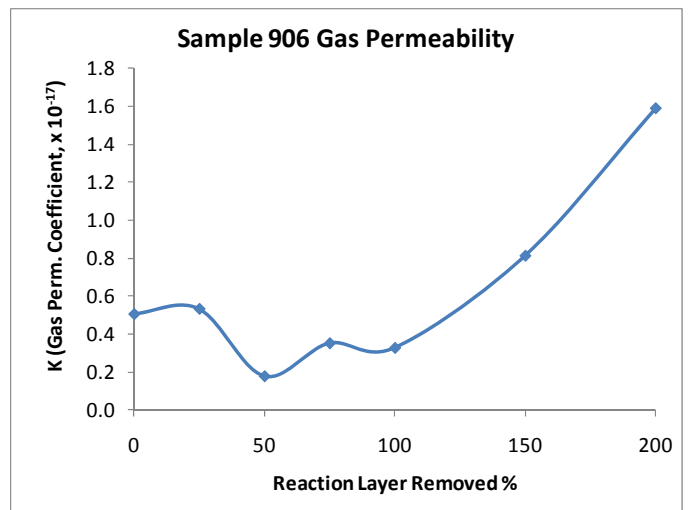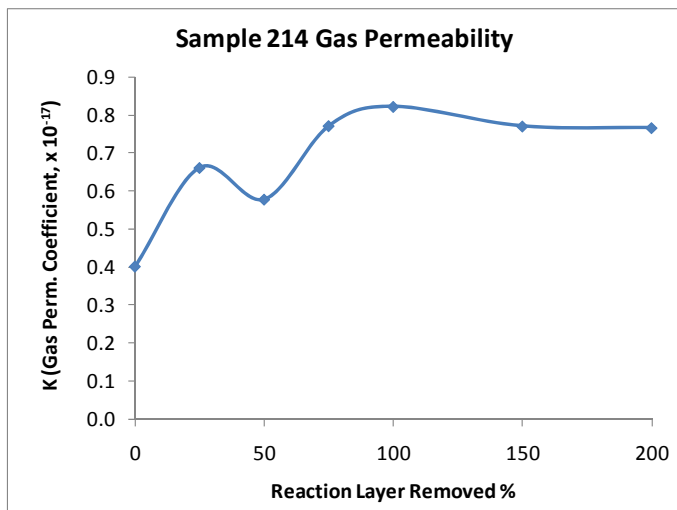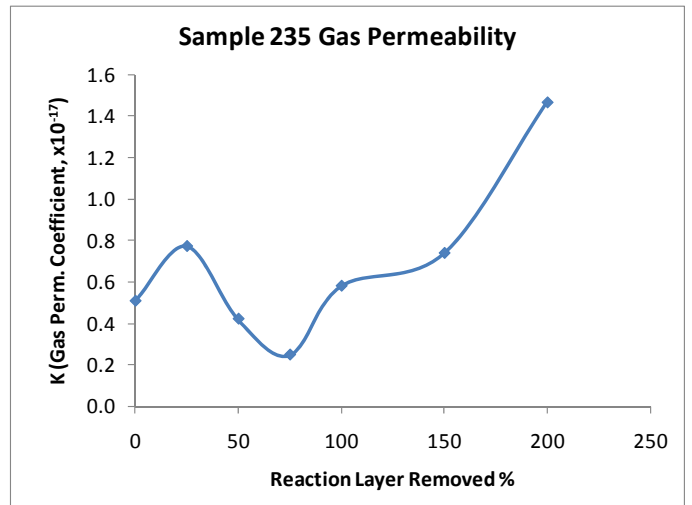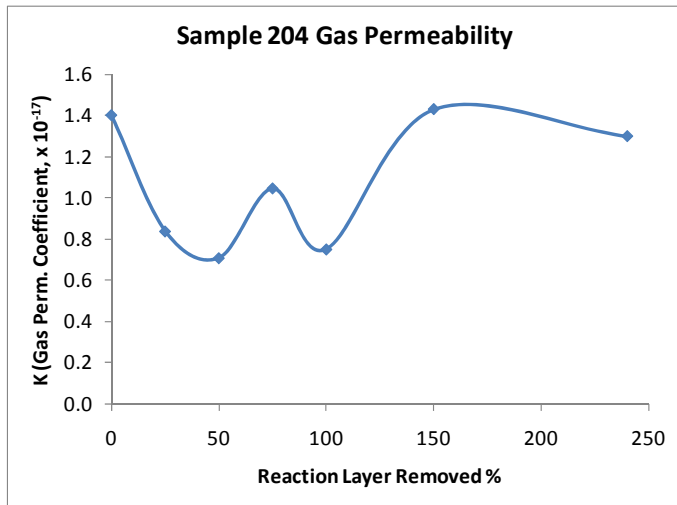
Figure 4.5: Gas permeability of select NETL samples as a function of reaction layer removal.

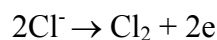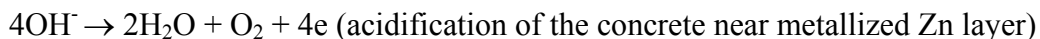### *4.2.1.3 Summary of Findings from the NETL Samples*

In summary, the select NETL electrochemically aged concrete samples showed a Zn-rich reaction layer of approximately 1 mm. With few exceptions, once the reaction layer was completely removed by sandblasting, the electrical resistivity, equivalent capacitance, and gas permeability of the resulting concrete specimen tended to increase. This suggests that relative to the concrete matrix itself, the Zn-rich reaction layer was generally less permeable but more electrically conductive. This was likely due to the electromigration of ionic species and chemical or electrochemical reactions that occurred at the zinc–concrete interface during the process of electrochemical aging, as detailed in the next section.
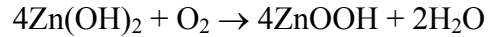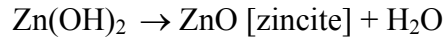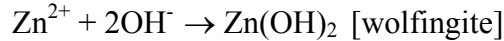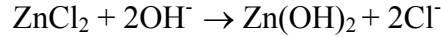
The adhesion strengths of thermal sprayed coating on metallic substrates can be as high as 3000 psi to 5000 psi, whereas those on concrete substrates are typically lower than 400 psi. Both the "exposed rock" and the thermal compatibility aspects help to explain why the thermally sprayed zinc has a much stronger bond to a steel substrate than to a concrete substrate. The bulk mass of most concrete structures is "rock" (i.e., coarse aggregates such as those with diameter 0.25″ or bigger), whereas fine aggregates (e.g., sand) and cement paste accounts for 20–30 percent of the mass. Once the outer paste layer is removed, aggregates are exposed. The coefficient of thermal expansion (CTE) for concrete and zinc raise some concerns as well. The CTE for zinc is 16.5×10^{-6} (inches expansion per inches of material per °F) while CTE of concrete is 5.5×10^{-6}. Considering that zinc will expand three times as much linearly as concrete, it helps explain how the initial bond strength is impaired by the temperature cycling in the service environment. The initial shrinkage of the rapidly cooling zinc on the rigid concrete structure may cause local cracking and splitting of the materials at the zinc–concrete interface. Zinc also has a thermal conductivity (116 W/mK) which is 68 times as great as that of concrete (1.7 W/mK). When the sun shines on the structure, the zinc will increase in temperature much faster than the concrete beneath, potentially causing cracking or stresses at the interface.

4.2.2 Chemical Considerations during the Electrochemical Aging

In addition to physical considerations, there are also chemical aspects to consider in light of various chemical and electrochemical reactions that may occur during the electrochemical aging of the thermally sprayed zinc anodes. All these reactions can affect the properties of the Zn-concrete interface, the durability of the Zn-concrete bond, and the removal of aged anode.
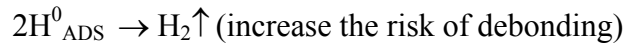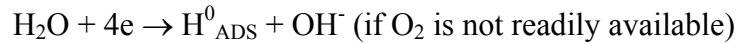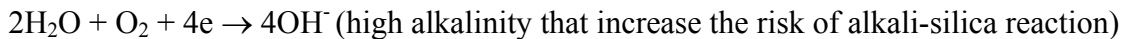
Depending on the electrochemical potential of the anode and local availability of chemical species, the anodic reactions may include but are not limited to:

$$4OH^- \rightarrow 2H_2O + O_2 + 4e \text{ (acidification of the concrete near metallized Zn layer)}$$

$$2Cl^- \rightarrow Cl_2 + 2e$$

$$Zn \rightarrow Zn^{2+} + 2e$$

$$Zn^{2+} + 2Cl^- \rightarrow ZnCl_2$$

$$ZnCl_2 + 2OH^- \rightarrow Zn(OH)_2 + 2Cl^-$$

$$Zn^{2+} + 2OH^- \rightarrow Zn(OH)_2 \text{ [wolfingite]}$$

$$Zn(OH)_2 \rightarrow ZnO \text{ [zincite]} + H_2O$$

$$4Zn(OH)_2 + O_2 \rightarrow 4ZnOOH + 2H_2O$$

In light of previous studies, other products that have been observed from the Zn-concrete interface of laboratory or field samples include: $Zn_7(CO_3)_2(OH)_{10}$, $ZnCO_3$, $Zn(OH)Cl$, $Zn_5(OH)_8Cl_2 \bullet H_2O$ [simonkolleite], $Zn_4(OH)_6(SO_4) \bullet xH_2O$ [hydrated zinc hydroxide sulfates], and $Zn_4(OH)_6(CO_3) \bullet H_2O$. In the concrete layer beneath the metallized Zn layer, there may be depletion of Ca^{2+} and other cations (Na^+, K^+, Zn^{2+} etc.) as these cations migrate towards the rebar under the externally applied electric field.

Depending on the electrochemical potential of the cathode (rebar) and local availability of chemical species, the cathodic reactions may include but are not limited to:

$$2H_2O + O_2 + 4e \rightarrow 4OH^- \text{ (high alkalinity that increase the risk of alkali-silica reaction)}$$

$$H_2O + 4e \rightarrow H^0{}_{ADS} + OH^- \text{ (if } O_2 \text{ is not readily available)}$$

$$2H^0{}_{ADS} \rightarrow H_2\uparrow \text{ (increase the risk of debonding)}$$

In the concrete layer near the rebar, there may be enrichment of cations (Ca^{2+}, Na^+, K^+, etc.) coupled with depletion of anions (especially Cl^-), as a result of the externally applied electric field.

4.3 A PRELIMINARY INVESTIGATION INTO ZINC ANODE REMOVAL AND CONCRETE SURFACE PREPARATION

The last section addressed the issue of how much of the TS-Zn coated surface needs to be removed in order to get rid of the TS-Zn coating as well as zone 1 and zone 2 affected by acidification of the interface (as shown in Figure 1.1). If an existing zinc anode surface has to be replaced, removing the old zinc coating (typically less than 15–20 mils, or 375–500 μm) and profiling the surface would effectively remove the majority of the reaction layer (typically 1 mm thick). The following section aims to explore another fundamental question, i.e., how to prepare the concrete surface to obtain good initial bond strength of the new TS-Zn.

Brousseau et al. (*1993*) of the National Research Council of Canada performed some earlier research on the bond strength of TS-Zn. They revealed that in order to achieve good TS-Zn bond strength, it was desirable to have concrete with good surface cohesion strength, minimal moisture content, and relatively high surface temperature; to use harder and denser grit material and a lower air pressure for abrasive blasting; to avoid the exposure of too much aggregate phase; to have a thinner coating per pass during arc-spray operations; and to have a thinner overall Zn coating layer (less than 20 mils) *(Brousseau et al. 1993)*.

While the adhesion of metallized zinc on concrete does not appear to be influenced by severe freeze-thaw cycling, the loss of adhesion was observed with high current densities and long polarization times, likely due to the oxidation of "anchors" that usually provide the mechanical bonding *(Brousseau et al. 1996a)*. The adhesion of zinc on a concrete surface was found to be mainly governed by the mechanical interaction of molten zinc droplets with the surface, and the root mean square (RMS) roughness obtained from a depth profile was the main parameter that could be related to the TS-Zn bond strength *(Legoux and Dallaire 1995)*. For the Single Wire Arc Plasma process, a short standoff distance (7 cm) was found to be most preferred for spraying large structures as it led to a reasonably high deposition efficiency (> 60%) and adequate bond strength (>2.07 MPa, i.e., 300 psi) *(Berndt et al. 1995)*.

Surface preparation is a critical factor in the performance of coatings and repair materials applied to concrete. Proper preparation provides a dry, even and level surface free of dirt, dust, oil and grease. For conductive coating anodes, a surface profile with appropriate anchor pattern and adequate bond strength to the concrete substrate is the key to achieving desired performance of the CP system and long service life of the new anode. In the case of thermal spray (TS) coatings (see Figure 4.6), "a high degree of surface preparation is essential," which can "only be achieved by abrasive blasting with a good quality, properly sized angular blast media" *(USACE 1999b)*. Abrasive blasting typically uses compressed air to propel a high-speed stream of solid media (e.g., sand, steel shot, aluminum oxide grit, plastic beads) from a nozzle, in order to remove surface layers of concrete. The large volumes of abraded concrete and abrasives are collected by an industrial vacuum and workers usually wear self-contained breathing equipment. The selection of an abrasive should consider hazards associated with the use of the abrasive.
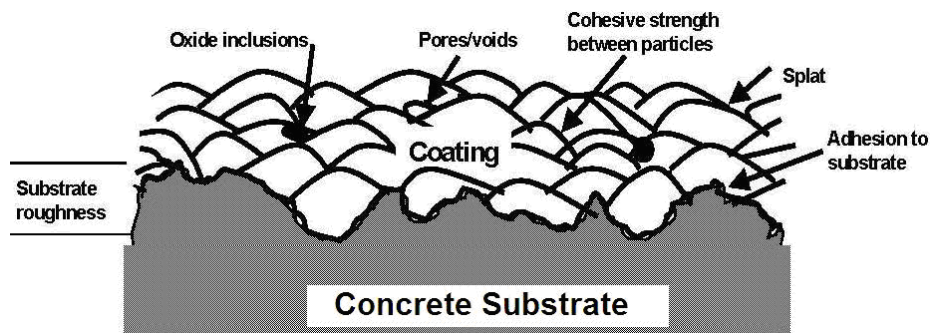

Figure 4.6: Typical cross section of a thermal spray coating (*USACE 1999a*).

To gain a better understanding of what parameters affect the initial zinc–concrete bond (as indicated by bond strength), the research team prepared many sets of samples and traveled to Oregon in the Spring of 2010 to have them sprayed by a current ODOT contractor, Great Western Corporation. The observations from this field trip that were not critical to this project but potentially useful are included as Appendix E.

Following the ODOT specifications and current protocol, the field work, sandblasting and arc-spraying took place inside the containment enclosure shown in Figure 4.7 as Great Western was working on the McCullough Bay Bridge project.

Figure 4.7: Containment enclosure at the McCullough Bay Bridge.

The samples that were sprayed and subsequently tested included small pieces from the original six NETL samples that had been extensively studied, large pieces of rock intended to simulate the coarse aggregates used in concrete, and nine-month old Portland cement concrete (PCC) panels that were fabricated based on the mix design used for the Yaquina Bay Bridge (as detailed in Section 4.4.1.1). The sample surfaces were prepared so that a minimum of three pull-off dollies could be applied per sample. Each dolly was 50 mm in diameter and required a test area slightly larger than the dolly itself (as shown in Figure 4.8). The bond strength was obtained by pulling off each dolly using a Defelsko Bond Tester as shown in Figure 4.9.

Figure 4.8: NETL samples with dollies epoxied in place ready for testing.

Figure 4.9: DeFlesko Posi-Test adhesion tester and metalized PCC sample ready for testing.

4.3.1 Sample Preparation

4.3.1.1 Samples with reaction Layer

The NETL samples were prepared so that the influence of the reaction layer on the zinc–concrete bond could be determined,[3] since the zinc–concrete bond was known to be one of the key factors defining the field performance and service life of CP systems. Most NETL samples had electrochemically aged TS-Zn layer on them. To ensure the TS-Zn and reaction layers were fully removed; 4.0 mm was ground from the original surface. This was achieved by grinding the surface of half of the NETL samples with a diamond-impregnated concrete polishing disc. The method was effective in removing material without introducing excessive heat or vibration. Figure 4.10 shows the NETL samples before and after profiling.

(a)

(b)
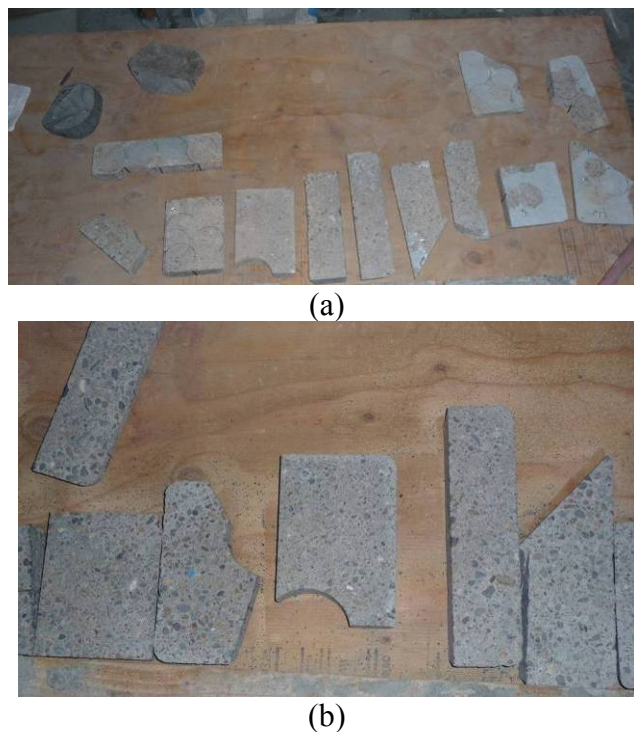
Figure 4.10: NETL samples (a) after removal of reaction layer by grinding; and (b) after the profiling process.

---

[3] There were hypotheses made before traveling to Oregon regarding the influence of surface moisture on the thermal spray process and subsequent bond strength. It became obvious when the research team watched and participated in the thermal spraying process that moisture is a concern but not to the extent hypothesized. The effort to track moisture content was abandoned from this field work because the problem is minor if the structure is properly enclosed and vented.

The NETL samples that did not have the reaction layer removed via grinding served as the control. These samples more realistically modeled what happens in the field when an concrete surface is profiled using current techniques.[4]

It was observed that to affectively remove the zinc a large percentage of "rock" (i.e., coarse aggregates) was exposed, leaving the concrete surface visually rough but texturally smooth. This resulted because conventional concrete aggregate is many times harder than structural grade concrete; consequently, the cement mortar binding the large aggregates was eroded away from the rock and the profiling left the smooth tops of the rock higher than the surrounding mortar.

4.3.1.2 Samples without reaction Layer

Large rock (diameter of 0.25–1.0″) accounts for at least 40–60 percent of the mass of concrete, so the interaction between the rock, zinc and mortar are parameters to consider for TS-Zn ICCP systems. As such, many of the samples (rock and PCC) that were profiled and arc-sprayed did not have a reaction layer. These samples were used to determine if the bond strength was influenced by the physical characteristics (percent of exposed rock, size of rock, surface profile) of the sample at the time of arc-spraying. Note that there were several different treatments to the rock samples. Some rock samples were profiled using the same method as used to profile the concrete, others were left in the natural state, and some were ground with the diamond polishing disc. After profiling, the PCC samples showed a more dramatic surface change relative to the rock samples (as shown in Figure 4.11).

Figure 4.11: PCC samples (left) and rock samples (right) after profiling and before arc-spraying.

---

[4] The overall thickness of the non-ground samples was measured in multiple locations using Verneer calipers prior to the profiling process. The measurement locations were marked on the edge of the samples to facilitate the follow-up measurements. Once the samples were profiled, the thickness was re-measured prior to the arc-spraying process.

4.3.2 Profiling

The PCC samples were used to investigate the effects of sandblasting to generate the surface profile (e.g., roughness). The profiling process involved blasting the surface with sand through a nozzle. The degree of material removal was influenced by many factors including but not limited to operator experience, travel speed, dwell time, and standoff distance. The intensity of material removal was influenced by many factors besides the four listed above; however, these four factors were the dominant parameters with respect to profiling. Soundness of the base material being profiled would have a significant influence on the final surface to be metalized. Softer base concrete experiences greater mass loss than more mature, harder concrete, which would result in more exposed larger aggregate.

There are many equipment parameters to consider when sandblasting a surface to generate a specific profile. Some of the major considerations are: blast media particle size and shape, air pressure, nozzle size, and output volume. The equipment used for this field work was also being used for the McCullough Bay Bridge project[5] so the research team decided only to manipulate the travel speed and dwell time to achieve the desired surface profiles. Extended dwell time or slow travel speeds over the samples resulted in larger concentrations of aggregates being exposed on the surface than shorter dwell times or higher travel speeds.

4.3.3 Zn Spraying

Figure 4.12 shows the arc-spraying of zinc onto the PCC samples by a Great Western worker. This process was very time consuming and labor intensive. The skill, attention to detail, and level of ownership by the operator had a direct impact on the finished product. For instance, if the operator had forgotten to blow down the area to be sprayed, failure could have resulted because the zinc–concrete bond would have been compromised by surface dust. In order to have a uniform bond over the entire concrete structure, the surface was all prepared in the same manner. Great care was taken to ensure that the thickness of the TS-Zn was uniform. The target thickness was 17 mils, which was achieved by making eight passes over the surface to be sprayed. Each pass was orthogonal to the previous pass. To verify the applied thickness, several small sections of duct tape were randomly placed on the surface being sprayed. When the spraying was completed, the operator removed the zinc from the surface of the tape and measured it with a micrometer. Typically, a spray section was approximately one square yard.

---

[5] The blasting/profiling operation on the McCullough Bay Bridge appeared to be operating as efficiently and consistently as could be expected. The profiled surfaces had varying concentrations of exposed aggregates but the overall surface consistency was good. The McCullough Bay Bridge is over 70 years old and has experienced substantial paste loss from the surface that is being prepared for metallization. This paste loss certainly does not help when trying to minimize the percentage of exposed aggregate by profiling. The arc-spray operation that the research team witnessed at the McCullough Bay Bridge project was also very organized and controlled, leading to a high level of quality.

Figure 4.12: Arc-spraying the PCC samples.

4.3.4 Bond Strength as a Function of Individual Factors

Six electrochemically aged NETL concrete samples were profiled to receive arc-spray zinc. Once the samples were profiled and arc-sprayed with zinc, the bond of the new zinc to the concrete surface was measured using pull-off dollies 50 mm in diameter. Each NETL sample was cut into two pieces, one of which had 4 mm of the surface layer ground off prior to profiling and spraying and the other was left intact until it was profiled. Figure 4.13 shows a NETL sample and a rock after bond testing.

Figure 4.13: Typical NETL sample (left) and rock sample (right) after bond testing.

4.3.4.1 Bond Strength vs. Reaction Layer

The bond strength of new zinc to concrete is influenced by the presence of the reaction layer but it depends on the electrochemical equivalent age of the layer. Each NETL sample was prepared such that half of it was tested with the reaction layer intact and the other half with the reaction layer removed via 4 mm of grinding by diamond disc. This was designed to unravel the role of reaction layer on the bond strength of new TS-Zn to the concrete surface. Figure 4.14 presents the average bond strengths of the NETL samples with and without the reaction layer. Samples 204 and 235 (with equivalent

73

electrochemical age of 5 and 8.6 years, respectively) exhibited higher bond strengths when the reaction layer was only partially removed during the profiling process. The bond strength for these two samples decreased when the reaction layer was completely removed prior to profiling and arc spraying. This relationship changed as the electrochemical equivalent age increased. Samples 214, 906, 905, and 1003 (with equivalent electrochemical ages of more than 22 years old) all had higher bond strengths when the reaction layer was completely removed prior to profiling and arc spraying. These data suggest that as the reaction layer matures (>8 years), the bond strength would be better if the reaction layer is completely removed prior to profiling and arc spraying.
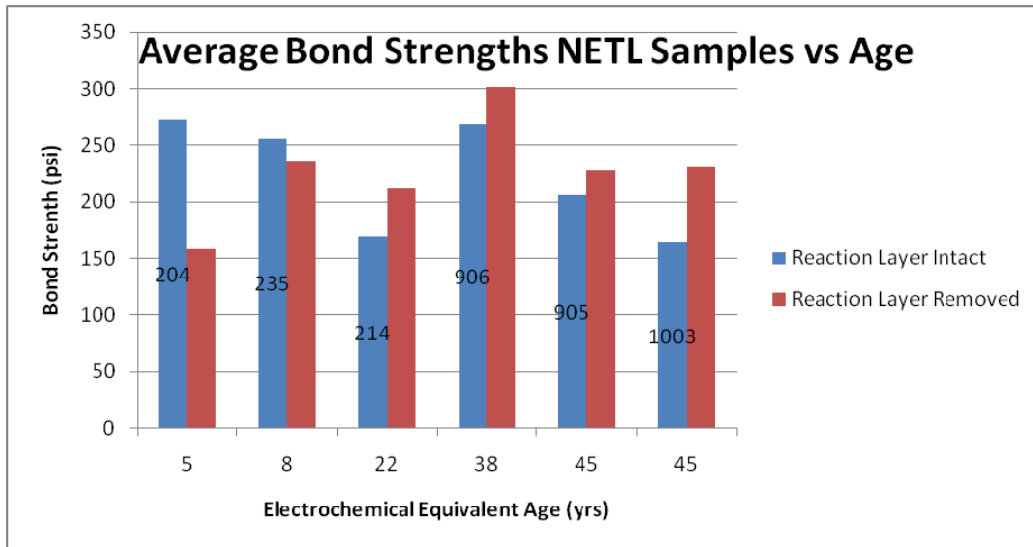

Figure 4.14: Average NETL bond strength as a function of electrochemical age.

4.3.4.2 Bond Strength vs. Surface Profile

The bond strength of new zinc to concrete is also influenced by the profile of the concrete surface (quantified by roughness measures). The PCC and NETL samples were prepared to achieve various surface profiles and levels of exposed aggregates by varying the travel speed and dwell time. After bond tests had been performed the surface roughness was measured on all the bond test locations. The standard operating procedures for measuring the 2-D surface macro-roughness, percent of exposed aggregates, surface micro-roughness, and root mean square (RMS) surface macro-roughness are detailed in Appendices E through H, respectively.

Figure 4.15 presents the average bond strength of the PCC and NETL samples as a function of surface micro-roughness. It is evident that if a surface was too smooth at the microscopic level (with micro-roughness < 3 μm) then the zinc would not bond well to it. On average, a microscopically rougher surface tended to lead to higher bond strength, as it provided more "anchor points" for the molten zinc to adhere to.
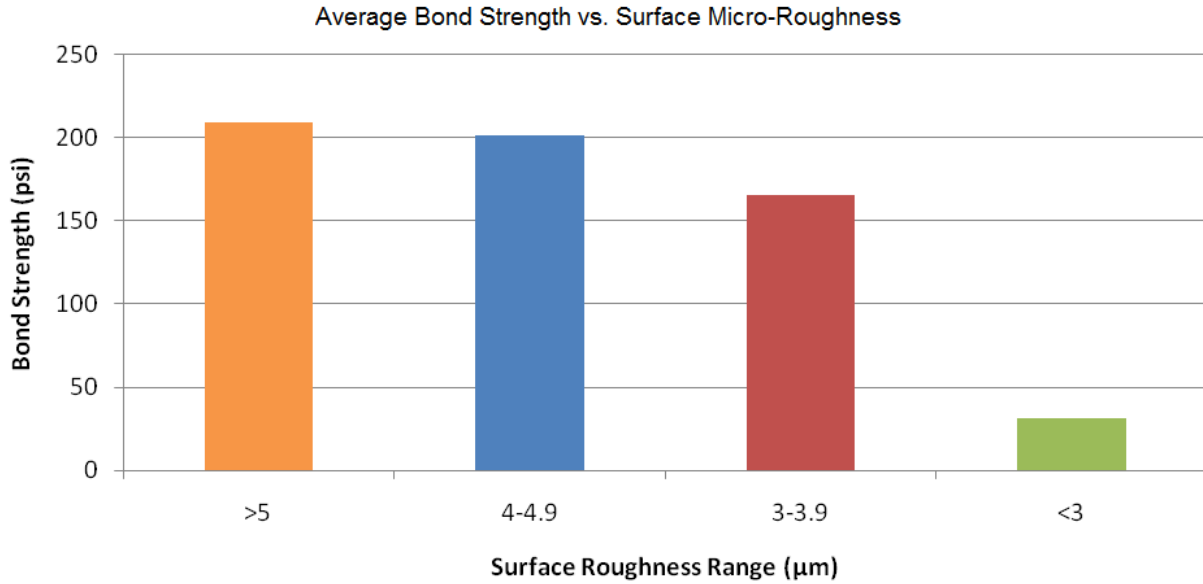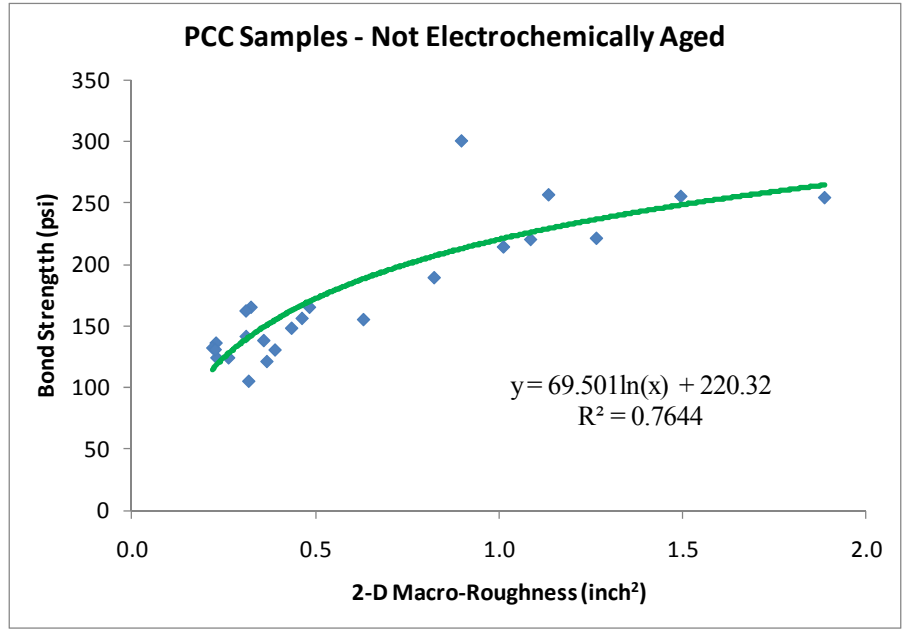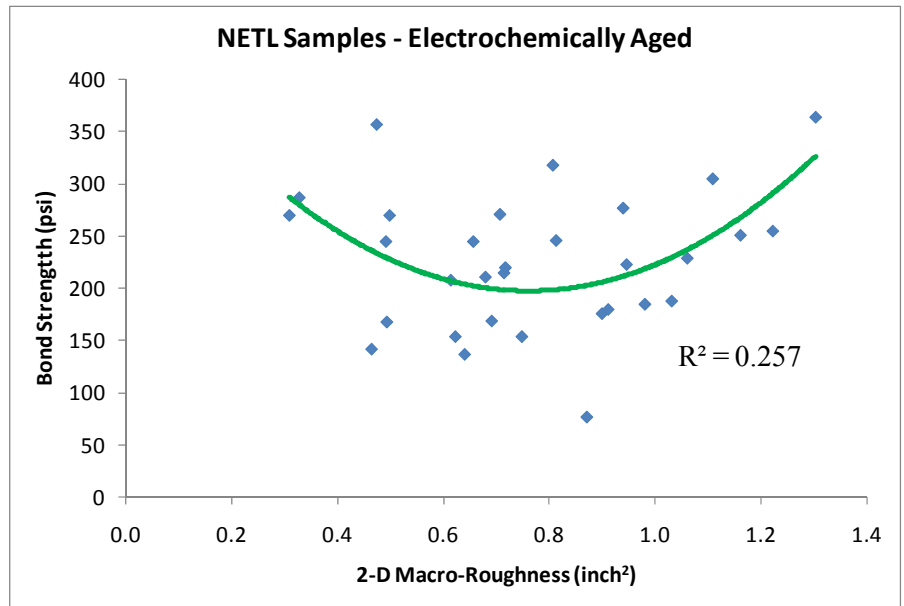
Figure 4.15: Average bond strength as a function of surface micro-roughness.

Figure 4.16(a) and (b) present the average bond strengths of the PCC and NETL samples as a function of 2-D surface macro-roughness, respectively. The PCC samples exhibited a strong correlation between its surface macro-roughness and the resulting zinc–concrete bond strength. If a concrete surface was not altered by electrochemically aging, a macroscopically rougher surface tended to lead to higher bond strength, as it provided more and larger "anchor points" for the molten zinc to adhere to. The electrochemically aged NETL samples, however, exhibited a very weak correlation between its surface macro-roughness and the resulting zinc–concrete bond strength.

(a)

(b)

Figure 4.16: Average bond strength as a function of 2-D surface macro-roughness.

4.3.4.3 Bond Strength vs. Surface Composition

Sandblasting the surface tends to increase the exposure of aggregates. Common responses from thermal spray contractors were that "rock" (i.e., coarse aggregates such as those with diameter 0.25″ or bigger) is a problem and that each time the surface is altered by blasting, the rock problem is exacerbated. For this study, the bond strength of zinc to rock samples ranged between 0 and 90 psi. Several contractors have mentioned that

treating the aggregate or coating it with some material that improves the bond to zinc would provide a better finished product and potentially reduce installation costs.

Figure 4.17 presents the average bond strength of the PCC and NETL samples as a function of surface composition. Note that while the percent of exposed aggregates was assessed after bond test using a procedure similar to that detailed in the Appendix F, only large aggregates (with diameter 0.125″, i.e., 3.2 mm or bigger) were considered as "rock" (see Figure 4.18). The PCC samples featured surfaces with 14.8–51.9% of exposed rock, and the NETL samples featured surfaces with 14.9–74.0% of exposed rock. Figure 4.17 suggests that an ideal surface composition for higher bond strength should have 45–54% of exposed rock (diameter 3–19 mm). This deviates from thermal spray practitioners' perspective that the concrete surfaces with less exposed rock should have higher bond strength. It should be noted that the bond of zinc to rock phase is much weaker than that of zinc to mortar phase and more prone to compromises and localized debonding.
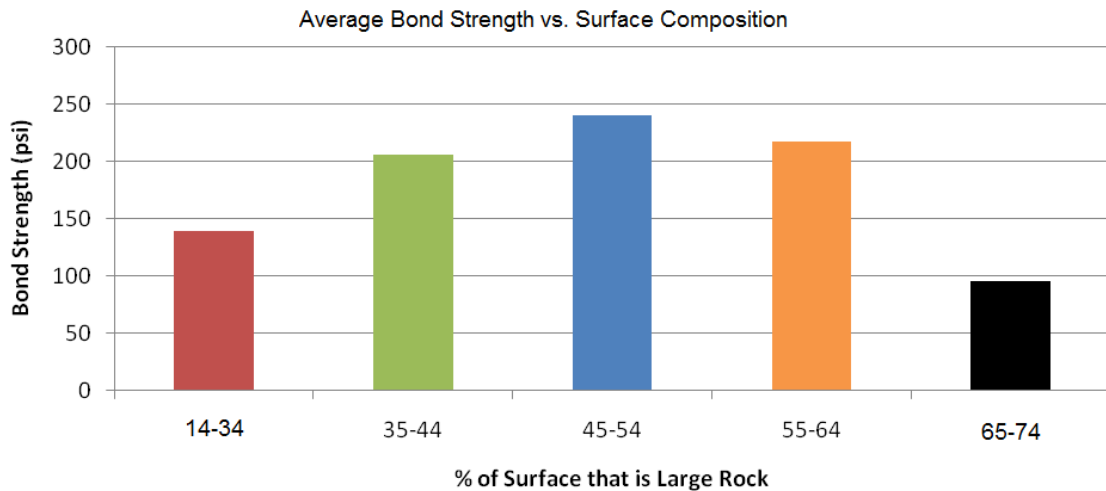

Figure 4.17: Average bond strength as a function of surface composition.
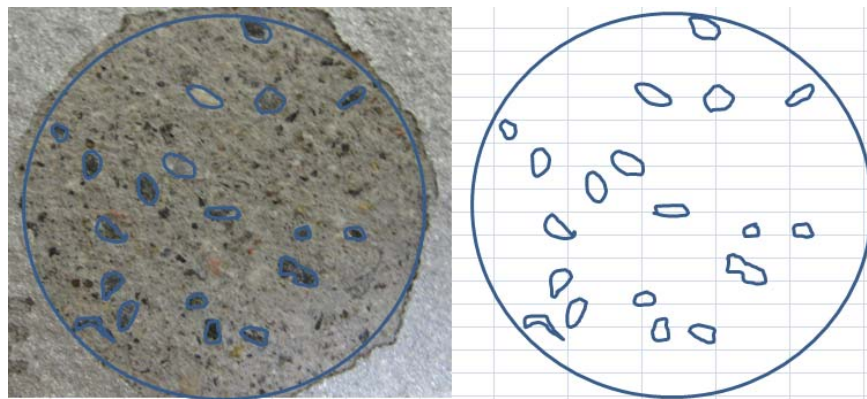

Figure 4.18: A step used in quantifying the percent of exposed rock at the bond test site.

Figure 4.19 shows a rock coated with TS-Zn that debonded within 48 hours of application without induced stress. This de-bonding from the rock is probably related to the significant differences in the coefficient of thermal expansion (CTE) between the zinc and the rock. Nonetheless, as the rock size decreases (e.g., from a real rock to a coarse aggregate), the TS-ZN spats are expected to form better and deeper anchors around the aggregate.

Figure 4.19: TS-Zn debonded from a rock sample.

The complex relationship between the percentage of exposed rock and the bond strength could stem from multiple mechanisms at work. On the one hand, as more large rock is exposed on the concrete surface, there is more areas with weak bonding with the zinc, leading to lower bond strength averaged over the rock and cement mortar areas. On the other hand, the interface between the aggregate and mortar appears to provide reasonable anchorage locations for the sprayed zinc, leading to higher bond strength averaged over the rock and cement mortar areas.

The aggregate phases tend to significantly decrease the permeability of the concrete by acting as physical barriers. This slows down the ingress of chlorides and generally improves the durability of the concrete, but it also slows down the chloride removal via CP and demands higher protective potential for CP to overcome the concrete resistivity. In the absence of best practices for aggregate preparation or sufficient mixing during construction, there is a possibility to form a so-called "interfacial transition zone (ITZ)" on the surface of coarse aggregates. In such cases, the ITZ is a highly permeable layer as a result of locally high water-to-cementitious-materials ratio on coarse aggregates, which degrades the impermeability of the concrete.

It is hypothesized that the safe way to ensure high initial bond strength as well as continued high bond strength over the CP system service life is to minimize the exposure of large aggregates (e.g., diameter > ¾″) yet maintain the exposure of small aggregates (e.g., diameter no more than 0.25″) at a moderate level. It is cautioned, however, for the existing ODOT bridges, it is nearly impractical to achieve both targets simultaneously

since the amount of small and large aggregates in the concrete was proportioned at the time of construction.[6]

4.3.4.4 Bond Strength vs. Surface Profile and Composition

To further illustrate the bond strength as a function of surface profile and composition, Figure 4.24 presents the individual bond strength values for surfaces with various micro-roughness and percent of exposed rock. The larger the size of the dot in Figure 4.20, the higher concentration of exposed rock was observed on the concrete surface. It can be seen that an optimum surface featured a micro-roughness of 3.5–5 µm and a moderate level of exposed rock. It is interesting to note that for surfaces with a high level of exposed rock the bond strength was always low independent of their micro-roughness.
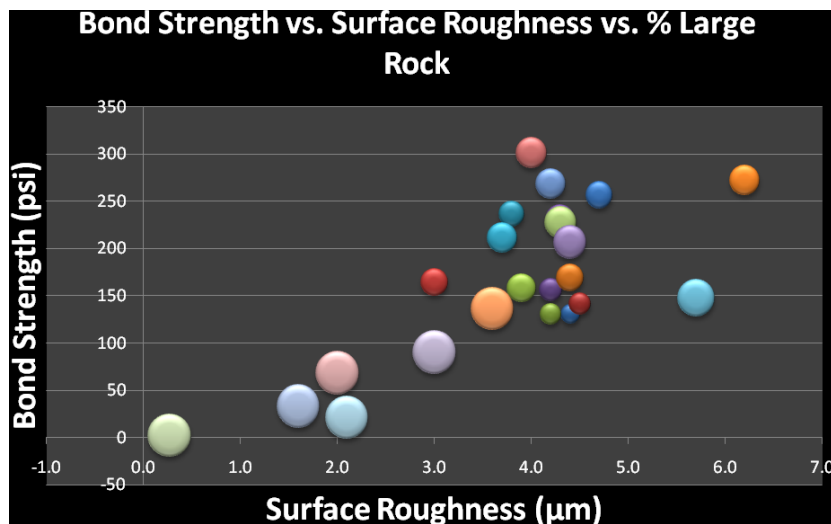
Figure 4.20: Bond strength as a function of surface micro-roughness and exposed rock.

4.3.5 Neural Network Modeling of Bond Strength

To study the complex cause-and-effect relationships inherent between the potential influential factors and the initial zinc–concrete bond strength, artificial neural networks (ANNs) was elected as a modeling alternative to establish predictive models.

ANNs are powerful tools to model the non-linear cause-and-effect relationships inherent in complex processes where conventional modeling techniques (e.g., multiple regression) fail. This is generally accomplished without knowing the form of the predictive relationship *a priori*.

---

[6] One potential solution is to apply a highly permeable cementitious mortar after the removal of old zinc and profiling of the concrete surface. This interlayer could be engineered so the bond with the substrate is optimized based on the constituents of the substrate and ideally also feature good conductivity and compatible CTEs with the concrete matrix as well as the TS-Zn layer. Such an inter-layer could be based on existing ODOT patch material, with adjustments in aggregate contents and admixtures for workability etc. However, the ODOT has raised concerns over this solution as its cost-effectiveness and implementation costs are not known at this stage.

ANNs provide non-parametric, data-driven, self-adaptive approaches to information processing *(Shi et al. 2004)*.

ANNs offer several advantages over traditional model-based methods. First, ANNs are robust and can produce generalizations from experience even if the data are incomplete or noisy, as long as over-fitting is avoided with intervention by experts of the relevant knowledge domain. Second, ANNs can learn from examples and capture subtle functional relationships among case data. Prior assumptions about the underlying relationships in a particular problem, which in the real world are usually implicit or complicated, need not be made. Third, ANNs provide universal approximation functions flexible in modeling linear and nonlinear relationships.

The ANN paradigm adopted in this study was the multiplayer feed-forward neural network, of which a typical architecture is shown in Figure 4.21. The nodes in the input and output layers consist of input variables and output variable(s), respectively, whereas the topological structure of the hidden layer(s) depends on the complexity of the relationships. In this study, a modified back propagation (BP) algorithm was employed for the ANN training. Signals are propagated from the input layer through the hidden layer(s) to the output layer, and each node in a layer is connected in the forward direction to every node in the next layer. Every node simulates the function of an artificial neuron. The inputs are linearly summated utilizing connection weights and bias terms and then transformed via a non-linear transfer function. The network learns by adjusting its weights and bias terms to reduce the difference between its output for each input pattern with a target output for that pattern. The learning process continues with multiple samples until the sum of the mean squared error (SMSE) in the output layer converged to an acceptable level. A thorough treatment of the BP ANNs is beyond the scope of this report, and the detailed description of data normalization, transfer function, and error propagation algorithm is provided elsewhere (*Rumelhart et al. 1986*). It is cautioned that the predictive quality of any model would not exceed the quality of the data used to construct it.
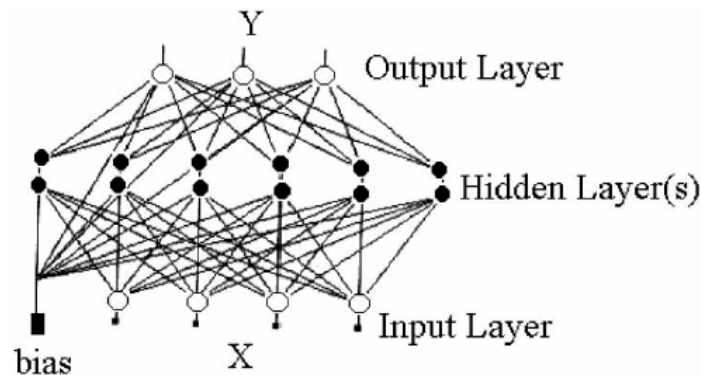
Figure 4.21: A typical multi-layer feed-forward ANN architecture.

For ANN modeling, the following four influential factors were chosen as input variables: equivalent electrochemical age, percent exposed rock area, 2-D macro-roughness, and micro-roughness. The initial zinc–concrete bond strength was chosen as the output variable. The ANN model was established by appropriately choosing the architecture and training process. The model was trained and tested using the data from both NETL and PCC samples. The topological

structure of the ANN model was determined to be 4-7-1 on the basis of trial-and-error. The sum of the mean squared error (SMSE) from the training data set (49 samples) and testing data set (one sample) was 0.039 and 0.059, respectively. The model performance is shown in Figure 4.22 which indicates that the established model has good "memory" and the trained matrices of interconnected weights and bias ("fabric" of the ANN) reflect the hidden functional relationship well. As such, the model was used to predict the bond strength as a function of influential factors. In the following sections, the model predictions are presented in the form of 3-D response surfaces to best illustrate the complex interactions between influential factors. Predictions were made with each influential factor varying in the range of training data, since ANNs are not suitable for extrapolation.
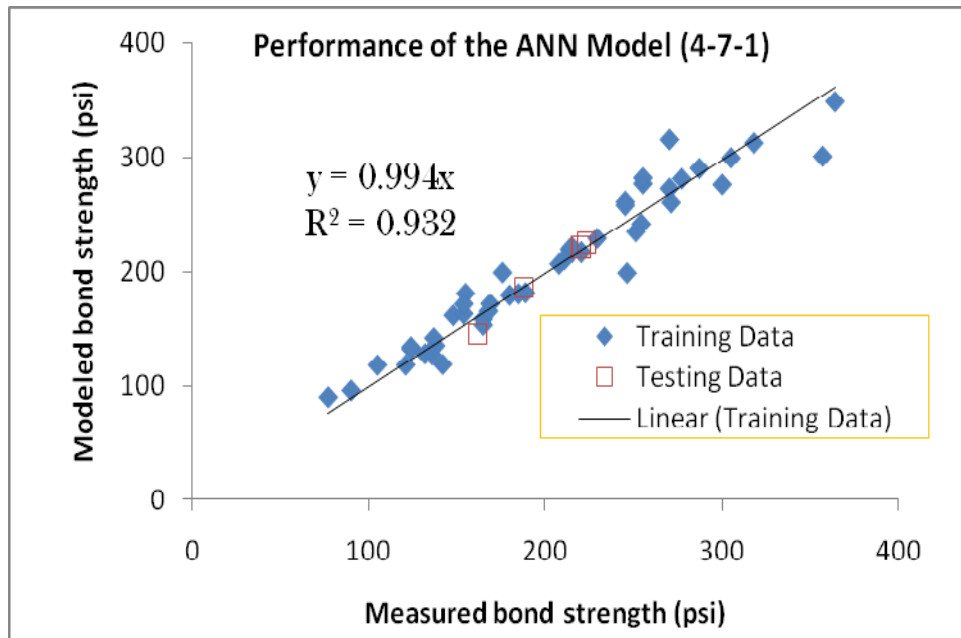
Figure 4.22: Performance of the ANN 4-7-1 model for bond strength.

From a modeling perspective, ANN was used to achieve better understanding of the complex cause-and-effect relationships inherent in the zinc–concrete system and was successful in finding meaningful, logical results from the bond strength data. As shown in Figure 4.23, for concrete with an electrochemical age of nine years and 35% exposed rock, the bond strength generally increased with the 2-D macro-roughness whereas the dependency of bond strength on micro-roughness was more of a function of the RMS macro-roughness and less significant.

Figure 4.23: Predicted bond strength as a function of 2-D macro-roughness and micro-roughness.

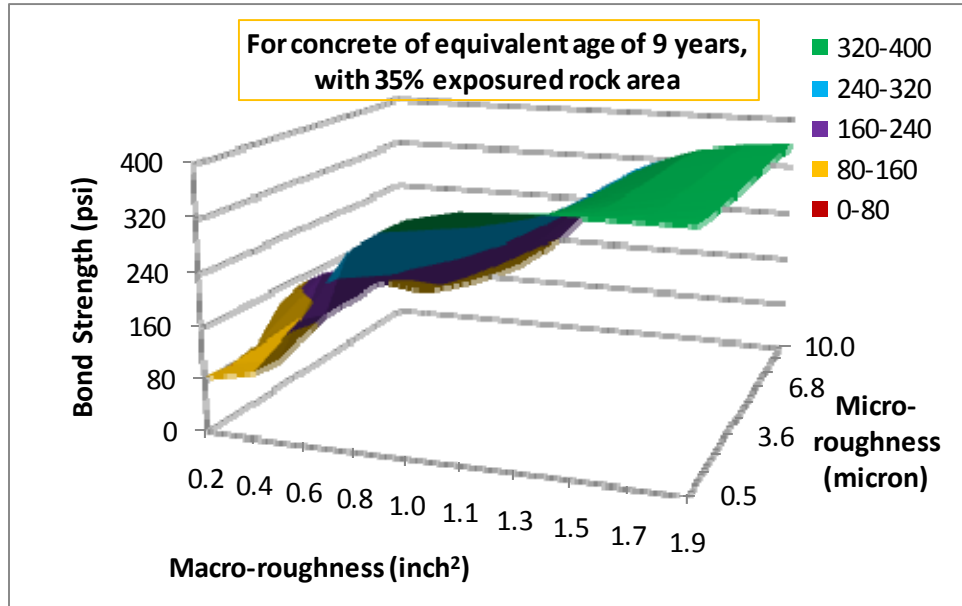As shown in Figure 4.24, for concrete with a 0.59-inch² 2-D macro-roughness and a 1.75-μm micro-roughness, there was not a straightforward dependency of bond strength on the electrochemical age of the concrete or the percent exposed rock area. The highest bond strength values were found on surfaces with 43% exposed rock and 18-27 years of electrochemical age, followed by surfaces with 15% exposed rock and 0-9 years of electrochemical age. Independent of the electrochemical age, concrete surfaces with more than 60% exposed rock generally had bond strengths lower than 110 psi, confirming the deleterious role of too much exposed rock. It is cautioned that these trends were modeled based on a limited number of data points and may change as more bond strength measurements of various concrete surfaces are included (as discussed later).
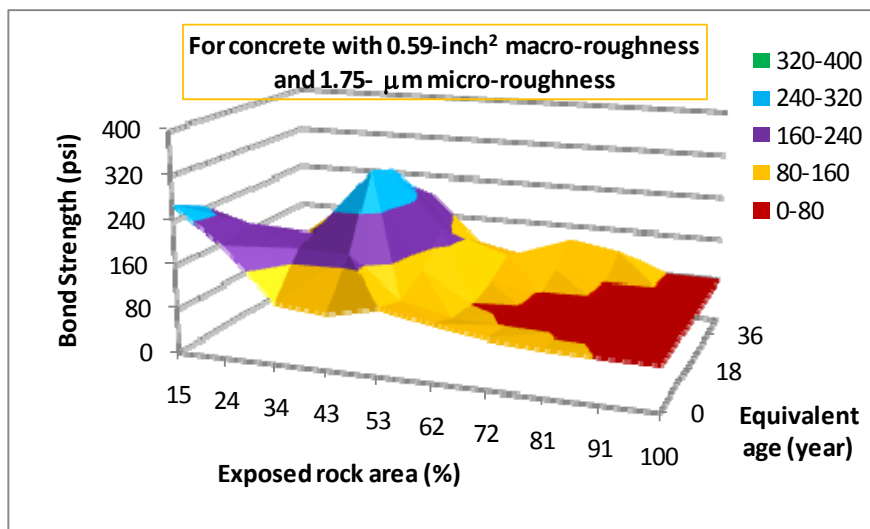

Figure 4.24:Predicted bond strength as a function of surface composition and equivalent electrochemical age.

4.4 A SYSTEMATIC INVESTIGATION INTO ZINC ANODE REMOVAL AND CONCRETE SURFACE PREPARATION

To further validate or improve the modeling results shown in the last section, the following section presents a systematic study into zinc anode removal and concrete surface preparation. To better understand what factors influenced the initial bond behavior between a profiled concrete surface and thermally applied zinc anode, the research team prepared additional sets of samples and traveled to Oregon in Fall 2010 to have them sprayed by Great Western Corporation. A design of experiments was also carried out to investigate how operational parameters might affect the resulting surface profile and composition and the initial bond strength of zinc to concrete or mortar. Cement mortar samples were fabricated, fully cured, and then used to provide baseline information to aid in the analysis of the bridge and concrete sample data. By removing the aggregates with diameter 0.25″ or bigger, the mortar samples had one of the influential variables removed, prior to surface profiling and arc-spraying of zinc. Furthermore, sections on the Pier 9 of the Yaquina Bay Bridge were selected as the "canvas" to investigate the relationship between surface profiling and the resulting bond strength of new TS-Zn to concrete. The Pier 9 (zone 16, with a surface area of 5,419 ft^2) was under ICCP with a nominal current density of 0.2 mA/ft^2 for approximately 14 years (1996–2010). The observations from this field trip that were not critical to this project but potentially useful are included as Appendix J.

4.4.1 Concrete and Mortar Samples

4.4.1.1 Mix design

The Portland cement concrete (PCC) samples produced in the laboratory were intended to represent the actual concrete used to construct the Yaquina Bay Bridge decades ago. Even though the maturity and phase changes of these PCC samples could not be matched to the existing bridge concrete, the basic mix constituent proportions were based on the information provided in the document "Specifications and Contract Agreement for Bridge Construction." The document was issued in May of 1929 by ODOT, which was the reference for all concrete and mortar mix designs used during the laboratory testing portion of this project.

Both materials, concrete and mortar, were cast into rectangular blocks that measured 12″ × 18″ × 1.5″. The concrete was placed into the forms and vibrated with an external vibration stinger. The final surface tooling did not occur until the bleed water dissipated from the surface. Once the surface was trowelled smooth the samples were covered with plastic for 24 hours. The samples were then uncovered, de-molded and subsequently placed into a fog-curing room with 100% humidity for six days. Thereafter, the samples were placed on pallets and stored outside in the elements until testing began.

The aggregate source and gradation for these laboratory mixtures were different than those used for the actual bridge construction. The maximum size aggregate for these laboratory mixes was ¾″ (19 mm) whereas the maximum aggregate size allowed during the construction of the Yaquina Bay Bridge was as big as 1.5″ (38 mm). There are differences in the composition of aggregate obtained in Oregon versus Montana but it

was decided that these differences in composition would not bias the planned test matrix in any obvious manner so Montana aggregates were used to produce the laboratory samples. Both the coarse and fine aggregates met the requirements of ASTM C33 for concrete aggregate. The minimum coarse aggregate size was a No. 4 (4.76 mm) and the maximum size aggregate was ¾″ (19 mm). A small percentage of the fine aggregate was finer than a 100 sieve, i.e., 149 μm (which was the smallest sieve used for the sand gradation).

Mix proportions for 1 cubic yard of concrete:

        Water–City of Bozeman   310 lbs
        Type I/II Portland Cement   563 lbs
        Coarse aggregate   2108 lbs
        Fine aggregate   1218 lbs

The quality of each batch of concrete was quantified in the plastic state by measuring the slump, air content and mix temperature. The average slump for this mix design was 5.0″ and the total air content ranged between 1.3 and 2.2 percent for the 17 mixes completed. This mix design did not have air entraining admixtures, and the measured air content was assumed to be entrapped air only. Each batch of concrete was also tested in the hardened state for compressive strength. For Class A concrete described in the ODOT document from 1929, the minimum 28-day strength was 2200 psi. The lab samples were tested only to see that the minimum strength requirement had been reached. It turned out that each of the concrete mixtures achieved in excess of 4000 psi at seven days.

Mortar samples were also prepared using the same basic mix design with some modifications. The primary change to the mix design was in the ratio of cement to sand. For the mortar mixes this ratio was 0.26, and for the concrete mixes the ratio was 0.46.

Mix proportions for 1 cubic yard of mortar

        Water-City of Bozeman   310 lbs
        Type I/II Portland Cement   563 lbs
        Fine aggregate   2108 lbs

The mortar was tested for compressive strength at 7 days to make sure it exceeded the minimum 28-day strength of 2200 psi. Much like the concrete mixes, the mortar exceeded 4000 psi at 7 days.

4.4.1.2 Surface profiling

To determine what surface features had significant influence on the initial bond strength between thermally sprayed zinc and concrete, 48 concrete samples and 24 mortar samples were profiled, thermally sprayed with zinc and bond tested. This work was completed at the McCullough Bay Bridge in North Bend, Oregon, according to a statistical design of experiments as shown in Table 4.2. Note that these PCC and mortar samples were 1

month old at the time of surface profiling; as such, they may not have been fully cured and are defined as "New PCC" and "New Mortar" in the discussions later.

Table 4.2: A Uniform Design table for sandblasting the PCC and mortar samples: U24(33).
http://www.math.hkbu.edu.hk/UniformDesign/

Air Pressure	Nozzle Size	No. of Passes
2	2	2
2	2	2
1	3	2
2	3	3
2	1	1
2	2	2
2	2	2
3	3	2
1	2	3
3	2	1
1	2	1
1	1	2
3	1	2
1	3	3
3	3	3
2	3	1
1	1	3
1	1	1
3	3	1
3	2	3
1	3	1
2	1	3
3	1	3
3	1	1
1=low	1=small	1=low
2=medium	2=medium	2=medium
3=high	3=large	3=high

The PCC and mortar samples were loaded into a containment enclosure on the bridge and allowed to acclimate for 24 hours as shown in Figure 4.25. The containment room temperature ranged between 80ºF and 90ºF throughout the work. The average sample surface temperature was in the low 80s ºF. The test matrix was separated into groups based on nozzle size, number of passes and sand volume. For this project, three nozzles sizes were used (#4, #6, #8). The sand volume (adjusted by pressure) had three levels: Low (L), Medium (M), High (H). The number of passes across the surface also had three levels: 1, 2, and 3. For example, a typical sample could have a designation of (8H2)

which translates to, a #8 nozzle, high sand volume and two passes across the surface. All of the samples (concrete and mortar) with the same treatment settings were profiled at the same time to minimize equipment changes.

Figure 4.25: PCC and mortar samples acclimatizing in enclosure.

Figure 4.26 shows a PCC test sample being profiled by a Great Western worker. This containment room was the remaining portion of the larger enclosure used by Great Western for application of zinc anode to the McCullough Bay bridge. As such, the environmental conditions were as close to production spraying conditions as possible.

Figure 4.26: Great Western worker profiling a concrete test sample.

For practical reasons, the surface profile was quantified in root mean square (RMS) macro-roughness (in place of 2-D macro-roughness and micro-roughness). RMS macro-roughness is a more common method of characterizing the surface profile. Figure 4.27 presents the relationship between the RMS roughness and the 2-D macro-roughness using the data from the preliminary investigation discussed earlier, which were strongly correlated for the PCC samples that were not electrochemically aged (ODOT) but less so

for those subjected to zinc spraying, electrochemical aging and subsequent zinc removal (NETL).
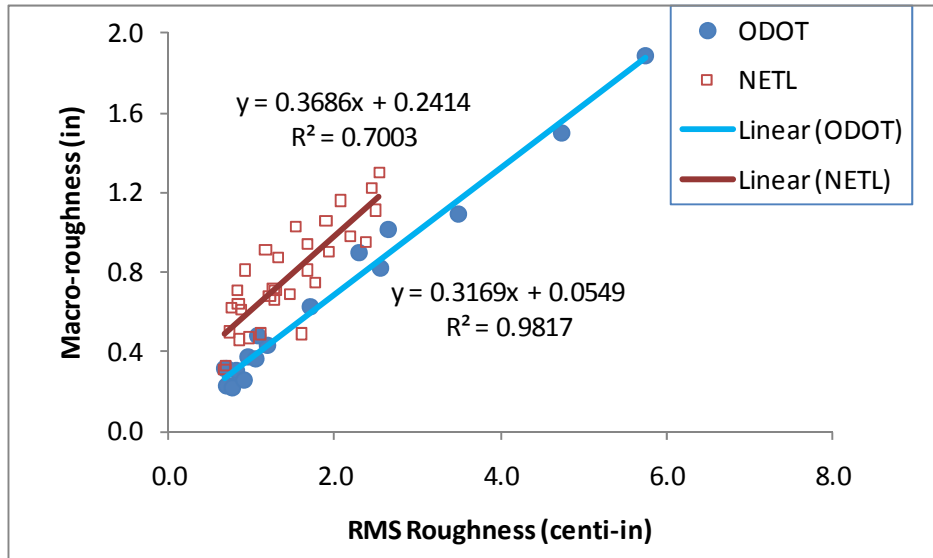

Figure 4.27: Relationship between 2-D macro-roughness and RMS macro-roughness.

Once the sample surface was fully profiled, three bond test sites were identified on each surface. A template was used to locate each of the three bond test sites on every sample. Each bond test site was outlined with a permanent marker on the surface so that RMS macro-roughness measurements could be made both before the application of TS-Zn and after the bond test in the exact same location (defined as "pre-roughness" and "post-roughness," respectively). Each RMS macro-roughness value was averaged from three measurements taken from the same bond test site. More details are provided in Appendix I.

The PCC samples featured much smoother surfaces after profiling, with pre-roughness values ranging from 0.2 and 1.1 centi-inches (averaged at 0.6), relative to the mortar samples (0.5-2.6, averaged at 1.2) and the Yaquina Bay Bridge concrete sections (0.5-2.4, averaged at 1.2). Similarly, the PCC samples featured much smoother surfaces after bond testing, with post-roughness values ranging from 0.2 to 1.2 centi-inches (averaged at 0.6), relative to the mortar samples (0.5-3.1, averaged at 1.4) and the Yaquina Bay Bridge concrete sections (0.3-2.9, averaged at 1.3). One likely explanation is that the PCC surface concrete was much stronger than the mortar surface or the bridge surface concrete and thus less prone to cement paste removal by aggressive sandblasting.

Since we did not measure the pre-roughness of the NETL samples investigated earlier, it was desirable to estimate their pre-roughness based on the measured post-roughness and some other relevant parameter (e.g., percent exposed aggregates). To this end, a 2-4-1 ANN model was trained and tested using the experimental data from the new PCC and mortar samples. As shown in Figure 4.28, the established model has relatively good "memory" and the trained matrices of interconnected weights and bias reflected the hidden functional relationship well. As such, the model was used to predict the pre-

roughness of the bond test sites as a function of the post-roughness and percent exposed aggregates.
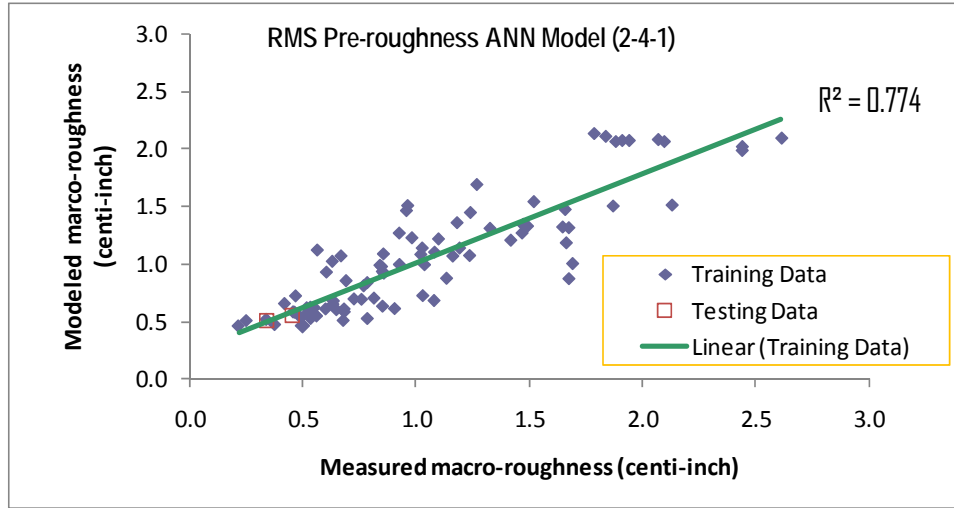

Figure 4.28: Performance of the ANN 4-7-1 model for pre-roughness.

As shown in Figure 4.29, the surfaces with high pre-roughness values tended to coincide with the surfaces with high post-roughness values and high concentration of exposed aggregates. Furthermore, the pre-roughness of bond test sites was generally lower than their post-roughness. This was due to the removal of additional mortar phase during the bond strength testing. Similarly, the percent exposed aggregates measured after the bond strength test was observed to be generally higher than that right after the surface profiling. For this project, a destructive chemical method (see Appendix G) was used to quantify the percent exposed aggregates. As such, only the percent of exposed aggregates after the bond testing was measured.
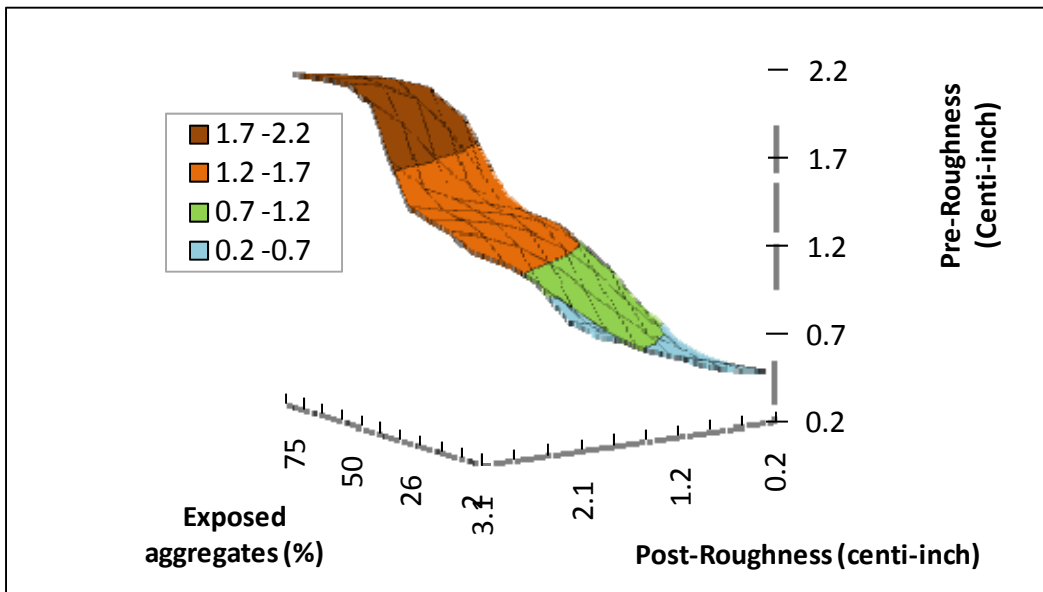

Figure 4.29: Predicted pre-roughness as a function of post-roughness and surface composition.

4.4.1.3 Arc-spraying with zinc

All of the concrete and mortar samples were sprayed with zinc, alternating the direction of travel top to bottom and side to side for each pass. The goal was to achieve a layer of zinc 17 mils (432 μm) thick. Mil tape (slices of duct tape) was placed on the surface of the samples so that the zinc thickness could be measured in real time. This was a method used by the zinc applicator to check his work so he could make additional passes if the layer was too thin. To achieve the 17-mil thickness, a minimum of eight passes, four in each direction, were required, and in some instances as many as 12 passes were made.

It should be noted that prior to applying the zinc, the surfaces of the samples were blown down with compressed air to remove any loose debris. The standoff distance for applying the zinc was roughly 8 to 12 inches. Due to the configuration of the zinc application gun and the changing geometry of a typical bridge structure, it was unrealistic to expect an exact standoff distance all of the time. The operator was very consistent with his movement of the application gun from start to finish of each pass but it should be noted that the bulkiness of the equipment certainly influenced the standoff distance. Fatigue was another factor that could manifest in variable standoff distances especially in the latter half of the work shift. The PCC and mortar samples that were sprayed for this investigation were on the ground in the containment enclosure and the applicator had unobstructed access to the sample from any direction so fatigue and standoff consistency were not much of an issue.

4.4.1.4 Bond testing

A total of 144 bond tests were completed on the 48 concrete samples and 72 tests on the 24 mortar samples. After the samples were sprayed with zinc, they were allowed to reacclimatize for a few hours before the bond dollies were epoxied to the surface. The template that was used to mark the surface of the samples before spraying with zinc was used to locate the bond test sites on the freshly zinc-coated surface. The dollies, 50 mm in diameter, were glued to the zinc surface using a high strength fast setting epoxy (Devcon^{TM} by ITW Performance Polymers). This product had a published tensile strength of 1250 psi at 1 hour. The epoxy was allowed to cure for 14 hours prior to starting the bond testing. Figure 4.30 shows the PCC and mortar samples in the enclosure with the bond dollies attached and being tested. The bond tester was a DeFlesko Posi-Test adhesion tester as shown earlier in Figure 4.9. Before the test samples were removed from the enclosure, the surface roughness was re-measured at the same locations that were measured before spraying and bond testing. The samples were then packed to protect the surfaces and brought back to the lab at WTI to measure the percentage of exposed aggregates versus paste at each bond test site. The standard operating procedure for quantifying the percent of exposed aggregates is provided in Appendix G.

Figure 4.30: PCC and mortar samples being bond tested.

It should be noted that the preliminary study discussed earlier defined exposed "rock" as aggregates with diameter 0.125″ or bigger, but the term "exposed aggregates" for the field-sprayed specimens included any visible aggregate that could be identified in the photo analysis program. This procedure was different from that illustrated in Figure 4.23 and led to higher readings of percent exposed aggregates. For instance, despite the absence of any aggregates with diameter 0.25″ or bigger, the mortar samples reported 2–54% exposed aggregates (averaged at 28%), slightly more than that of PCC samples (2–50%, averaged at 18%) and less than that of the Yaquina Bay Bridge concrete sections (5–75%, averaged at 36%).

Despite the absence of aggregates with diameter 0.25″ or bigger, the mortar samples did not show bond strengths that were significantly different from those of PCC samples. The mortar samples had bond strengths ranging from 115 to 286 psi (averaged at 193 psi), whereas the PCC samples had bond strengths ranging from 104 to 309 psi (averaged at 196 psi). As detailed earlier in section 4.4.1.1, the main difference between the PCC samples and the mortar samples was that the former had coarse aggregates (4.76 - 19 mm in diameter) added in them. As such, the bond strength results implied that the addition and exposure of these coarse aggregates (4.76 - 19 mm in diameter) had no significant influence on the bond strength of new zinc. The specific reason for this merits further investigation, which is also related to the feasibility of applying a cementitious mortar after the removal of old zinc and profiling of the concrete surface in the effort to enhance the bond strength of new zinc.

4.4.2 Field Trial at Yaquina Bay Bridge

The test sections on the Yaquina Bay Bridge were successfully profiled, sprayed and bond tested. The intent of field trials was to document the bond strength after different levels of abrasive blasting (and consequently, different levels of roughness and aggregate exposure). The

test sections included 12 ft by 12 ft areas that were profiled to different roughness and then arc-sprayed with zinc. These bridge sections were selected mainly based on the quality of existing concrete (e.g., level of cracking and air void characteristics), the condition of the old zinc anode, and the accessibility of the sections. Multiple bond tests were conducted on each section to further the effort to correlate surface condition to initial zinc–concrete bond strength. It was anticipated that these additional bond testing would increase the spread of data and improve the data distribution necessary to build a more robust ANN predictive model than the one described earlier (see Figure 4.28). The field trial took place on the south pier structure #8. The Great Western Corporation (GWC) was hired as the contractor to construct the containment enclosure, remove the failed anode by sandblasting, and to re-apply the 17-mil zinc anode to the south side of the pier structure from the ground level up to about 12 feet. Figure 4.31 shows the containment enclosure at the base of the pier, note the negative pressure. The atmospheric conditions during the field trial were fairly harsh, with high wind accompanied by rain during the profiling and zincing operations. The contractor did an outstanding job at keeping the surface free of moisture and at a temperature above 80ºF for the duration of the work.

Figure 4.31: Containment enclosure with negative pressure system and blast pot assembly: (left) external view; (right) internal view.

4.4.2.1 Anode removal and surface profiling

The pier structure was divided into nine sections; each section was used to try different blasting equipment configurations with respect to surface profiling. The entire south face on the west pier was used as the control. GWC was instructed to remove the failed zinc anode on this section using methods and techniques currently being employed at the McCullough Bay Bridge in North Bend, Oregon (#8 nozzle and high pressure). The remaining sections, the pile cap between the piers and the east face of the east pier were divided into eight experimental sections to accommodate the different sandblasting equipment configurations. Figure 4.32 shows the pile cap roughly outlined for six different sandblasting equipment settings (for #6 and #4 nozzles respectively). Notice that some of the anode was already debonded from the concrete before the profiling process started.

Figure 4.32: The bridge sections before anode removal by: (left) #6 nozzle; (right) #4 nozzle.

When the pressure was set at high, the #8, #6, and #4 nozzles featured an average sand volume of 11.8, 10.4, and 2.8 lbs/min for sandblasting operation. When the pressure was set at medium, the #8, #6, and #4 nozzles featured an average sand volume of 10.5, 7.3, and 2.4 lbs/min for sandblasting operation. When the pressure was set at low, the #8, #6, and #4 nozzles featured an average sand volume of 9.8, 7.3, and 2.9 lbs/min for sandblasting operation. Note that these sand volumes are roughly measured by the GWC personnel for information only.

Figure 4.33 shows the east pier after anode removal and subsequent profiling using a #8 nozzle and Figure 4.34 and Figure 4.35 show the pile cap after being profiled using various air pressure settings and #6 and #4 nozzles, respectively. The black circle outlines on the concrete surface are where the bond dollies were placed after the surface was applied with new TS-Zn. Each bond test site was selected based on how well it represented the overall surface condition for that test section.

Figure 4.33: The bridge section profiled by a #8 nozzle with medium and low sand volume. Medium profile is to the left of the red line.

(a)

(b)

(c)

Figure 4.34: The bridge section profiled by a #6 nozzle and (a) high, (b) medium, or (c) low sand volume.

(a)

(b)

(c)

Figure 4.35: The bridge section profiled by a #4 nozzle and (a) high, (b) medium, or (c) low sand volume.

It was observed that the old anode was mostly debonded from the concrete surface prior to this project work. As a result, the removal process was somewhat random with respect to the number of passes over the surface. In most places one or two passes was sufficient to remove the old anode. But as seen in the pictures above, the anode was well bonded at the form lines in the concrete surface which required more than two passes in most cases. The contractor made sure that any anode remaining after sand blasting was soundly bonded to the concrete. Areas where the old zinc anode had rough edges that would prohibit the new anode from bonding to the surface of the concrete were detailed by hand to smooth the edges down, in order to limit the surrounding concrete's exposure to sandblasting.

The visual and textural effects of the sandblasting on the Yaquina Bay Bridge concrete were significantly different from what occurred on the PCC and mortar samples. The surface texture of the bridge concrete after blasting had a denser burnished feel whereas the PCC and mortar samples had a more fractured roughness feel, similar to a coarse grit sand paper. The overall surface flatness of the bridge concrete at any given location was much less than it was for the laboratory-fabricated samples. This was in part due the age of the bridge structure and the maximum size aggregate used in its construction. The majority of the original mortar surface was either lost before the original anode was installed or more likely at the time of profiling the surface to install the original anode. As the paste eroded past the leading edges of the larger aggregates, depressions and crevices formed leading to the un-flatness of the surface and exposing a high percentage of larger rocks. Because this bridge was operating the ICCP for approximately 14 years, the surface composition also underwent significant changes that had an apparent hardening effect on the mortar fraction of the concrete surface. Figure 4.36 is an example of the irregular surface with a large concentration of exposed aggregates. The rough areas covered with new zinc had high concentrations of exposed aggregates; some areas had aggregate tops exposed that were over one inch in diameter.

Figure 4.36: Irregular concrete surface due to paste loss.

4.4.2.2 Bond test sites

After all of the sections were profiled, bond test sites were located and outlined on the surface with a permanent marker as shown in the previous pictures. The west pier was used as the control and had 12 bond test sites; the east pier was divided into two sections each with six bond test sites. Both of the pier sections were profiled with a #8 nozzle with the three different sand contents. The west pier (control) was profiled with a high volume of sand and the east pier had two levels of sand content, medium and low. The pile cap was split into six sections, three for the #6 nozzle at the three sand volumes and three sections for the #4 nozzles at the three sand volumes.

4.4.2.3 Zinc application

Re-application of the zinc anode to the bridge structure was completed using methods currently in practice at the McCullough Bay Bridge. The entire concrete surface was blown down with compressed air to remove any dirt or loose debris prior to starting the zincing process. This blowing step was repeated for every spray set-up, which was about every 9 square feet. The metalizer visually divided the surface into squares measuring approximately 3 ft per side and used the form lines on the surface or other visual references to define the spray area. Inside each of these "spray boxes," 3 pieces of mil tape were randomly placed so that the thickness measurements could be made after the arc-spray operation. The operator made eight passes, four in each direction and then checked the mil tape for thickness using a micrometer. If the layer was too thin, one or more passes would be made until the target thickness was obtained. For this investigation the target thickness was 17 mils, with the actual thicknesses ranging from 16 to 18 mils on the bridge sections.

Figure 4.37 shows the arc-spraying of new zinc onto the west pier. Notice the standoff distance was about 12 inches and the angle of the gun to the surface was approximately 90 degrees (see the left photo) or less (see the right photo). When the angle of spray incidence was less than 90 degrees, it generally increased the effective standoff distance. Figure 4.38 shows the arc-spraying of new zinc onto the pile cap section of pier structure, in which the metalizer was standing on the ground. These two figures illustrate that standoff distance was a variable that was mainly controlled by three factors during the real operations: the bulky configuration of the application gun with attached feed lines, the operator's stamina over an entire shift, and the geometry of the bridge section to be metalized. If these three variables are assumed inseparable and standoff distance is a critical parameter to successful anode application, then there is an inherent problem with the current methods.

Figure 4.37: GWC worker applying new anode to the south face of the west pier.

Figure 4.38: GWC worker applying new anode to the pile cap section of pier structure.

4.4.2.4 Bond testing

Figure 4.39 to Figure 4.41 show the west pier, the pile cap, and the east pier after applying the bond test dollies to the newly zinced surfaces respectively. Duct tape was

used to hold the dollies in place while the epoxy cured. Figure 4.42 is a close-up of a dolly bonded to the wall ready to have the excess epoxy around the edges and the drips removed, before conducting the bond tests. Removing the excess epoxy ensured that the bond test site being tested was truly a circle that was 50 mm in diameter.

The pile cap between the west and east pier was divided into six sections (Figure 4.40). Three sections were profiled with the #6 nozzle at the high, medium, and low sand contents. The #6 nozzle section was defined by the three areas to the far left in the picture outlined in red. The far left area was profiled with the high sand volume; the very next area was profiled with medium sand volume; and the last area in the # 6 series was profiled with the low sand content. The three areas to the right in the picture defined the #4 nozzle sections with the high sand volume section being the third area from the right-hand side of the picture.

Figure 4.39: South face of the west pier profiled with a #8 nozzle and high sand, control section.
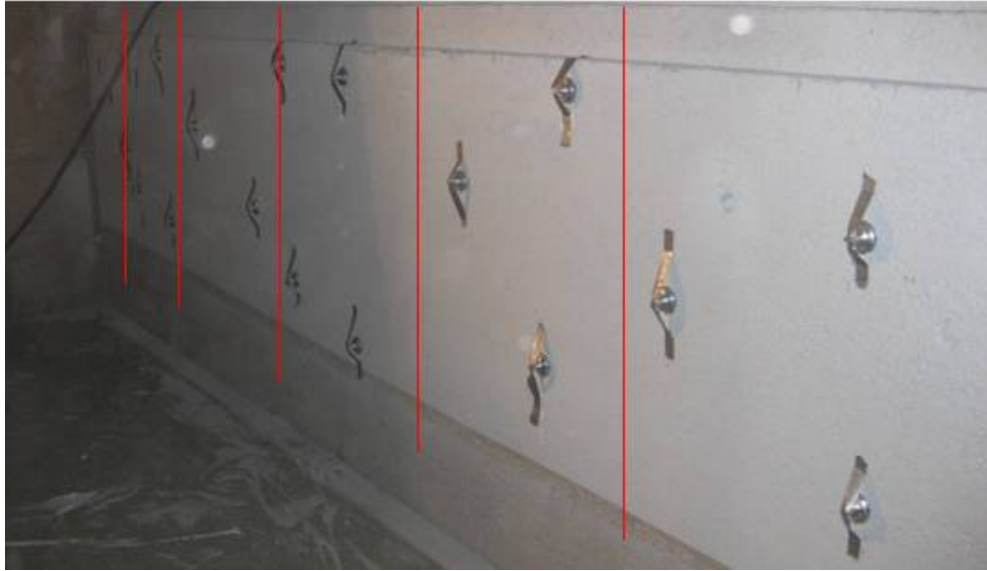
Figure 4.40: Pile cap section divided into the six test sections.

Figure 4.41: South face of the east pier divided into two sections, high and low sand content. Low sand content section is below the red line in the picture.

Figure 4.42: Close-up of test dolly bonded to the surface. The excess epoxy was removed before bond testing.

The Yaquina Bay Bridge concrete sections featured much lower bond strengths (43–248 psi, averaged at 151 psi) compared to the PCC samples (104-309 psi, averaged at 196 psi). One likely reason was the difference in the maximum aggregate size between the two. The maximum size aggregate for the PCC samples was ¾″ (19 mm), whereas the

99

maximum aggregate size allowed during the construction of the Yaquina Bay Bridge was as big as 1.5″ (38 mm). These results implied that once exposed by surface profiling the aggregates larger than ¾″ degraded the bond strength of new zinc. Another possible reason was that the current sandblasting protocol was too aggressive and might have "bruised" the bridge concrete surfaces and generated defects that led to poor bond of zinc to them. This was suggested by the fact that the bridge concrete samples had much rougher surfaces after profiling and validated by later findings related to the modeling of operating parameters for PCC and bridge concrete. It was hypothesized that a less aggressive sandblasting protocol and/or a more abrasion-resistant mortar treatment to the concrete surface after the old zinc was removed would have led to higher Zn–concrete or Zn–mortar bond strength.

Each of the 42 bond test sites on the bridge structure was treated with a phenolphthalein ($C_{20}H_{14}O_4$) solution to provide contrast between the cement paste fraction and the aggregate fraction for photographic analysis. The photographs for each bond test site were then run through an imaging program, ultimately generating a breakdown of the surface area with respect to what percentage was exposed aggregates and what percentage was paste. Figure 4.43 shows a close-up photo of a bond test site that was profiled with a #4 nozzle and low sand volume, as well as the pile cap section after phenolphthalein treatment.
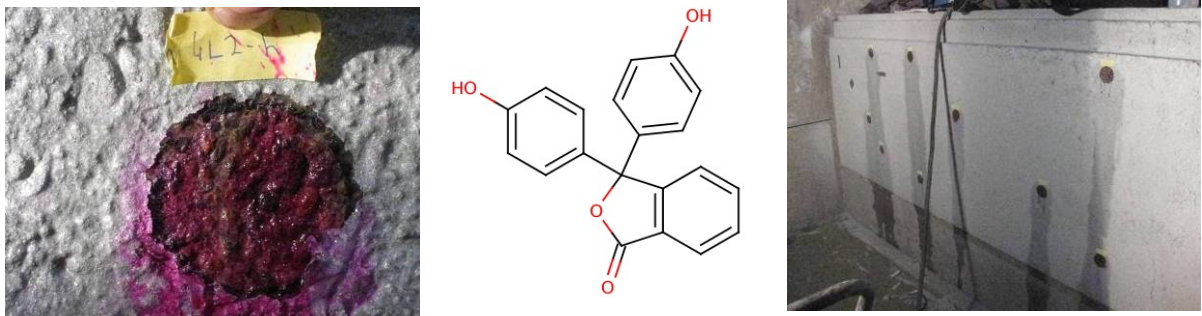

Figure 4.43: A bond test site treated with phenolphthalein (left), the molecular structure of phenolphthalein (middle), and a portion of pile cap after the treatment (right).

4.4.2.5 Measuring the percent exposed aggregates on bridge concrete

After all the photographs were taken, the phenolphthalein solution was washed from the surface of the concrete and new zinc using de-ionized water. The contractor hand detailed every bond test site prior to re-zincing the bond test sites to ensure there was no loose zinc that would inhibit the bond.

4.4.3 ANN Modeling of Bond Strength and Operating Parameters

4.4.3.1 Bond strength of new mortar samples

For ANN modeling of new mortar samples (1-month old, with equivalent electrochemical age of 0 years), three influential factors were chosen as input variables, i.e., percent

exposed aggregate area, RMS pre-roughness, and thickness of new zinc. The zinc-mortar bond strength was chosen as the output variable. The ANN model was established by appropriately choosing the architecture and training process. The model was trained and tested using the 24 data points obtained from measurements of mortar samples. Each data point was averaged from measurements from three bond test sites that were treated under a certain set of operating parameters, following the design shown in Table 4.2. To determine what surface features had significant influence on the initial bond strength between thermally sprayed zinc and concrete, 48 concrete samples and 24 mortar samples were profiled, thermally sprayed with zinc and bond tested. This work was completed at the McCullough Bay Bridge in North Bend, Oregon, according to a statistical design of experiments as shown in Table 4.2. Note that these PCC and mortar samples were 1 month old at the time of surface profiling.

The topological structure of the ANN model was determined to be 3-6-1 on the basis of trial-and-error. The SMSE from the training data set (23 samples) and testing data set (1 sample) was 0.105 and 0.081 respectively. The model performance is shown in Figure 4.44 which indicates that the established model has good "memory" and the trained matrices of interconnected weights and bias reflect the hidden functional relationship well. As such, the model was used to predict the bond strength as a function of influential factors. In the following sections, the model predictions are presented in the form of 3-D response surfaces to best illustrate the complex interactions between influential factors.
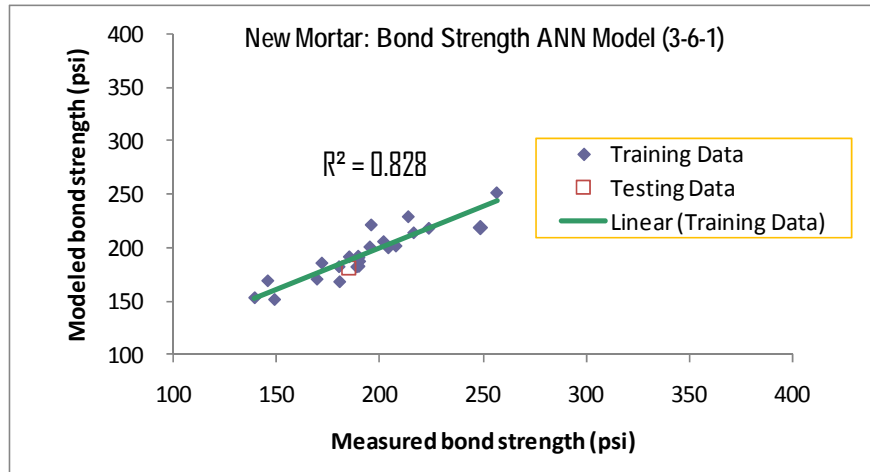

Figure 4.44: Performance of the ANN 3-6-1 model for bond strength of new mortar.

From a modeling perspective, ANN was used to achieve better understanding of the complex cause-and-effect relationships inherent in the zinc-mortar system and was successful in finding meaningful, logical results from the bond strength data. As shown in Figure 4.45, for mortar with an electrochemical age of 0 years and 28% exposed aggregates, the bond strength exhibited two main trends with 12-20 mils of new Zn: for rougher surface, the thicker the Zn layer, the higher the bond strength; for the smoother surface, the thinner the Zn layer, the higher the bond strength. Furthermore, too rough or too smooth a mortar surface would not lead to high bond strength, which is also illustrated in Figure 4.46. The figure also reveals that for mortar with an electrochemical

age of 0 years and 17.5 mils of new Zn, higher bond strength values generally coincided with mortar surfaces with a moderate level of surface macro-roughness, but the dependency of bond strength on exposed fine aggregates was less significant.
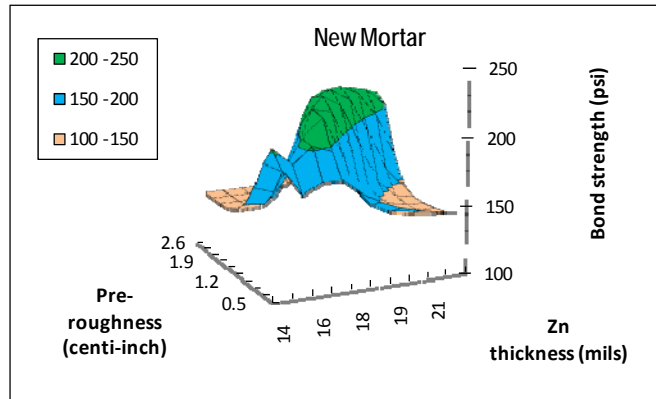

Figure 4.45: Predicted bond strength of new mortar as a function of pre-roughness and Zn thickness, with an electrochemical age of 0 years and 28% exposed aggregates.
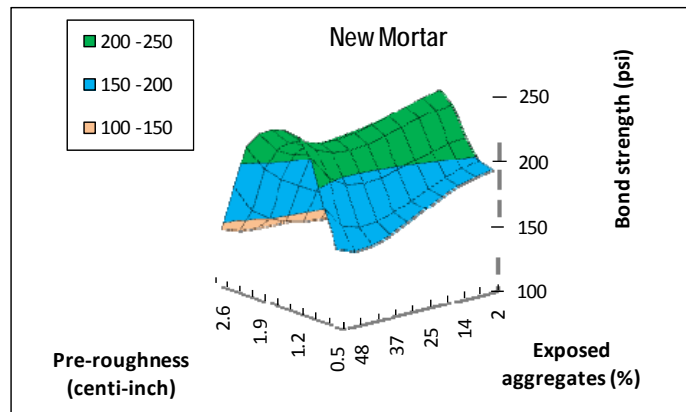

Figure 4.46: Predicted bond strength of new mortar as a function of pre-roughness and surface composition, with an electrochemical age of 0 years and 17.5 mils of new Zn.

For new mortar samples with an electrochemical age of 0 years, it should be noted that their pre-roughness featured a strong correlation with their concentration of exposed aggregates (as shown in Figure 4.47). In other words, it was practically difficult to achieve a surface with high concentration of exposed aggregates but low roughness or with low concentration of exposed aggregates but high roughness.
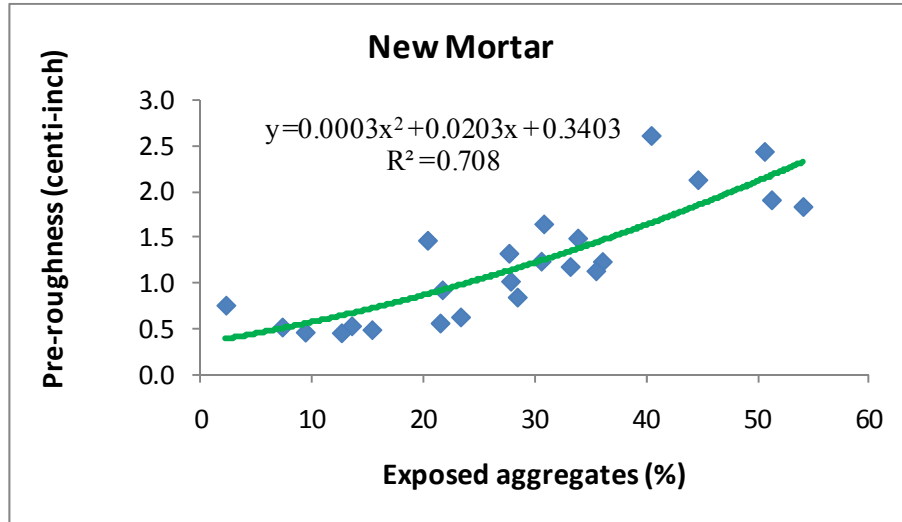
New Mortar

$$y=0.0003x^2+0.0203x+0.3403$$
$$R^2=0.708$$

Figure 4.47: Relationship between pre-roughness and surface composition of mortar samples.

4.4.3.2 Operating parameters for new mortar samples

For ANN modeling of new mortar samples (1-month old, with equivalent electrochemical age of 0 years), three influential factors were chosen as input variables: nozzle size, sand volume, and number of passes. The output variable was defined as pre-roughness, delta-roughness (i.e., post-roughness – pre-roughness), and zinc-mortar bond strength respectively. The topological structure of these three ANN models was determined to be 3-4-1 on the basis of trial-and-error. All the SMSE values from the training data set (23 samples) and testing data set (one sample) were in the range of 0.085 and 0.098, suggesting reasonable performance of these models. As the influential factors are non-continuous variables, the model predictions could not be presented in the form of 3-D response surfaces. Instead, the established ANN models were used to predict the outcome of every possible combination of operating parameters, as shown in Table 4.3.

Table 4.3 shows that five operating configurations (8H3, 8H2, 6M3, 6L3, 6M2 highlighted in green color) led to the highest bond strengths of new zinc to the profiled mortar surface, whereas five other operating configurations (6L2, 8L3, 4M3, 4M2, 4M1) led to the lowest bond strengths. The most desirable operating configuration seemed to be 8H3, i.e., a #8 nozzle, high sand volume and three passes across the mortar surface. This specific operating configuration also led to a high level of exposed fine aggregates (32.8%), a high pre-roughness (1.68 centi-inches), and a moderate reduction in the macro-roughness after the bond testing (0.17 centi-inches).

103

Table 4.3: ANN prediction of new mortar samples processed by various operating configurations

NozzleSize	Sand Volume	# of Passes	% rock	Pre-roughness (centi-inch)	delta-roughness (centi-inch)	Bond Strength (psi)
4	L	1	28.7	1.03	0.15	202
4	L	2	18.6	1.48	0.15	185
4	L	3	14.5	0.51	0.19	181
4	M	1	14.2	0.52	0.16	142
4	M	2	27.0	0.47	0.15	142
4	M	3	33.1	1.18	0.16	143
4	H	1	5.5	0.77	0.50	170
4	H	2	6.7	0.46	0.16	185
4	H	3	7.9	0.56	0.15	190
6	L	1	13.9	0.53	0.17	192
6	L	2	18.2	1.72	-0.39	160
6	L	3	25.6	0.86	0.08	217
6	M	1	23.1	0.94	0.19	204
6	M	2	38.1	1.30	0.36	216
6	M	3	40.3	2.41	0.19	217
6	H	1	28.5	1.24	0.77	172
6	H	2	39.6	0.46	0.77	196
6	H	3	48.3	1.89	0.46	214
8	L	1	20.6	0.50	0.76	192
8	L	2	35.8	1.23	-0.26	191
8	L	3	44.3	2.61	0.50	149
8	M	1	27.2	1.24	0.18	192
8	M	2	36.3	1.41	-0.35	164
8	M	3	46.9	2.44	-0.23	190
8	H	1	38.2	1.24	-0.35	190
8	H	2	41.1	2.13	-0.34	224
8	H	3	32.8	1.68	-0.17	248

Note: The green and yellow colors indicate extreme values in the bond strength or surface conditions.

4.4.3.3 Bond strength of new PCC samples

For ANN modeling of new PCC samples (1 month old, with equivalent electrochemical age of 0 years), three influential factors were chosen as input variables, i.e., percent exposed aggregate area, RMS pre-roughness, and thickness of new zinc. The zinc–concrete bond strength was chosen as the output variable. The ANN model was established by appropriately choosing the architecture and training process. The model was trained and tested using the 24 data points obtained from measurements of mortar samples. Each data point was averaged from measurements from three bond test sites that were treated under a certain set of operating parameters, following the design shown in Table 4.2. The topological structure of the ANN model was determined to be 3-5-1 on the basis of trial-and-error. The SMSE from the training data set (23 samples) and testing data set (1 sample) was 0.093 and 0.076 respectively. The model performance is shown in Figure 4.48, which indicates that the established model has good "memory" and the trained matrices of interconnected weights and bias reflect the hidden functional relationship well. As such, the model was used to predict the bond strength as a function

of influential factors. In the following sections, the model predictions are presented in the form of 3-D response surfaces to best illustrate the complex interactions between influential factors.
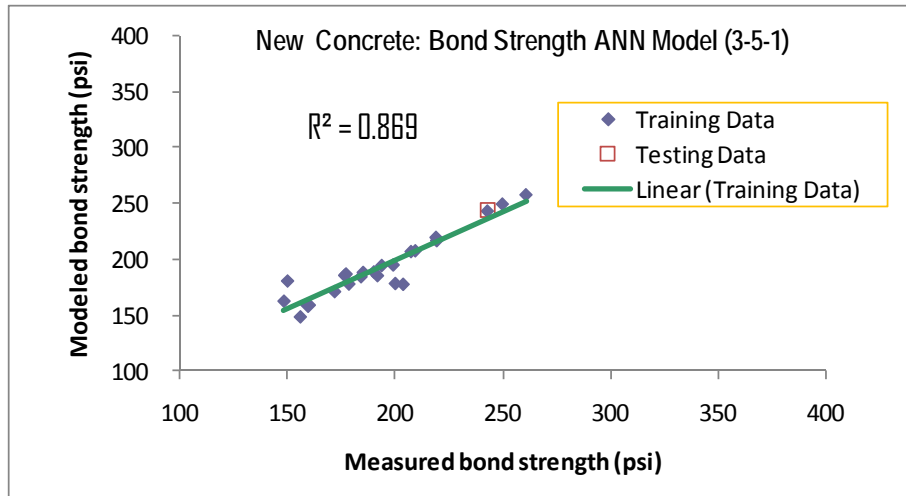

Figure 4.48: Performance of the ANN 3-5-1 model for bond strength of new PCC.

From a modeling perspective, ANN was used to achieve a better understanding of the complex cause-and-effect relationships inherent in the zinc-concrete system and was successful in finding meaningful, logical results from the bond strength data. As shown in Figure 4.49, for PCC with an electrochemical age of 0 years and 13.4% exposed aggregates, the highest bond strength values were found with the rough surfaces (0.9 -1.1 centi-inches), in which case the effect of Zn thickness (12-20 mils) was negligible. For the smooth surfaces (0.2-0.3 centi-inches), the relative high bond strength values corresponded with intermediate Zn thickness (15-17 mils), which coincided relatively well with the target thickness of current ODOT specifications. Figure 4.50 also reveals that for PCC with an electrochemical age of 0 years and 16.8 mils of new Zn, the highest bond strength values were found for surfaces with less exposed aggregates (<13%), in which case the rougher surfaces were generally beneficial. The rougher surface likely provided more and larger "anchor points" for the molten zinc to adhere to. Another preferred combination featured a very smooth surface (0.2-0.3 centi-inches) and a moderate level of exposed aggregates (18%-34%), for unknown reasons.
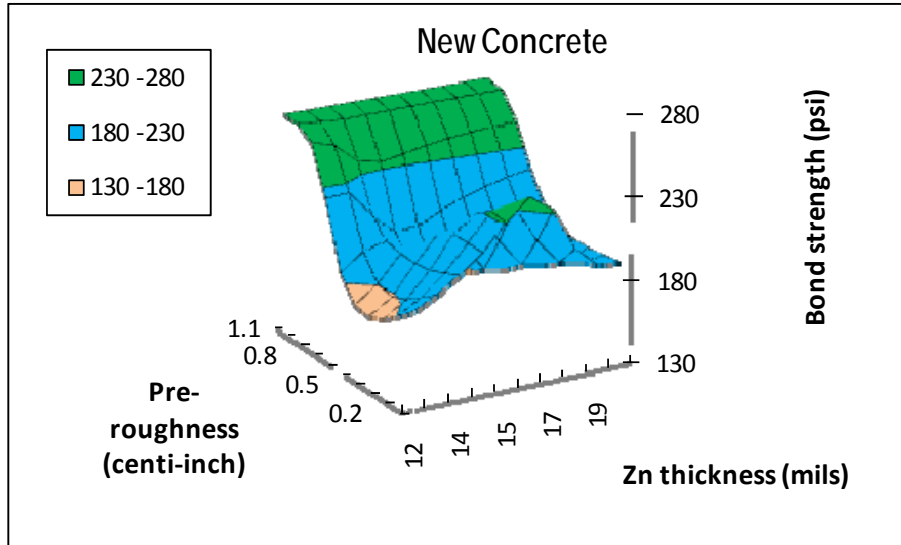
Figure 4.49: Predicted bond strength of new PCC as a function of pre-roughness and Zn thickness, with an electrochemical age of 0 years and 13.4% exposed aggregates.
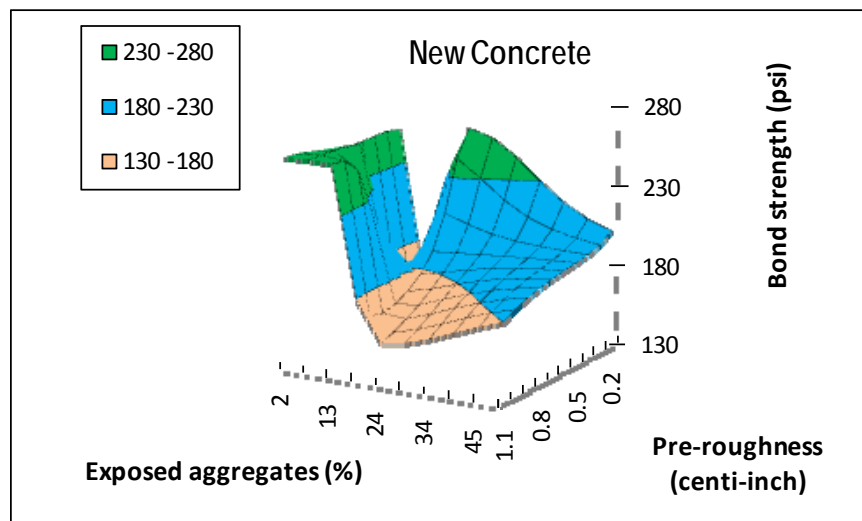

Figure 4.50: Predicted bond strength of new PCC as a function of pre-roughness and surface composition, with an electrochemical age of 0 years and 16.8 mils of new Zn.

For new PCC samples with an electrochemical age of 0 years, it should be noted that their pre-roughness featured a relatively strong correlation with their concentration of exposed aggregates (as shown in Figure 4.51). In other words, it was practically difficult to achieve a surface with high concentration of exposed aggregates but low roughness or with low concentration of exposed aggregates but high roughness.
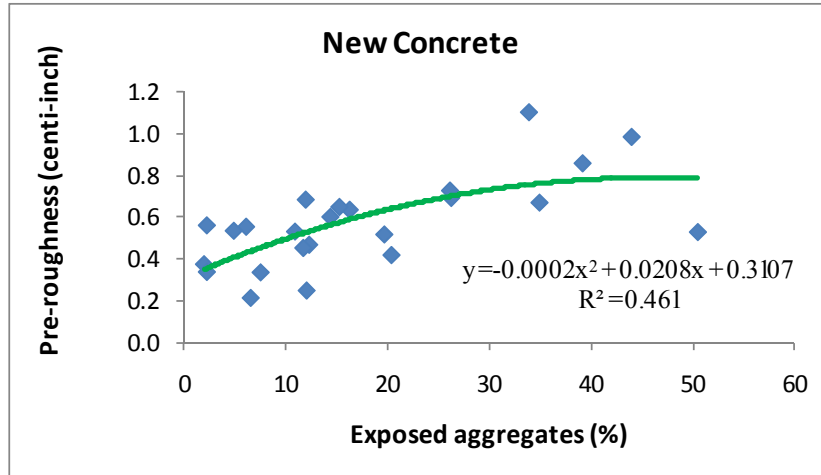
Figure 4.51: Relationship between pre-roughness and surface composition of new PCC samples.

4.4.3.4 Operating parameters for new PCC samples

For ANN modeling of new PCC samples (1-month old, with equivalent electrochemical age of 0 years), three influential factors were chosen as input variables: nozzle size, sand volume, and number of passes. The output variable was defined as pre-roughness, delta-roughness, and zinc–concrete bond strength respectively. The topological structure of these three ANN models was determined to be 3-4-1 on the basis of trial-and-error. All the SMSE values from the training data set (23 samples) and testing data set (1 sample) were in the range of 0.050 and 0.086, suggesting reasonable performance of these models. As the influential factors are non-continuous variables, the model predictions could not be presented in the form of 3-D response surfaces. Instead, the established ANN models were used to predict the outcome of every possible combination of operating parameters, as shown in Table 4.4.

Table 4.4: ANN prediction of new PCC samples processed by various operating configurations.

NozzleSize	Sand Volume	# of Passes	% rock	Pre-roughness (centi-inch)	delta-roughness (centi-inch)	Bond Strength (psi)
4	L	1	2.1	0.37	0.07	261
4	L	2	2.1	0.32	-0.15	243
4	L	3	12.1	0.30	0.16	178
4	M	1	2.5	0.48	0.00	250
4	M	2	3.2	0.34	-0.19	148
4	M	3	5.1	0.51	-0.05	192
4	H	1	6.7	0.31	0.09	158
4	H	2	8.6	0.25	-0.02	219
4	H	3	10.3	0.48	0.07	200
6	L	1	10.3	0.46	0.47	190
6	L	2	39.4	0.52	0.26	156
6	L	3	50.0	0.51	-0.09	205
6	M	1	16.3	0.57	0.13	182
6	M	2	25.6	0.62	0.17	171
6	M	3	16.9	0.70	-0.07	207
6	H	1	18.1	0.42	0.26	220
6	H	2	14.6	0.53	0.24	259
6	H	3	13.9	0.71	-0.05	207
8	L	1	15.4	0.53	0.08	149
8	L	2	15.5	0.58	0.04	176
8	L	3	39.1	0.83	0.10	193
8	M	1	14.8	0.60	0.04	242
8	M	2	12.5	0.66	0.05	160
8	M	3	43.6	0.99	0.11	174
8	H	1	8.7	0.53	0.07	207
8	H	2	26.2	0.68	0.06	200
8	H	3	33.4	1.04	0.11	154

Note: The green and yellow colors indicate extreme values in the bond strength or surface conditions.

Table 4.3 shows that five operating configurations (4L1, 6H2, 4M1, 4L2, 8M1) led to the highest bond strengths of new zinc to the profiled PCC surface, whereas five other operating configurations (4H1, 6L2, 8H3, 8L1, 4M2) led to the lowest bond strengths. The most desirable operating configuration seems to be 4L1, i.e., a #4 nozzle, low sand volume and only one pass across the mortar surface. This specific operating configuration also led to a very low level of exposed aggregates (2.1%), a low pre-roughness (0.37 centi-inches), and a small increase in the macro-roughness after the bond testing (0.07 centi-inches). It should be noted that these PCC surfaces did not have any existing zinc to be removed; consequently, one pass of sandblasting was sufficient to achieve the desired surface profile featuring a low concentration of exposed aggregates and a low macro-roughness. The findings shown in Table 4.4 are very useful in defining the operating protocol for profiling new concrete surfaces prior to the installation of TS-Zn coating or potentially other types of thermally sprayed coating.

4.4.3.5 Bond strength of Fully Cured Concrete

For ANN modeling of fully cured concrete samples, three influential factors were chosen as input variables: percent exposed aggregate area, RMS pre-roughness, and equivalent electrochemical age. The zinc–concrete bond strength was chosen as the output variable. The ANN model was established by appropriately choosing the architecture and training process. The model was trained and tested using the data points from the preliminary investigation (31 ten-year old NETL samples, 18 nine-month old PCC samples, and three rock samples) as well as 42 data points from the seventy-five year old Yaquina Bay Bridge sections. Each data point was averaged from measurements from three bond test sites that were treated under a certain set of operating parameters. Note that the missing pre-roughness data of some samples were estimated from post-roughness and percent exposed aggregates using the predictive model discussed earlier.

The topological structure of the ANN model was determined to be 3-11-1 on the basis of trial-and-error. The SMSE from the training data set (91 samples) and testing data set (three samples) was 0.079 and 0.095, respectively. The model performance is shown in Figure 4.52, which indicates that the established model has good "memory" and the trained matrices of interconnected weights and bias reflect the hidden functional relationship well. As such, the model was used to predict the bond strength as a function of influential factors. In the following sections, the model predictions are presented in the form of 3-D response surfaces to best illustrate the complex interactions between influential factors.
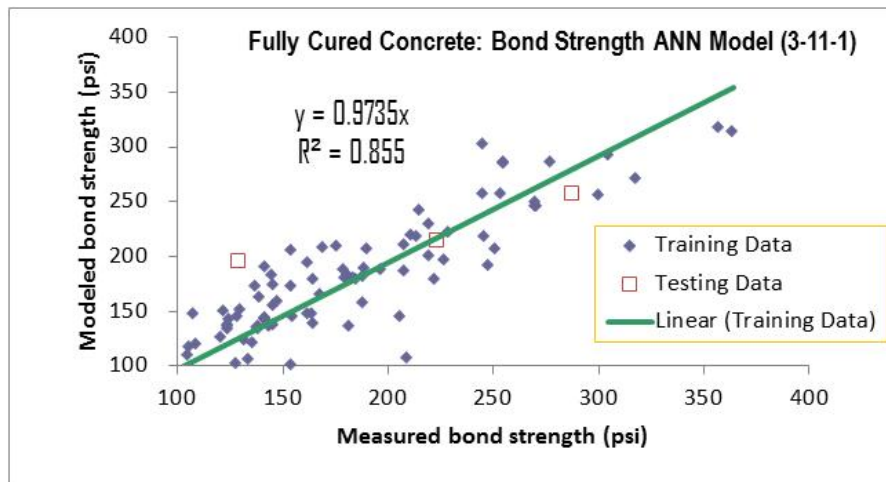

Figure 4.52: Performance of the ANN 3-11-1 model for bond strength of fully cured concrete.

From a modeling perspective, ANN was used to achieve better understanding of the complex cause-and-effect relationships inherent in the zinc-concrete system and was successful in finding meaningful, logical results from the bond strength data.

As shown in Figure 4.53, for fully cured concrete with a moderate level of exposed aggregates (35%), the ideal surface macro-roughness varied significantly with the electrochemical age of the concrete. For concrete with an electrochemical age of 0-5

years, the surface macro-roughness after profiling should be maintained at higher than 1.1 centi-inches. The ideal surface macro-roughness changed to 0.8-1.5, 1.3-1.5, 0.4-0.8, and 0.4-1.3 centi-inches, for concrete with an electrochemical age of 10, 15, 20, and 25 years respectively. As the electrochemical age of concrete further increased, the highest bond strengths tended to gradually shift to smoother surfaces.
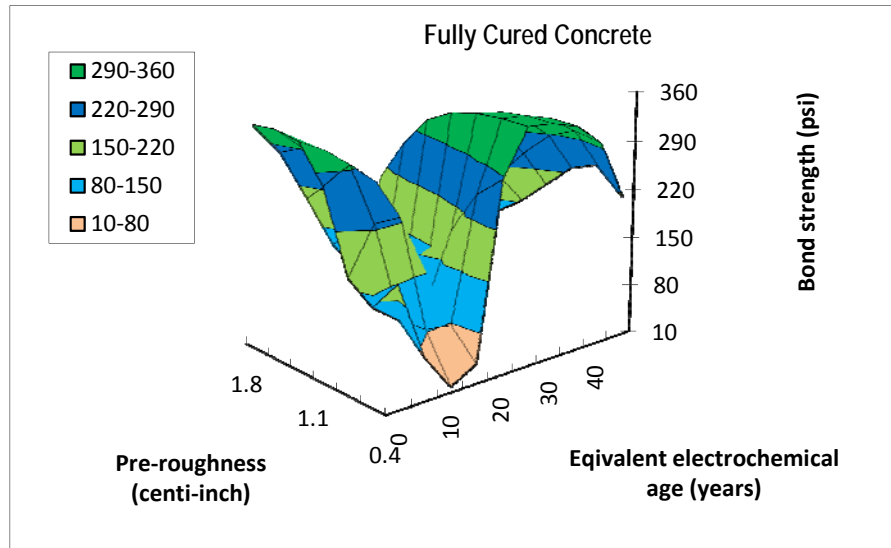

Figure 4.53: Predicted bond strength of fully cured concrete as a function of pre-roughness and electrochemical age, with 35% exposed aggregates and 17 mils of new Zn.

The change of ideal surface roughness with electrochemical age was likely linked to how the chemistry and microstructure of the concrete surface layer beneath the arc-sprayed zinc evolved over the duration of electrochemical aging. As discussed earlier in Chapter 1, Holcomb et al. *(1997)* proposed a four-parameter empirical model to account for the evolution of anode adhesion strength over the electrochemical age (see Figure 1.2). They also proposed the following strengthening and weakening mechanisms for the TS-Zn adhesion on concrete: "The initial zinc coating had a purely mechanical bond to the concrete… Upon electrochemical aging, the ZnO that formed decreased the mechanical bonding due to a volume expansion. With additional aging, secondary mineralization locally strengthened the bond at the coating–concrete interface and led to an increase in adhesion strength. With increased electrochemical aging, inhomogeneities in the ZnO thickness … created stresses and cracking within zone 1 and at the zone 1–zone 2 interface. The cracking eventually decreased the adhesion strength of the zinc coating to zero."

Figure 4.57 also shows that the lowest bond strength values are expected near the electrochemical age of 14, which coincides with that of the Yaquina Bay Bridge Pier 9. It is cautioned that the bridge concrete that provided the data points for electrochemical age of 14 years had been in service for 75 years, whereas the laboratory concrete samples that provided the data points of other electrochemical ages (0, 5, 9, 22, 38, 45) was never in service. As such, the model might have been skewed by the data points from the bridge sections. As discussed earlier, the Yaquina Bay Bridge concrete sections featured much

lower bond strengths (43–248 psi, averaged at 151 psi) than the PCC samples (104–309 psi, averaged at 196 psi). One likely reason is the difference in the maximum aggregate size between the two. The maximum size aggregate for the PCC samples was ¾″ (19 mm) whereas the maximum aggregate size allowed during the construction of the Yaquina Bay Bridge was as big as 1.5″ (38 mm). These results implied that once exposed by surface profiling, the aggregates larger than ¾″ degraded the bond strength of new zinc. Another possible reason was that the current sandblasting protocol was too aggressive and might have "bruised" the bridge concrete surfaces and generated defects that led to poor bond of zinc to them. This was implied by the fact that the bridge concrete samples had much rougher surfaces after profiling and validated by later findings related to the modeling of operating parameters for PCC and bridge concrete. It was hypothesized that a less aggressive sandblasting protocol and/or a more abrasion-resistant mortar treatment to the concrete surface after the old Zn is removed would lead to higher Zn–concrete or Zn–mortar bond strength.

Figure 4.54 also reveals that for PCC with an electrochemical age of 0 years and 17 mils of new Zn, the highest bond strength values generally coincided with surfaces with a moderate level of macro-roughness (1.1-1.8 centi-inches) and relatively low concentration of exposed aggregates (5-36%).
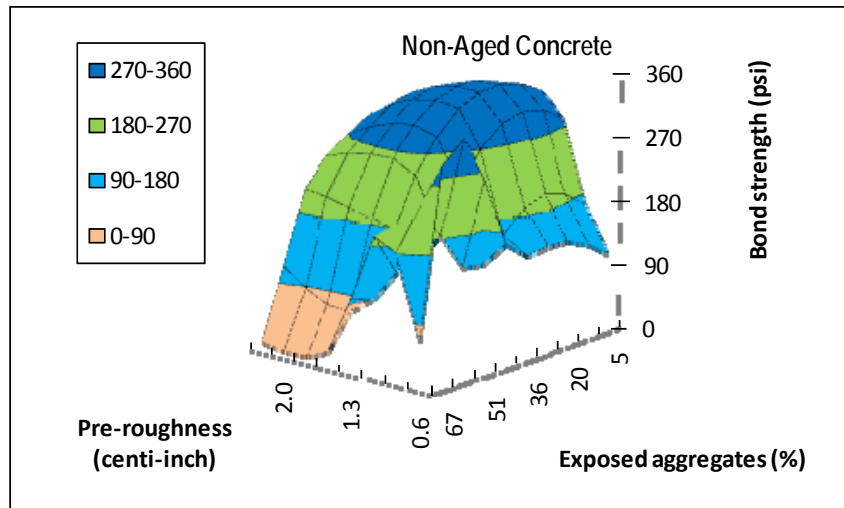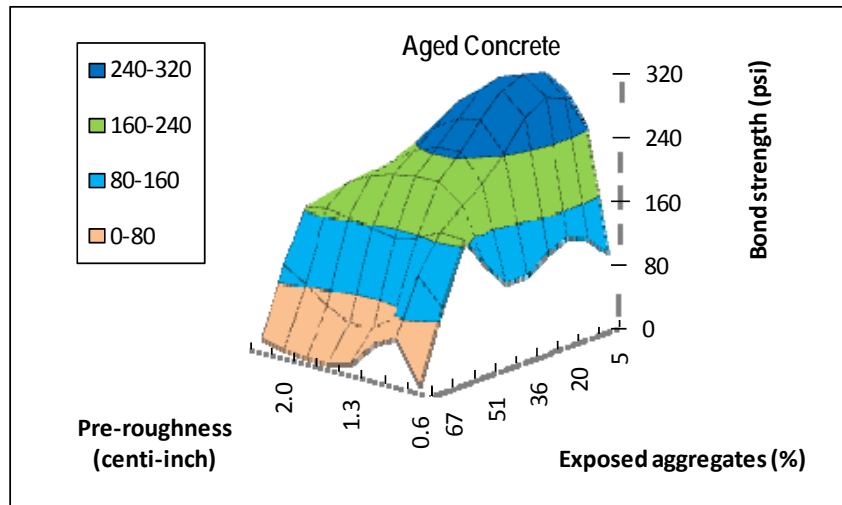

Figure 4.54: Predicted bond strength of fully cured concrete as a function of pre-roughness and surface composition, with electrochemical age of 0 yrs and 17 mils of new Zn.

Figure 4.55 also reveals that for existing concrete with relatively young electrochemical age (eight years under CP current density of 0.2 mA/ft^2) and 17 mils of new Zn, the highest bond strength values generally coincided with surfaces with a moderate level of macro-roughness (1.1-1.5 centi-inches) and relatively low concentration of exposed aggregates (12-36%).

111

Figure 4.55: Predicted bond strength of fully cured concrete as a function of pre-roughness and surface composition, with electrochemical age of eight yrs and 17 mils of new Zn.

Figure 4.56 also reveals that for existing concrete with relatively high electrochemical age (14 years under CP current density of 0.2 mA/ft^2) and 17 mils of new Zn, the highest bond strength values generally coincided with surfaces with a moderate level of macro-roughness (1.1-1.5 centi-inches) and a moderate level of exposed aggregates (44-67%). If too much aggregate phase were exposed (e.g., 67–75%), it would expose a proportionally high concentration of large aggregates and thus negatively affect the bond strength of new zinc. This unravels the complex role of exposed aggregates in affecting the initial bond strength of arc-sprayed zinc to the profiled concrete surface, with the surface of large aggregates providing poor bonding to TS-Zn but small aggregates providing beneficial "anchor" spots around them. While not experimentally validated in this work, it is also known that the exposure of too much aggregate phase (e.g., by deep profiling) can increase the electrical resistance of the anode-concrete interface and thus affect the performance of the ICCP system. In light of field observations and the caveats of the modeling discussed earlier, the ideal level of exposed aggregates should avoid the higher end of the model predictions (i.e., maintained at 44–55%). Wherever possible, large aggregates (e.g., diameters ¾″ and bigger) should be avoided for exposure by surface profiling.
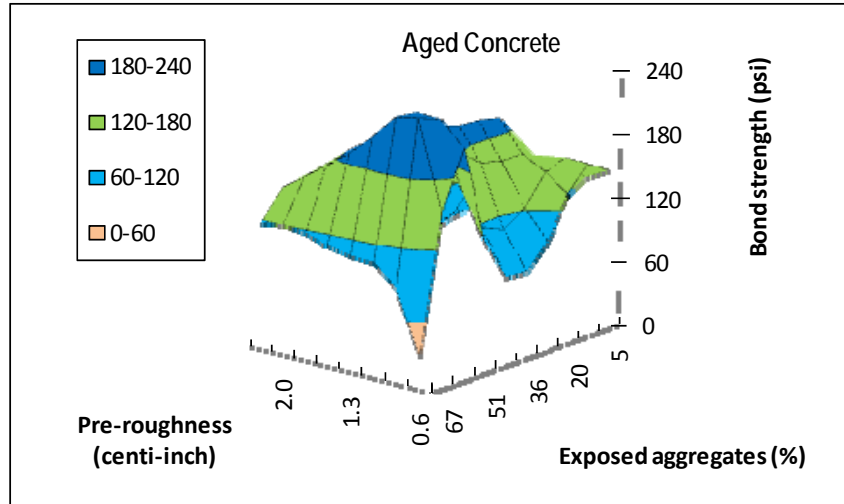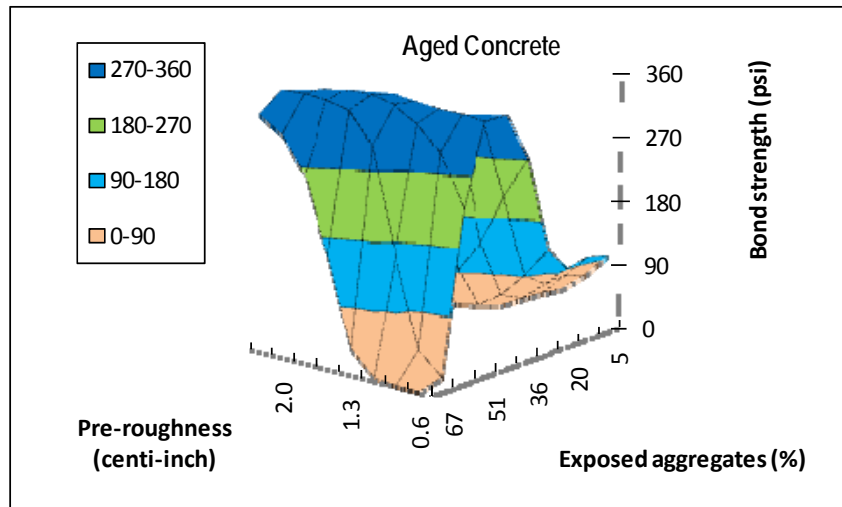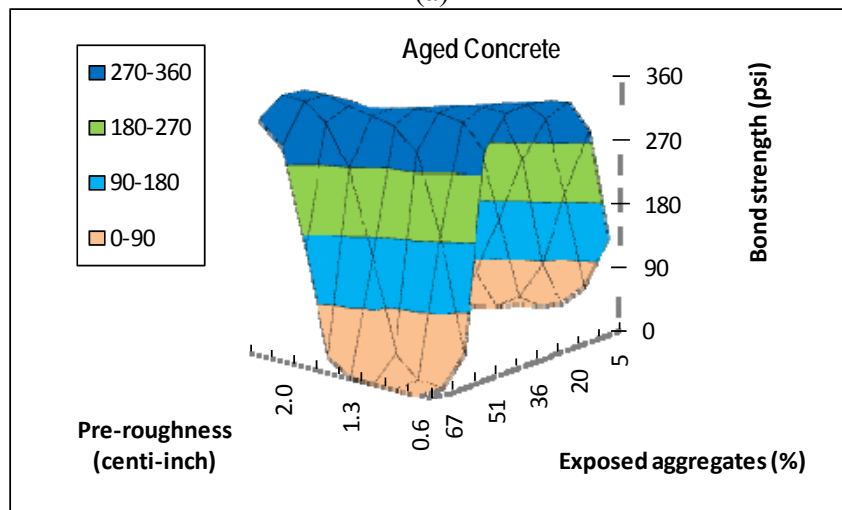
Figure 4.56: Predicted bond strength of fully cured concrete as a function of pre-roughness and surface composition, with electrochemical age of 14 yrs and 17 mils of new Zn.

Figure 4.57 also reveals that for existing concrete with high electrochemical age (20 years and 27 years under CP current density of 0.2 mA/ft^2) and 17 mils of new Zn, the highest bond strength values generally coincided with surfaces with a relatively low level of macro-roughness (0.6-1.1 centi-inches) and a moderate level of exposed aggregates (44–51%).

Figure 4.57: Predicted bond strength of fully cured concrete as a function of pre-roughness and surface composition, with 17 mils of new Zn and electrochemical age of (a) 20, and (b) 27 years.

4.4.3.6 Operating parameters for Yaquina Bay Bridge concrete

The previous sections shed light on the desired levels of surface profile and exposed aggregates, for a concrete with a given electrochemical age to achieve high initial bond strength of newly arc-sprayed zinc. As discussed earlier, for existing concrete with relatively high electrochemical age (14 years under CP current density of 0.2 mA/ft^2) and 17 mils of new Zn, the desirable surface after profiling should have a moderate level of macro-roughness (1.1-1.5 centi-inches) and a moderate level of exposed aggregates (44-55%). The following section will examine the influence of operating parameters on such surface properties of electrochemically aged concrete subsequent to the sandblasting.

For ANN modeling of Yaquina Bay Bridge concrete sections (with equivalent electrochemical age of 14 years), three influential factors were chosen as input variables,

i.e., nozzle size, sand volume, and percent exposed aggregates. The output variables were defined as pre-roughness, delta-roughness, and zinc–concrete bond strength. Note that the percent exposed aggregates was used as a surrogate variable for the number of passes since the number of passes for surface profiling on the bridge sections was not recorded (generally more than three passes). The topological structure of the models was determined to be 3-5-1, 3-5-1, and 3-7-1 for pre-roughness, delta-roughness, and bond strength, respectively, on the basis of trial and error. All the SMSE values from the training data set (40 samples) and testing data set (two samples) were in the range of 0.094 and 0.125, suggesting acceptable performance of these models. The relatively high SMSE values may be attributable to the fact that the number of passes data were missing and could not be used for the modeling.

Before proceeding to model prediction results, however, this section will examine some of the relevant cause-and-effect relationships using the 42 data points obtained from the bridge sections. As shown in Figure 4.58, relative to non-aged mortar and PCC samples (see Figure 4.51 and Figure 4.55), the macro-roughness of the electrochemically aged bridge featured a weaker correlation with their concentration of exposed aggregates. Nonetheless, it was practically difficult to achieve a surface with very high concentration of exposed aggregates but low roughness or with very low concentration of exposed aggregates but high roughness. As shown in Figure 4.59, when examined individually, the measured bond strength of new zinc to the profiled old concrete did not exhibit any statistically significant correlation with nozzle size or sand volume. Apparently there were strong interactions between these influential factors. That is why a more powerful tool such as ANN was needed to elucidate the complex cause-and-effect relationships. ANN models were established for predictions, as shown below, to illustrate the interactions between influential factors and to identify the ideal operating configurations for achieving the desired surface profile and bond strength.
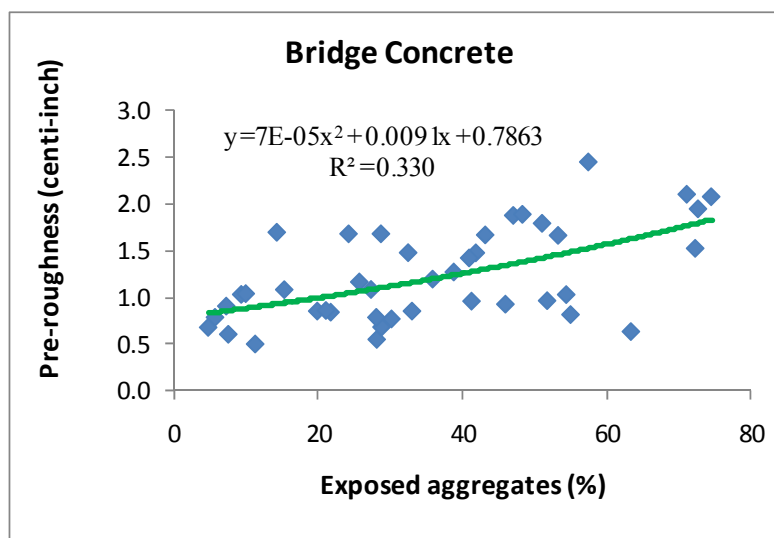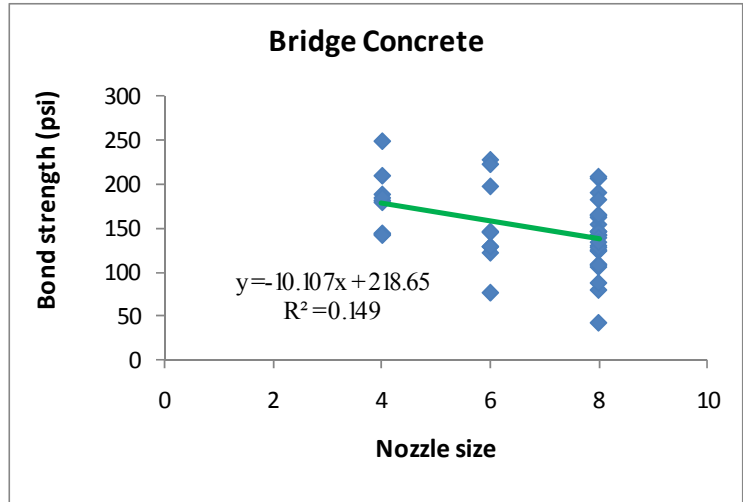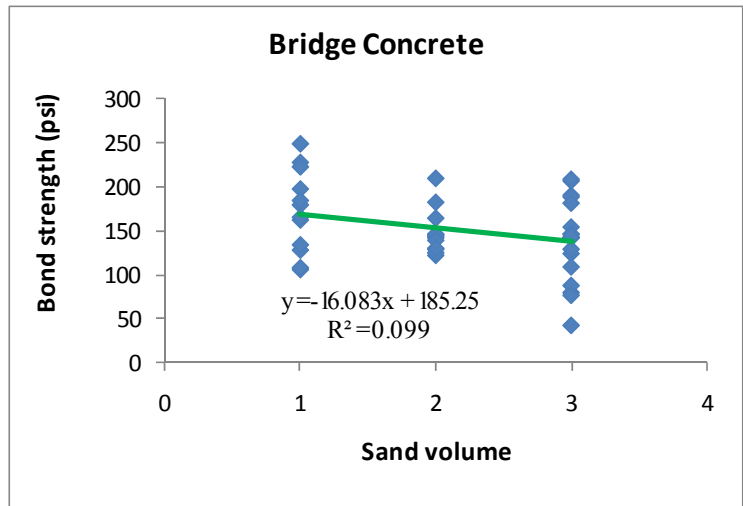

Figure 4.58: Relationship between macro-roughness and surface composition.

(a)

(b)

Figure 4.59: Relationship between bond strength and (a) nozzle size, and (b) sand volume.

To achieve the ideal surface composition and profile (44-55% exposed aggregates and macro-roughness of 1.1-1.5 centi-inches), Figure 4.60 suggests the following operating configurations are desirable: #4 nozzle with low or high sand volume; #6 nozzle with medium sand volume; or #8 nozzle with high sand volume. To achieve the highest bond strengths, Figure 4.61 suggests the following operating configurations and surface profiles are desirable: #4 nozzle with low sand volume and 51-75% exposed aggregates; #4 nozzle with medium sand volume and 20% exposed aggregates; or #6 nozzle with low sand volume and 30-44% exposed aggregates. With both macro-roughness and bond strength taken into consideration, the desirable operating configuration becomes: *#4 nozzle with low sand volume*. Note that this ideal configuration is significantly less aggressive than the current practice i.e. #8 nozzle with high sand volume, and thus may require more number of passes (thus higher labor cost) for surface profiling. As such, a balanced alternative configuration would be *#6 nozzle with low sand volume*, which with reasonable number of passes would expose 30-44% aggregates and according to

Figure 4.61 and Figure 4.62 produce a surface pre-roughness of 1.2-2.1 centi-inches and delta-roughness of 0.5-1.0 centi-inches. This high level of change in macro-roughness after bond test implies that the bond strength is so high that the pull-off test removed some additional paste rather than failing the zinc–concrete interface.
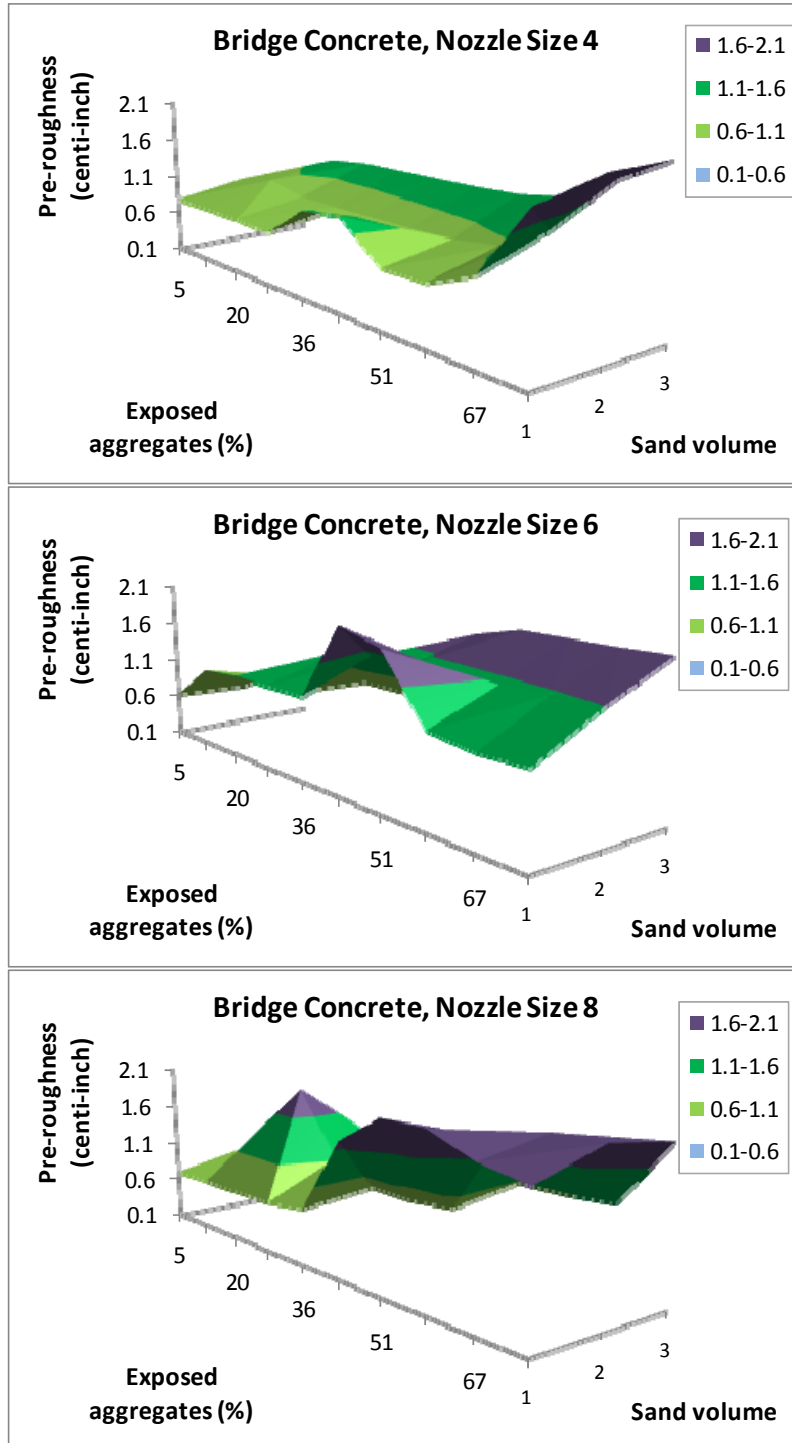

Figure 4.60: Predicted macro-roughness as a function of surface composition, sand volume, and nozzle size.
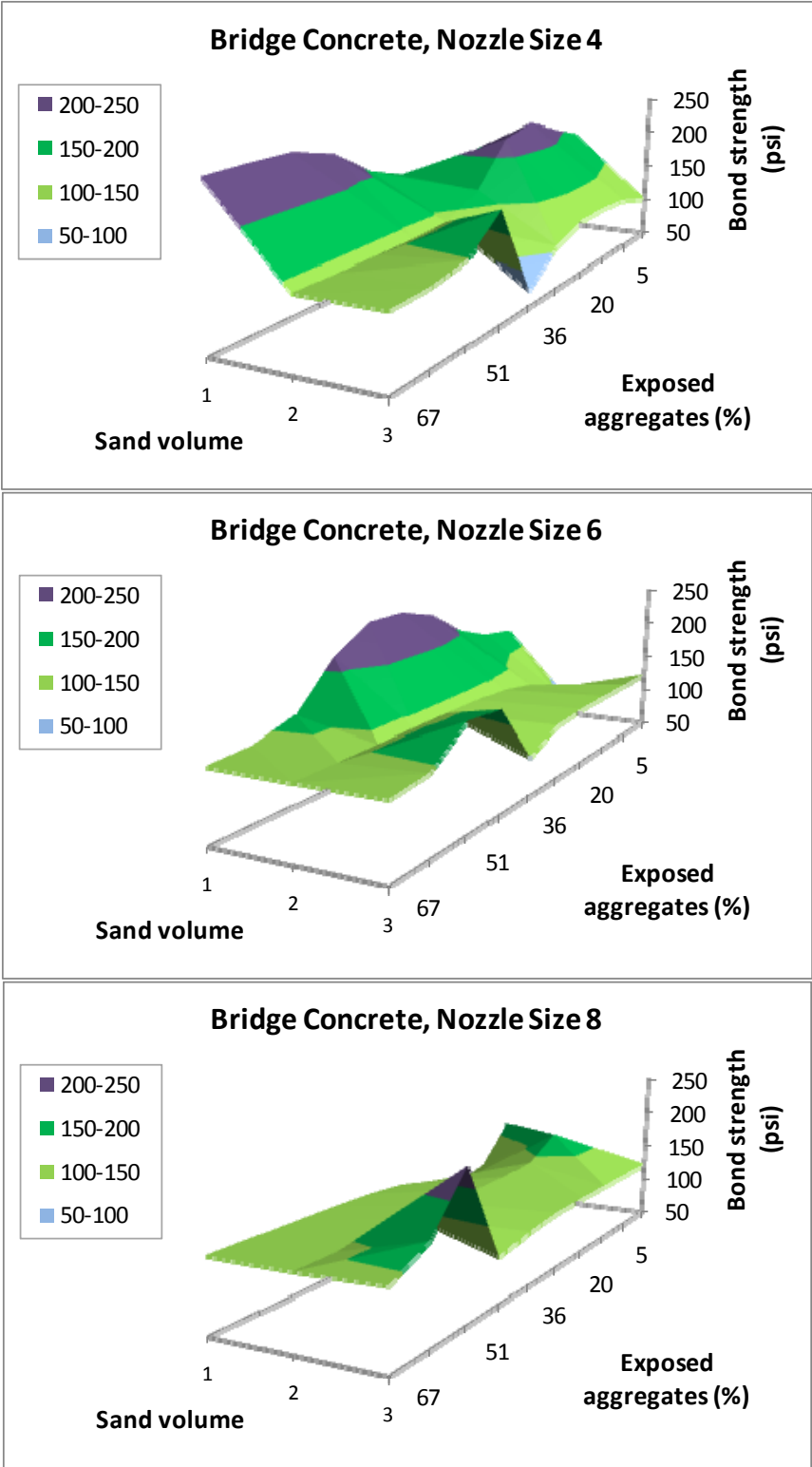
Figure 4.61: Predicted bond strength as a function of surface composition, sand volume, and nozzle size.
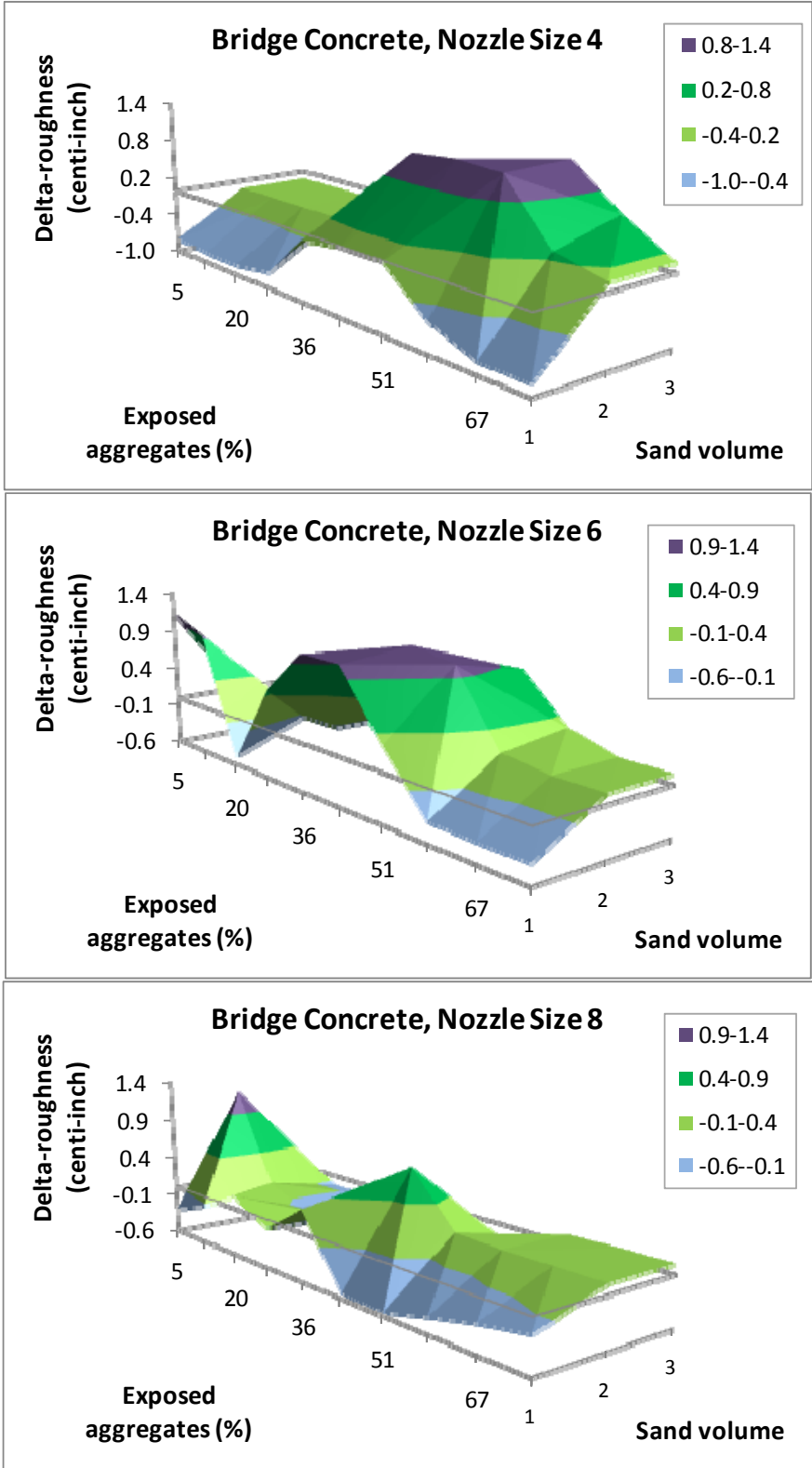
Figure 4.62: Predicted change in macro-roughness as a function of surface composition, sand volume, and nozzle size.

Since it is practically difficult to assess the percentage of exposed aggregates during the surface profiling operations, one way for quality assurance is to measure the macro-roughness of the concrete surface after old zinc removal and surface profiling, with a target RMS macro-roughness in the range of 1.2-2.1 centi-inches (0.3-0.5 mm). Furthermore, a micro-roughness of 3.5-5 μm is desirable (see Figure 4.24).

5.0 CONCLUSIONS AND IMPLEMENTATION RECOMMENDATIONS

Many cathodic protection (CP) systems with thermally sprayed Zn anodes will reach or exceed their design life in the near future and thus may function improperly or insufficiently, making it necessary to replace the aged anodes. Prior to this project, however, little was known about the most cost-effective method to remove existing zinc anodes that were arc-sprayed onto the concrete surface for CP systems, or the desired surface profile and composition after surface profiling and the appropriate operating configuration to achieve it. Furthermore, questions remained on the thickness of reaction layer at the old zinc–concrete interface and how it would affect the bond strength of new zinc to the profiled concrete surface. In this context, this research aimed to address these questions underlying the replacement of arc-sprayed zinc anodes on cathodically protected steel reinforced concrete bridges and to develop a protocol to prepare the concrete surface for the new anode, through a combination of literature review, practitioner surveys, laboratory studies, and field investigation (Pier 9 of the Yaquina Bay Bridge, Oregon). The main findings from this project are provided as follows.

5.1 MAIN FINDINGS

CP of reinforced concrete can be used to effectively mitigate chloride-induced corrosion of rebar, thereby extending the service life of reinforced concrete structures exposed to a marine environment or chemical deicers. Technological advances have made CP more attractive by providing new alternatives to engineers, which is manifested by improvements in new electronic equipment that facilitates the effective monitoring and control of the operational system. Continuous and incremental improvements to existing materials, equipment, and characterization techniques for CP are anticipated. More research is also needed to enhance the electrical properties of concrete overlay and backfill materials so as to enable a conductive circuit in dry-climate areas. The development of enhanced monitoring systems for universal applications is highly desirable but technically challenging. Such systems would feature the capability to analyze external inferences on the CP performance and to rectify/adjust the system parameters accordingly.

In this project, efforts were directed towards developing and testing a method for determining the "suitability" of a concrete surface for applying thermally sprayed zinc.

- The combined use of scanning electron microscopy (SEM) and energy-dispersive X-ray spectroscopy revealed that for concrete samples with an equivalent electrochemical age of 5 to 45 years, their Zn-rich reaction layer was approximately 1 mm. Relative to the concrete matrix itself, the Zn-rich reaction layer was generally less permeable but more electrically conductive, likely due to the electromigration of ionic species and chemical or electrochemical reactions that occurred at the zinc–concrete interface during the process of electrochemical aging.

121

- The bond strength of new zinc to concrete was influenced by the presence of the reaction layer but it depended on the electrochemical equivalent age of the layer. As the reaction layer matured (>8 years), the bond strength would be better if the reaction layer were completely removed by 4 mm of grinding prior to profiling and arc spraying. [7]

- From a modeling perspective, artificial neural network (ANN) was used to achieve better understanding of the complex cause-and-effect relationships inherent in the zinc–concrete system and was successful in finding meaningful, logical results from the bond strength and other types of data. Some of the key findings in the new TS-Zn bond strength to new mortar and new PCC are summarized in Table 5.1. These findings imply that the exposure of a moderate amount of fine aggregates is beneficial for the bonding of new TS-Zn whereas the exposure of coarse aggregates is not.

- For PCC with a moderate level of exposed aggregates (35%), the ideal surface macro-roughness varied significantly with the electrochemical age of the concrete. For concrete with an electrochemical age of 0-5 years, the surface macro-roughness after profiling should be maintained at greater than 1.1 centi-inches. The ideal surface macro-roughness changed to 0.8-1.5, 1.3-1.5, 0.4-0.8, and 0.4-1.3 centi-inches, for concrete with an electrochemical age of 10, 15, 20, and 25 years respectively. As the electrochemical age of concrete further increased, the highest bond strengths tended to gradually shift to smoother surfaces. The change of ideal surface roughness with electrochemical age was likely linked to how the chemistry and microstructure of the concrete surface layer beneath the arc-sprayed zinc evolved over the duration of electrochemical aging. Other key findings in the new TS-Zn bond strength to aged concrete are summarized in Table 5.2.

- It was practically difficult to achieve a surface with high concentration of exposed aggregates but low roughness or with low concentration of exposed aggregates but high roughness.

- With both macro-roughness and bond strength taken into consideration, the desirable operating configuration for existing concrete with relatively high electrochemical age (14 years under CP current density of 0.2 mA/ft^2) becomes: #4 nozzle with low sand volume. Note that this ideal configuration is significantly less aggressive than the current practice i.e. #8 nozzle with high sand volume, and thus may require more number of passes (thus higher labor cost) for surface profiling. As such, a balanced alternative configuration would be #6 nozzle with low sand volume, which with reasonable number of passes would expose 30–44% aggregates and produce a surface pre-roughness of 1.2-2.1 centi-inches.

---

[7] Even though direct surface profiling could remove at least part of the reaction layer, the data indicated that 4-mm grinding to remove the reaction layer before profiling could lead to higher bond strength of the new TS-Zn to the concrete surface.

Table 5.1: Predicted trends in the new TS-Zn bond strength to new mortar or new PCC.

Sample Type	Equivalent Electro-chemical Age (yrs)	Exposed Aggre-gates	Observed Trends	Desirable Operating Configuration
Mortar	0	28%	12-20 mils of new Zn: for rougher surface, the thicker the Zn layer, the higher the bond strength; for the smoother surface, the thinner the Zn layer, the higher the bond strength. 17.5 mils of new Zn: higher bond strength values generally coincided with mortar surfaces with moderate level of surface macro-roughness.	#8 nozzle, high sand volume & three passes: exposed <u>fine aggregates</u> (33%) & pre-roughness (1.7 centi-inches).
PCC	0	13.4%	The highest bond strength values were found with rough surfaces (0.9–1.1 centi-inches), regardless of the Zn thickness (12-20 mils). For the smooth surfaces (0.2-0.3 centi-inches), the relative high bond strength values corresponded with intermediate Zn thickness (15-17 mils). 16.8 mils of new Zn: highest bond strength values were with rough surfaces with less exposed aggregates (<13%), followed by very smooth surfaces (0.2-0.3 centi-inches) with a moderate level of exposed aggregates (18%-34%).	#4 nozzle, low sand volume & one pass[8]: exposed aggregates (2%) & pre-roughness (0.4 centi-inches).

---

8 These PCC surfaces did not have any existing zinc to be removed; as such, one pass of sandblasting was sufficient to achieve the desired surface profile featuring a low concentration of exposed aggregates and a low macro-roughness.

Table 5.2 Predicted trends in the new TS-Zn bond strength vs. electrochemical aging of concrete (assuming 17 mils of new Zn).

Equivalent Electro-chemical Age (yrs)	Surface Features to Maximize Bond Strength
0	A moderate level of macro-roughness (1.1-1.8 centi-inches) and relatively low concentration of exposed aggregates (5-36%)
8	A moderate level of macro-roughness (1.1-1.5 centi-inches) and relatively low concentration of exposed aggregates (12-36%)
14	A moderate level of macro-roughness (1.1-1.5 centi-inches) and a moderate level of exposed aggregates (44-67%). In light of field observations and the caveats of the modeling discussed earlier, the ideal level of exposed aggregates should avoid the higher end of the model predictions (i.e., maintained at 44-55%). Wherever possible, large aggregates (e.g., diameters ¾″ and bigger) should be avoided for exposure by surface profiling.
20-27	A relatively low level of macro-roughness (0.6-1.1 centi-inches) and a moderate level of exposed aggregates (44-51%).

5.2   RECOMMENDATIONS FOR IMPLEMENTATION

- Incorporate the following into the ODOT field specifications for old anode removal and surface preparation before new anode application: use a reasonably low air pressure and a reasonably hard and dense abrasive material for sandblasting; have a reasonably thin coating per pass during arc-spray operations; and have a slightly thinner overall Zn coating layer (15-17 mils vs. the currently used 17 mils). It is also desirable to have concrete with good surface cohesion strength (a minimum of 150 psi).

- Adjust the anode removal and surface profiling based on the electrochemical age of the existing concrete. For existing concrete with an equivalent electrochemical age of more than eight years, the reaction layer should be completely removed prior to profiling and arc spraying (e.g., 4 mm of grinding). [9] For concrete with an electrochemical age of 0 years, profile the surface to achieve a moderate level of macro-roughness (1.1-1.8 centi-inches) and relatively low concentration of exposed aggregates (5-36%). For existing concrete with relatively young electrochemical age (eight years), profile the surface to achieve a moderate level of macro-roughness (1.1-1.5 centi-inches) and relatively low concentration of exposed aggregates (12-36%). For existing concrete with relatively high

---

[9] Even though the Zn-rich reaction layer measured by SEM/EDX was only 1 mm thick, the bond strength data suggested that the 4-mm grinding was beneficial for improving the bond of new TS-Zn to concrete. The grinding removed the top concrete layer underlying the Zn-rich reaction layer, as both layers were likely compromised by electrochemical aging.

electrochemical age (14 years), profile the surface to achieve a moderate level of macro-roughness (1.1-1.5 centi-inches) and a moderate level of exposed aggregates (44-55%). For existing concrete with high electrochemical age (20 years and 27 years), profile the surface to achieve a relatively low level of macro-roughness (0.6-1.1 centi-inches) and a moderate level of exposed aggregates (44-51%). Minimize the exposure of large aggregates (e.g., diameter > ¾″) wherever possible, yet maintain the exposure of small aggregates (e.g., diameter no more than 0.25″) at a moderate level. These targets can be achieved in the field operations by adjusting the nozzle size, air pressure (i.e., sand volume), number of passes and possibly other parameters of the sandblasting equipment, with trial-and-error or with a design of experiments as described in this work.

- In order to achieve strong initial bond strength of new arc-sprayed zinc to existing concrete with relatively high electrochemical age (e.g., Yaquina Bay bridge after 14 years under CP current density of 0.2 mA/ft^2), the sandblasting configuration should be a #6 nozzle with low sand volume (approximately 7.3 lbs/min), which with reasonable number of passes would expose 30-44% aggregates and produce a surface pre-roughness of 1.2-2.1 centi-inches.

- Since it is practically difficult to assess the percentage of exposed aggregates during the surface profiling operations, one way for quality assurance is to measure the macro-roughness of the old concrete surface after old zinc removal and surface profiling, with a target RMS macro-roughness in the range of 1.2-2.1 centi-inches (0.3-0.5 mm). The method detailed in Appendix I can be used for this measurement. In addition to the macro-texture, a micro-texture with micro-roughness of 3.5-5 μm is desirable.

- A strong initial bond strength of arc-sprayed zinc to concrete is desirable, but it may not guarantee a long service life of the anode or a good performance of the CP system. Continued research is needed to investigate how the surface preparation affects the evolution of zinc–concrete interface and its bond strength (as well as circuit resistance) over the process of electrochemical aging by CP system operations. There is also the need to search for innovative anode materials and cost-effective methods for anode removal, surface profiling, and new anode application/installation to protect atmospherically exposed bridge substructures in the ODOT coastal environments.

- The main audience for this report will be ODOT bridge engineers, maintenance engineers, contractors, and other stakeholders. ODOT decision makers using the bridge management system can also benefit from the improved knowledge gained from this research on CP best practices. The institutions and individuals who might take leadership in applying the research product will be the ODOT bridge preservation engineers and contractors that hopefully will benefit from its implementation.

6.0 REFERENCES

Ahmad, S. Reinforcement Corrosion in Concrete Structures, its Monitoring and Service Life Prediction: A Review. *Cement and Concrete Composites,* Vol. 25, 2003, pp. 459–471.

Ahmad, S., and B. Bhattacharjee. A Simple Arrangement and Procedure for In-situ Measurement of Corrosion Rate of Rebar Embedded in Concrete. *Corrosion Science*, Vol. 37, No. 5, 1995, pp. 781–791.

Ali, M., and H. A. Al-Ghannam. Cathodic Protection for Above-water Sections of a Steel-Reinforced Concrete Seawater Intake Structure. *Materials Performance*, Vol. 37, No. 6, 1998, pp. 11–16.

Alonso, C., C. Andrade, M. Castellote, and P. Castro. Chloride Threshold Values to Depassivate Reinforcing Bars Embedded in a Standardized OPC Mortar. *Cement and Concrete Research, Vol.* 30, 2000, pp. 1047–1055.

Alshamsi, A. M., and H. D. Imran. Development of a permeability apparatus for concrete and mortar. *Cement and Concrete Research, Vol.* 32, 2002, pp. 923–929.

Amaya, K. Mathematical Modeling for Corrosion Analysis. *Modeling of Cathodic Protection Systems*, R. A. Adey, ed., WIT Press, Southampton, UK, 2005.

American Concrete Institute. ACI Committee 364 (Rehabilitation), *FAQ: What is "bruising," how is it evaluated, and how can it be minimized?* 2006. http://www.concrete.org/FAQ/afmviewfaq.asp?faqid=48.

Andrade, C., V. Castelo, C. Alonso, and J. A. Gonzalez. The determination of the corrosion rate of steel embedded in concrete by the polarization resistance and AC impedance methods. *Corrosion Effect of Stray Currents and the Techniques for Evaluating Corrosion of Rebars in Concrete.* ASTM Series, Vol. STP906, American Society for Testing Materials, Philadelphia, 1986.

Andrade, C., M. Keddam, X. R. Novoa, M. C. Perez, C. M. Rangel, and H. Takenouti. Electrochemical Behavior of Steel Rebars in Concrete: Influence of Environmental Factors and Cement Chemistry. *Electrochimica Acta,* Vol. 46, 2001, pp. 3905–3912.

Apostolos, J. A., D. M. Parks, and R. A. Carello. Cathodic Protection Using Metallized Zinc. CORROSION/1987, Paper No. 137, 1987.

Bandy, R. The Simultaneous Determination of Tafel Constants and Corrosion Rate—A New Method. *Corrosion Science,* Vol. 20, 1980, pp. 1017–1028.

Bazzoni, B., and L. Lazzari. A New Approach for Automatic Control and Monitoring of Cathodically Protected Reinforced Concrete Structures. *Materials Performance,* Vol. 31, No. 12, 1992, pp. 13-18.

Bennett, J. E., J. B. Bushman, K. C. Clear, R. N. Kamp, and W. J. Swiat. Cathodic Protection of Concrete Bridges: A Manual of Practice. *SHRP,* Report S-372, National Research Council, Washington, DC. 1993.

Bennett, J., and C. Firlotte. Zinc/Hydrogel System for Cathodic Protection of Reinforced Concrete Structures. *Materials Performance,* Vol. 36, 1997, pp. 14–20.

Bennett, J. E., and T. J. Schue. *Cathodic Protection Field Trials on Prestressed Concrete Components.* Publication FHWA-RD-97-153, FHWA, 1998.

Bennett, J. E., T. J. Schue, and G. McGill. A Thermally Sprayed Titanium Anode for Cathodic Protection of Reinforced Concrete Structures. CORROSION/1995, Paper No. 504, 1995a.

Bennett, J. E., T. J. Schue, and G. McGill. A Thermally-sprayed Titanium Anode for Cathodic Protection of Reinforced Concrete Structures. Proceedings of NACE Conference on Corrosion (March), Orlando, Florida, USA, Paper No. 504, 1995b.

Bennett, J. E., T. J. Shue, and G. McGill. Protecting Reinforced Concrete Using Thermally Sprayed Titanium Anode. *Materials Performance,* Vol. 34, No. 11, 1995c, pp. 23–27.

Berndt, C. C., S. Reddy, and M. L. Allan. Optimization of Thermal Spray Parameters for Cathodic Protection of Reinforced Concrete. CORROSION/1995, Paper No. 12, NACE International, Houston, TX, 1995.

Bertolini, L., F. Bolzoni, A. Cigada, T. Pastore, and P. Pedeferri. Cathodic Protection of New and Old Reinforced Concrete Structure. *Corrosion Science,* Vol. 35, No. 5-8, 1993, pp. 1633–1639.

Bertolini, L., F. Bolzoni, T. Pastore, and P. Pedeferri. Effectiveness of a Conductive Cementitious Mortar Anode for Cathodic Protection of Steel in Concrete. *Cement and Concrete Research,* Vol. 34, No. 4, 2004, pp. 681–694.

Bertolini, L., F. Bolzoni, P. Pedeferri, L. Lazzari, and T. Pastore. Cathodic Protection and Cathodic Prevention in Concrete. *Journal of Applied Electrochemistry,* Vol. 28, No. 12, 1998, pp. 1321–1331.

Bin Ismail, M., and M. S. R. bin Yusoff. Application of Intermittent Cathodic Protection Using Solar Power in Reinforced Concrete. *COSTAM,* 2002, September, Johor Bahru, 2002.

Bottenberg, R. Cathodic Protection of Historic Bridges. *Concrete International,* Vol. 30, No. 9, 2008, pp. 37–41.

Broomfield, J., and J. S. Tinnea. Cathodic Protection of Reinforced Concrete Bridge Components. *SHRP-C*, Report UWP-92-618, Strategic Highway Research Program/National Research Council, 1992.

Broomfield, J. P., D. A. Whiting, and M. A. Nagi. Laboratory Evaluation and Field installation of an Experimental Sacrificial Anode System for Reinforced Concrete Bridge Decks. *Corrosion of Reinforcement in Concrete Construction*. The Royal Society of Chemistry, Cambridge, UK, 1990, pp. 378-388.

Broomfield, J., and B. Wyatt. *Cathodic Protection of Steel in Concrete—The International Perspective.* Corrosion Protection Association Monograph 3. 2002. http://www.azom.com/details.asp?ArticleID=1316.

Brousseau, R., M. Arnott, and B. Baldock. Laboratory Performance of Zinc Anodes for Impressed Current Cathodic Protection of Reinforced Concrete. *Corrosion,* Vol. 51, No. 8, 1995, pp. 639–644.

Brousseau, R., M. Arnott, and B. Baldock. Long-Term Factors Influencing the Adhesion of Metallized Zinc to Concrete. *Journal of Thermal Spray Technology,* Vol. 5, No. 1, 1996a, pp.49–52.

Brousseau, R., M. Arnott, and B. Baldock. Metalized and Conductive Coatings as Impressed Current Anode for Reinforced Concrete. *Corrosion Prevention and Control,* Vol. 43, No. 5, 1996b, pp.119–123.

Brousseau, R., M. Arnott, and S. Dallaire. The Adhesion of Metallized Zinc Coatings on Concrete. CORROSION/1993, Paper No. 331, NACE International, Houston, TX, 1993.

Brousseau, R., B. Arsenault, S. Dallaire, D. Rogers, T. Mumby, and D. Dong. Sprayed Titanium Coatings for the Cathodic Protection of Reinforced Concrete. *Journal of Thermal Spray Technology,* Vol. 7, 1998, pp. 193–196.

Bullard, S. J., B. S. Covino, S. D. Cramer, G. R. Holcomb, J. H. Russell, C. B. Cryer, and H. M. Laylor. Alternative Consumable Anodes for Cathodic Protection of Reinforced Concrete Bridges. CORROSION/1999, Paper No. 99544. 1999.

Bullard, S. J., B. S. Covino, G. R. Holcomb, S. D. Cramer, J. H. Russell, H. M. Laylor, and C. B. Cryer. Anodes for Cathodic Protection of Reinforced Concrete. CORROSION/2000, Paper No. 00810, 2000.

Bullard, S. J., S. D. Cramer, B. S. Covino, G. R. Holcomb, and M. Ziomek-Moroz. CP System for Steel Reinforced Concrete Bridges. CORROSION/2004, Paper No. 04054, 2004.

Burke, N. D., and J. B. Bushman. *Corrosion and Cathodic Protection of Steel Reinforced Concrete Bridge Decks.* Publication FHWA-IP-88-007. FHWA. 1988.

Burns, W. R., and S. F. Daily. Cathodic Protection of a Coastal Bridge in Texas Using a Thermally Sprayed Aluminum Alloy. CORROSION/2004, Paper No. 04338, 2004.

Callon, R., D. F. Daily, and M. Funahashi. Selection Guidelines for Using Cathodic Protection Systems on Reinforced and Pre-stressed Concrete Structures. CORROSION/2004, Paper No. 04235, 2004.

Carello, R. A., D. M. Parks, and J. A. Apostolos. *Development, Testing and Field Application of Metalized Cathodic Protection Coatings on Reinforced Concrete Substructures*. Publication FHWA/CA/Tl-89/04. California Department of Transportation, 1989.

Chang, J. J., W. Yeih, R. Huang, and C. C. Hung. Effects of the Cathodic Current on the Alkali-Silica Aggregate Reaction. Presented at 16th International Corrosion Congress, Beijing, China, 2005.

Clemena, G.G., and D. R. Jackson. Long-Term Performance of Conductive-Paint Anodes in Cathodic Protection Systems for Inland Concrete Piers in Virginia. *Transportation Research Record,* No. 1642, Paper No. 98-0227, 1998, pp. 43–50.

Cotton, J. B. Platinum-faced Titanium for Electrochemical Anodes. *Platinum Metals Review,* Vol. 2, 1958, pp. 45–47.

Covino, B. S., S. D. Cramer, S. J. Bullard, G. R. Holcomb, W. K. Collins, and G. McGill. Thermally-sprayed Anodes for Impressed Current Cathodic Protection of Reinforced Concrete Structures. *Materials Performance,* Vol. 38, No. 1, 1999, pp. 27–33.

Covino, J. B. S., S. D. Cramer, S. J. Bullard, G. R. Holcomb, J. H. Russell, W. K. Collins, H. M. Laylor, and C. B. Cryer. *Performance of Zinc Anodes for Cathodic Protection of Reinforced Concrete Bridges.* Publication FHWA-OR-RD-02-10. Oregon Department of Transportation, 2002.

Cramer, S. D., and M. D. Anderson. *Zinc Anode Aging on the Arches and South Approach Sections of the Yaquina Bay Bridge.* Contract Number: EA 08BRPG3/201 P51 574. Oregon Department of Transportation, 2009.

Cramer, S. D., B. S. Covino, S. J. Bullard, G. R. Holcomb, J. H. Russell, F. J. Nelson, H. M. Laylor, and S. M. Soltesz. Corrosion Prevention and Remediation Strategies for Reinforced Concrete Coastal Bridges. *Journal of Cement and Concrete Composites,* Vol. 24, 2002, pp. 101–117.

Cramer, S. D., B.S. Covino, J. G. R. Holcomb, S. J. Bullard, W. K. Collins, R. G. Govier, R. D. Wilson, and H. M. Laylor. Thermally-sprayed Titanium Anode for Cathodic Protection of Reinforced Concrete Bridges. *Journal of Thermal Spray Technology,* Vol. 8, No. 1, 1999, pp. 133–145.

Daily, S. F. *Using Cathodic Protection to Control Corrosion of Reinforced Concrete Structures in Marine Environments*. Port Technology International, 1999.
http://www.epicuro.co.uk/uploads/cp1-4.pdf.

Davis, G. D., C. M. Dacres, and L. A. Krebs. In-Situ Sensor to Detect Moisture Intrusion and Degradation of Coatings, Composites, and Adhesive Bonds. Proceedings of the Tri-Services Conference on Corrosion, Myrtle Beach, South Carolina, 1999.

DePeuter, F., and L. Lazzari. New Conductive Overlay for CP in Concrete: Results of Long-Term Testing. CORROSION/1993, Paper No. 325, 1993.

Dhouibi-Hachani, L., E. Triki, J. Grandet, and A. Raharinaivo. Comparing the Steel–Concrete Interface State and its Electrochemical Impedance. *Cement and Concrete Research, Vol.* 26, 1996, pp. 253–266.

Eliaz, N., A. Shachar, B. Tal, and D. Eliezer. Characteristics of Hydrogen Embrittlement Stress Corrosion Cracking and Tempered Martensite Embrittlement in High-strength Steels. *Engineering Failure Analysis, Vol.* 9, 2002, pp. 167–184.

Enevoldsen, J. N., C. M. Hansson, and B. B. Hope. Binding of Chloride in Mortar Containing Admixed or Penetrated Chlorides. *Cement and Concrete Research*, Vol. 24, No. 8, 1994, pp. 1525–1533.

Feliu, S., J. A. Gonzalez, C. Andrade, and V. Feliu. *In-situ Determination of the Polarization Resistance in a Reinforced Concrete Beam*. Corrosion, Vol. 44, No. 10, 1988, pp. 761–765.

Fromm, H. J., and F. Pianca. *An Evaluation of Platinized Niobium Wire Anodes for Cathodic Protection of Bridge Support Structures*. Report No. MSP-81-03. Ontario Ministry of Transportation and Communications, 1981.

Genesca, J., and J. Juarez. Development and Testing of Galvanic Anodes for Cathodic Protection. *Contributions to Science, Vol.* 1, No. 3, 2000, pp. 331–343.

Gjørv, O. E., and Ø. Vennesland. Diffusion of Chloride Ions from Seawater into Concrete. *Cement and Concrete Research, Vol.* 9, No. 2, 1979, pp. 229–238.

Glass, G. K., and N. R. Buenfeld. The Presentation of the Chloride Threshold Level for Corrosion of Steel in Concrete. *Corrosion Science, Vol.* 39, No. 5, 1997, pp. 1001–1013.

Glass, G. K., A. M. Hassanein, and N. R. Buenfeld. Cathodic Protection Afforded by An Intermittent Current Applied to Reinforced Concrete. *Corrosion Science, Vol.* 43, 2001, pp. 1111–1131.

Gonzalez, J. A., S. Feliu, C. Andrade, and I. Rodriguez. On-site Detection of Corrosion in Reinforced Concrete Structures. *Mater. Struct.,* Vol. 24, 1991, pp. 346–350.

González, J. A., A. Molina, M. L. Escudero, and C. Andrade. Errors in the electrochemical evaluation of very small corrosion rates—II. Other electrochemical techniques applied to corrosion of steel in concrete. *Corrosion Science,* Vol. 25, 1985, pp. 519–530.

Gurrappa, I. Cathodic Protection of Cooling Water Systems and Selection of Appropriate Materials. *Journal of Materials Processing Technology,* Vol. 166, 2005, pp. 256–267.

Harriott, D. M., M. Laylor, J. P. Broomfield, A. Saccomano, and K. B. Brosseau. *Cathodic Protection of Reinforced Concrete Bridge Elements: A State-of-the-Art Report.* Publication SHRP-S-337. Strategic Highway Research Program, Washington, DC, 1993.

Hartt, W. H. Analytical Evaluation of Galvanic Anode Cathodic Protection Systems for Steel in Concrete. *Corrosion,* Vol. 58, No. 6, 2002, pp. 513–518.

Hassanein, A. M., G. K. Glass, and N. R. Buenfeld. Protection Current Distribution in Reinforced Concrete Cathodic Protection Systems. *Cement and Concrete Composites,* Vol. 24, 2002, pp. 159–167.

Holcomb, G. R., S. J. Bullard, B. S. Covino, Jr., S. D. Cramer, C. B. Cryer, and G. E. McGill. Electrochemical Aging of Thermal-Sprayed Zinc Anodes on Concrete. Proceedings of 9th National Thermal Spray Conference, in Thermal Spray: Practical Solutions for Engineering Problems. ASM International, Metals Park, OH, 1996, pp. 185–192.

Holcomb, G. R., S. J. Bullard, J. B. S. Covino, S. D. Cramer, C. B. Cryer, and G. E. McGill. *Electrochemical Aging of Thermally-sprayed Zinc Anodes on Concrete*. Publication ACR-97-001. DOE, 1997.

Holcomb, G. R., B. S. Covino, S. D. Cramer, H. J. Russell, S. J. Bullard, W. K. Collins, J. E. Bennett, S. M. Soltesz, and H. M. Laylor. *Humectants to Augment Current from Metallized Zinc Cathodic Protection Systems on Concrete.* Report No. FHWA-OR-RD-03-08. Oregon Department of Transportation, 2002.

Hong, S., and R. S. Harichandran. Nondestructive Evaluation of CFRP/Concrete Bond in Beams using Electrochemical Impedance Spetroscopy. Presented at Transportation Research Board 2004 Annual Meeting, 2004.

Hu, J., D. A. Koleva, and P. Stroeven. Efficiency of Cathodic Protection in Retarding Corrosion-Induced Cracking of Mortars Subjected to Aggressive Environments. Presented at 16th International Corrosion Congress, September 19–24, Beijing, China, 2005.

Isecke, B., and J. Mietz. The Risk of Hydrogen Embrittlement in High-Strength Prestressing Steels under Cathodic Protection. *Steel Research* (Germany), Vol. 64, No. 1, 1993, pp. 97–101.

Jankowski, J. Electrochemical Methods for Corrosion Rate Determination under Cathodic Polarization Conditions—A Review Part 2-AC, Methods. *Corrosion Reviews,* Vol. 20, No. 3, 2002, pp. 179–200.

John, D. G., P. C. Searson, and J. L. Dawson. Use of AC Impedance Technique in Studies on Steel in Concrete in Immersed Conditions. *British Corrosion Journal,* Vol. 16, 1981, pp. 102–106.

Jones, D. A. Electrochemical Fundamentals of Cathodic Protection. CORROSION/1987, Paper No. 317, 1987.

Kendig, M. W., and J. R. Scully. Basic Aspects of Electrochemical Impedance Application for the Life Prediction of Organic Coatings on Metals. *Corrosion,* Vol. 46, 1990, pp. 22–29.

Kendig, M. W., S. Jeanjaquet, and J. Lumsden. *Electrochemical Impedance of Coated Metal Undergoing Loss of Adhesion. Electrochemical Impedance: Analysis and Interpretation.* Publication ASTM STP 1188. American Society of Testing and Materials, Philadelphia, 1993, pp. 407–427.

Kessler, R. J., and R. G. Powers. Update on Cathodic Protection of Reinforcing Steel in Concrete Marine Substructures. CORROSION/1993, Paper No. 326, NACE International, Houston, TX, 1993.

Kessler, R. J., R. G. Powers, and I. R. Lasa. Intermittent Cathodic Protection Using Solar Power. *Materials Performance,* Vol. 37, No. 12, 1998a, pp. 14–19.

Kessler, R. J., R. G. Powers, and I. R. Lasa. Sacrificial Anode Protection of an Underground Steel Reinforced Concrete Structure. *Materials Performance,* Vol. 37, No. 3, 1998b, pp. 10–13.

Kessler, R. J., R. G. Powers, and I. R. Lasa. Battery Powered Impressed Current Cathodic Protection. NACExpo 2000, Paper No. 00815, NACE International, Houston, TX, 2000.

Kessler, R. J., R. G. Powers, and I. R. Lasa. An Update on the Long Term Use of Cathodic Protection of Steel Reinforced Concrete Marine Structures. CORROSION/2002, Paper No. 02254, 2002.

Klisowski, S., and W. H. Hartt. Qualification of Cathodic Protection for Corrosion Control of Pretensioned Tendons in Concrete, in *Corrosion of Reinforcement in Concrete Construction*, Society of Chemical Industry, 1996, pp. 354–368.

Koleva, D. A., J. H. W. de Wit, K. van Breugel, Z. F. Lodhi, and E. van Westing. Investigation of Corrosion and Cathodic Protection in Reinforcement Concrete. *Journal of the Electrochemical Society,* Vol. 154, No. 4, 2007, pp. 52–61.

Kranc, S. C., A. A. Sagues, and F. J. Presuel-Moreno. Computational and Experimental Investigation of Cathodic Protection Distribution in Reinforced Concrete Marine Piling. CORROSION/1997, Paper No. 231, 1997.

Legoux, J. G., and S. Dallaire. Adhesion Mechanisms of Arc-Sprayed Zinc on Concrete. *Journal of Thermal Spray Technology,* Vol. 4, No. 4, 1995, pp. 395–400.

Leroy, R. L. Evaluation of Corrosion Rates from Polarization Measurements. *Corrosion*, Vol. 31, 1975, pp. 173–177.

Liu, Z., and J. J. Beaudoin. An assessment of the relative permeability of cement systems using AC impedance techniques. *Cement and Concrete Research,* Vol. 29, 1999, pp. 1085–1090.

MacDonald, D. D., M. C. H. McKubre, and M. Urquidi-MacDonald. Theoretical Assessment of AC Impedance Spectroscopy for Detecting Corrosion of Rebar in Reinforced Concrete. *Corrosion,* Vol. 44, No. 1, 1988, pp. 2–7.

MacDowell, L. G., and J. J. Curran. *Liquid Galvanic Coating for Protection of Imbedded Metals*, U.S. Patent 6627065, 2003.

Mailvaganam, N. P. *Repair and Protection of Concrete Structures*. CRC Press, New York, 1991.

Manning, D. G., and J. Ryell. *A Strategy for the Rehabilitation of Concrete Bridge Decks*. Report No. ME-79-01. Ontario Ministry of Transportation and Communications, 1979.

Manning, D. G., and H. Schell. *Substructure Cathodic Protection in Ontario: Field Trials*. Report No. ME-87-05. Ontario Ministry of Transportation and Communications, 1987.

Mansfeld, F. Tafel Slopes and Corrosion Rates from Polarization Resistance Measurements. *Corrosion,* Vol. 29, 1973, pp. 397–402.

Martinez, I., C. Andrade, O. Vennesland, U. Evensen, R. B. Polder, and J. Leggedor. Efficiency Control of Cathodic Protection Measured Using Passivation Verification Technique in Different Concrete Structures. *Corrosion,* Vol. 63, No. 9, 2007, pp. 880–892.

Martinez, S., and I. Stern. A Mathematical Model for the Internal Cathodic Protection of Cylindrical Structures by Wire Anodes. *Journal of Applied Electrochemistry,* Vol. 30, 2000, pp. 1053–1060.

McGill, G., and T. Shike. Rehabilitation and Preservation of Oregon's Historic Concrete Coastal Bridges. *Transportation Research Record,* No. 1601, 1997, pp. 9–12.

McMahon, C. J. Hydrogen-induced Intergranular Fracture of Steels. *Engineering Fracture Mechanics,* Vol. 68, 2001, pp. 773–788.

Montemor, M. F., A. M. P. Simoes, and M. G. S. Ferreira. Chloride-induced Corrosion on Reinforced Steel; from the Fundamental to the Monitoring Techniques. *Cement and Concrete Composites,* Vol. 25, 2003, pp. 491–502.

Mishra, P. R., J. C. Joshi, and B. Roy. Design of a Solar Photovoltaic-powered mini Cathodic Protection System. *Solar Energy Materials & Solar Cells,* Vol. 61, 2000, pp. 383–391.

Miyata, Y., Y. Akira, T. Wakabayashi, and N. Mochizuki. Estimating Anode Consumption in Seawater from Cathode Potential. *Materials Performance,* Vol. 47, No. 2, 2008, pp. 32–35.

Mussinelli, G., M. Tettamanti, and P. Pedeferri. "The Effect of Current Density on Anode Behavior and on Concrete in the Anode Region." The 2nd International Conference on Deterioration and Repair of Reinforced Concrete in the Arabian Gulf, Bahrain, Vol. 1, 1987, pp. 99–120.

NACE International. *Cathodic Protection of Reinforcing Steel in Atmospherically Exposed Concrete Structures*. Standard RP0290-90, NACE International, Houston TX, 2000, p. 11.

NACE International. *Standard Practice – Cathodic Protection of Reinforcing Steel in Buried or Submerged Concrete Structure*. NACE SP0408-2008. NACE International, Houston, TX, 2008.

NACE International. *Standard Test Method TM105-2005, Test Procedures for Organic-Based Conductive Coating Anodes for Use on Concrete Structures*. NACE International, Houston, TX, 2005.

NACE International. *Standard Test Method TM0294-2007, Testing of Embeddable Anodes for Use in Cathodic Protection of Atmospherically Exposed Steel Reinforced Concrete.* NACE International, Houston, TX, 2007.

Nagumo, M. Function of Hydrogen in Embrittlement of High-strength Steels. *ISIJ International,* Vol. 41, 2001, pp. 590–598.

Nagumo, M., M. Nakamura, and K. Takai. Hydrogen Thermal Desorption Relevant to Delayed-Fracture Susceptibility of High-strength Steel. *Metallurgical and Materials Transactions A,* Vol. 32, 2001, pp. 339–347.

Naish, C., and M. McKenzie. Monitoring Cathodic Protection of Steel in Concrete. *Cathodic Protection of Steel in Concrete*. E & FN Spon Press, New York, 1998.

Nicholson, J. P. A New Approach to Cathodic Protection of Bridge Decks and Concrete Structures. Presented at the Transportation Research Board Meeting in Washington D.C., 1980.

Orazem, M., J. Esteban, K. Kennelley, and R. Degerstedt. Mathematical Model for Cathodic Protection of an Underground Pipeline with Coating Holidays: Part 1—Theoretical Development. *Corrosion,* Vol. 53, No. 4, 1997, pp. 264–272.

Orlikowski, J., S. Cebulski, and K. Darowicki. Electrochemical Investigations of Conductive Coatings Applied as Anodes in Cathodic Protection of Reinforced Concrete. *Cement and Concrete Composites,* Vol. 26, No. 6, 2004, pp. 721–728.

Page, C. L., and G. Sergi. Developments in Cathodic Protection Applied to Reinforced Concrete. *Journal of Materials in Civil Engineering,* Vol. 12, No. 1, 2000, pp. 8–15.

Parthiban, G. T., K. Bharanidharan, D. Dhayanand, T. Parthiban, N. Palaniswamy, and V. Sivan. Influence of Sacrificial Cathodic Protection on the Chloride Profile in Concrete. *International Journal of Electrochemical Science,* Vol. 3, 2008a, pp. 1162–1168.

Parthiban, G. T., T. Parthiban, R. Ravi, V. Saraswathy, N. Palaniswamy, and V. Sivan. Cathodic Protection of Steel in Concrete using Magnesium Alloy Anode. *Corrosion Science,* Vol. 50, No. 12, 2008b, pp. 3329–3335.

Pedeferri, P. Cathodic Protection and Cathodic Prevention. *Construction and Building Materials,* Vol. 10, No. 5, 1996, pp. 391–402.

Pianca, F., and H. C. Schell. Evaluation of New Sacrificial Anode Cathodic Protection Systems for Highway Bridge Decks. CORROSION/2004, Paper No. 04340, NACE International, Houston, TX, 2004.

Polder, R. B. *Current Distribution in Cathodic Corrosion Protection of Steel in Concrete.* TNO Report BI-90—125. TNO Institute for Building Materials and Structures, Delft,The Netherlands, 1990.

Polland, J. S., and J. A. Page. *Investigation of Chloride Migration in Reinforced Concrete under Application of Cathodic Protection.* Report No. ME-87-11. Ontario Ministry of Transportation, 1988.

Preiser, H. S. Cathodic Protection Applications Using Platinum Anodes. *Platinum Metals Review,* Vol. 3, No. 2, 1959, pp. 38–43.

Presuel, F. J., S. C. Kranc, and A. A. Sagues. Modeling and Measurements of Cathodic Prevention Distribution in Partially Submerged Reinforced Concrete. CORROSION/2002, Paper No. 02258, 2002a.

Presuel, F. J., S. C. Kranc, and A. A. Sagues. Modeling and Measurements of Cathodic Prevention Distribution. CORROSION/2002, Paper No. 02259, 2002b.

Pruckner, F., J. Theiner, J. Eri, and G. E. Nauer. In-situ Monitoring of the Efficiency of the Cathodic Protection of Reinforced Concrete by Electrochemical Impedance Spectroscopy. *Electrochemica Acta,* Vol. 41, No. 7/8, 1996, pp. 1233–1238.

Qiao, G., and J. Ou. Corrosion Monitoring of Reinforcing Steel in Cement Mortar by EIS and ENA. *Electrochemica Acta,* Vol. 52, 2007, pp. 8008–8019.

Rabiot, D., F. Dalard, J. J. Rameau, J. P. Caire, and S. Boyer. Study of Sacrificial Anode Cathodic Protection of Buried Tanks: Numerical Modeling. *Journal of Applied Electrochemistry,* Vol. 29, 1999, pp. 541–550.

Riemer, D. P., and M. E. Orazem. A Mathematical Model for the Cathodic Protection of Tank Bottoms. *Corrosion Science,* Vol. 47, 2005, pp. 849–868.

Rodriguez, P., E. Ramirez, and J. A. Gonzalez. Methods for Studying Corrosion in Reinforced Concrete. *Magazine of Concrete Research,* Vol. 46, No. 167, 1994, pp. 81–90.

Rothman, P. S., M. J. Szeliga, and S. Nikolakakos. Galvanic Cathodic Protection of Reinforced Concrete Structures in a Marine Environment. CORROSION/2004, Paper No. 04308, 2004.

Rumelhart, D. E., G.E. Hinton, and R.J. Williams. *Learning internal representations by error propagation.* Parallel Distributed Processing; MIT Press, Cambridge, MA, 1986, pp. 318–362.

Salt, B. K., R. L. Carrasquillo, R. C. Loehr, and D. W. Fowler. *Recycling Contaminated Spent Blasting Abrasives in Portland Cement Mortars Using Solidification/Stabilization Technology.* Texas Department of Transportation, 1995.

Schechirlian, S., M. Keddam, and H. Takenouti. Specific aspects of impedance measurements in low conductivity media, in *Electrochemical Impedance Analysis and Interpretation*, ASTMSTP, 1188, ASTM, Philadelphia, 1993.

Scully, J. R., D. C. Silverman, and M. W. Kendig, eds. *Electrochemical Impedance Analysis and Interpretation.* STP 1188. American Society for Testing and Materials, Philadelphia, PA., 1993, pp. 384–403.

Sehgal, A., D. Li, Y. T. Kho, K. Osseo-Asare, and H. W. Pickering. Reproducibility of Polarization Resistance Measurements in Steel-in-Concrete Systems. *Corrosion,* Vol. 48, 1992, pp. 706–715.

Sergi, G., and G. K. Glass. A Method of Ranking the Aggressive Nature of Chloride Contaminated Concrete. *Corrosion Science,* Vol. 42, No. 12, 2000, pp. 2043–2049.

Sharp, S. R., and M. C. Brown. *Survey of Cathodic Protection Systems on Virginia Bridges.* Report No. FHWA-VTCR-07-R35, Federal Highway Administration, 2007.

Shi, X., P. Schillings, and D. Boyd. Applying artificial neural networks and virtual experimental design to quality improvement of two industrial processes. *International Journal of Production Research,* Vol. 42, No. 1, 2004, pp. 101–118.

Shi, X., Z. Yang, T. A. Nguyen, Z. Suo, R. Avci, and S. Song. *Science in China, Series E: Technological Sciences,* Vol. 52, No. 1, 2009, pp. 52–66.

Shreir, L. L. *Impressed Current Anodes, Cathodic Protection Theory and Practice.* Ellis Horwood Ltd, Chichester, UK, 1986.

Sohanghpurwala, A. A. Long-term Effectiveness of Galvanic Cathodic Protection Systems for Reinforced Concrete Highway Structures. CORROSION/2004, Paper No. 04341, NACE International, 2004a.

Sohanghpurwala, A. A. Long-term Effectiveness of Impressed Current Cathodic Protection Systems for Reinforced Concrete Highway Structures. CORROSION/2004, Paper No. 04347, 2004b.

Sohanghpurwala, A. A. *Cathodic Protection for Life Extension of Existing Reinforced Concrete Bridge Elements.* NCHRP Synthesis 398. Transportation Research Board, Washington, DC, 2009. http://onlinepubs.trb.org/onlinepubs/nchrp/nchrp_syn_398.pdf.

Sohanghpurwala, A. A., and W. T. Scannell. *Long-Term Effectiveness of Cathodic Protection Systems on Highway Structures.* Report No. FHWA-RD-01-096, Federal Highway Administration, 2000.

Song, H.-W., and V. Saraswathy. Corrosion Monitoring of Reinforced Concrete Structures—A Review. *International Journal of Electrochemical Science,* Vol. 2, 2007, pp. 1–28.

Song, F. M., and N. Sridhar. Modeling Pipeline Crevice Corrosion under a Disbonded Coating with or without Cathodic Protection under Transient and Steady State Conditions. *Corrosion Science,* Vol. 50, 2008, pp. 70–83.

Spriestersbach, J., A. Melzer, J. Wisniewski, A. Winkels, and M. Knepper. Lifetime Extension of Thermally Sprayed Zinc Anodes for Corrosion Protection of Reinforced Concrete Structures by Using Organic Topcoatings, in Proceedings of EuroCor '99, Aachen, Germany, 1999. http://www.kks-beton.de/downloads/Eurocorr99eng.pdf.

Stockert, L., J. Junker, H. Bergner, J. Brust, and P. Kess. Cathodic Corrosion Protection of Steel in High-Performance Concrete. 16th International Corrosion Congress, Sept. 19–24, Beijing, China, 2005.

Stratfull, R. F. Experimental Cathodic Protection of a Bridge Deck. *Transportation Research Record, No.* 500:1–15, 1974.

Sun, W., and K. M. Liu. Numerical Solution of Cathodic Protection Systems with Nonlinear Polarization Curves. *Journal of the Electrochemical Society,* Vol. 147, No. 10, 2000, pp. 3687–3690.

Sun, X. Online Monitoring of Corrosion Under Cathodic Protection Conditions Utilizing Coupled Multielectrode Sensors. CORROSION/2004, Paper No. 04094, 2004.

Swiat, W. J., and J. B. Bushman. *Further Improvements in Cathodic Protection.* Publication FHWA-RD-88-267. 1989.

Szabó, S., and I. Bakos. Cathodic Protection with Sacrificial Anodes. *Corrosion Reviews , Vol.* 24, Nos. 1-2, 2006a, pp. 1–50.

Szabó, S., and I. Bakos. Impressed Current Cathodic Protection. *Corrosion Reviews,* Vol. 24, Nos. 3-4, 2006b, pp. 1–24.

Talavera, M. A., T. Perez, and J. Genesca. EIS Measurements on Cathodically Protected Steel in Concrete. CORROSION/2000, Paper No. 00794, NACE International, Houston, TX, 2000.

Tang, B. *Building More Durable Bridges.* Federal Highway Administration *FOCUS*, Publication FHWA-RD-99-107. 1999. http://www.fhwa.dot.gov/publications/focus/99sep/building.cfm.

Thompson, N. G., K. M. Lawson, and J. A. Beavers. Monitoring Cathodically Protected Steel in Concrete Structures with Electrochemical Impedance Technique. *Corrosion , Vol.* 44, 1988, pp. 581–588.

Tinnea, J., K. M. Howell, and M. Figley. Triple System Galvanic Protection of Reinforced Concrete Energizing and Operation, CORROSION/2004, Paper No. 04337, NACE International, 2004.

Toumi, A., R. Francois, and O. Alvarado. Experimental and Numerical Study of Electrochemical Chloride Removal from Brick and Concrete Specimens. *Cement and Concrete Research,* Vol. 37, No. 1, 2007, pp. 54–62.

U. S. Army Corps of Engineers (USACE). *Engineer Manual: Thermal Spraying: New Construction and Maintenance*, EM 1110-2-3401; Chapter 2: Thermal Spray Fundamentals. 1999a. http://140.194.76.129/publications/eng-manuals/em1110-2-3401/c-2.pdf.

USACE. *Engineer Manual: Thermal Spraying: New Construction and Maintenance*, EM 1110-2-3401, Chapter 5: Thermal Spray Coating Selection. 1999b. http://140.194.76.129/publications/eng-manuals/em1110-2-3401/c-5.pdf.

Van Blaricum, V. L., and W. R. Norris. *Remote Monitoring Equipment for Cathodic Protection Systems.* U.S. Army Construction Engineering Research Laboratories, Champaign, IL. 1997. http://owww.cecer.army.mil/TechReports/Vancprem/Vancprem.pdf.

Virmani, Y. P. *FCP Annual Progress Report – Year Ending September 30, 1982—Project 4 K*, Federal Highway Administration, 1982.

Virmani, P., and G. G. Clemena. *Corrosion Protection—Concrete Bridges.* Federal Highway Administration, Publication FHWA-RD-98-088. 1998. http://www.tfhrc.gov/structur/corros/results.htm.

Webster, M. T., and R. C. Loehr. Recycling of Spent Abrasive Media in Nonstructural Concrete. *Journal of Environmental Engineering,* Vol. 22, No. 9, 1996, pp. 840–849.

Wenger, F., and J. Galland. Study of Corrosion of Steel in Concrete by Electrochemical Impedance Measurements. *Materials Science Forum,* Vol. 44-45, 1989, pp. 375–386.

Whiting, D. A., M. A. Nagi, and J. P. Broomfield. Laboratory Evaluation of Sacrificial Anode Materials for Cathodic Protection of Reinforced Concrete Bridges. *Corrosion,* Vol. 52, No. 6, 1996, pp. 472–479.

Whitney, D., L. Etcheverry, and H. Wheat. *Performance Evaluation of Cathodic Protection Systems for Queen Isabella PR 100*, Research Project 7-2945, 2003.

Wrobel, L. C., and P. Miltiadou. Genetic Algorithm for Inverse Cathodic Protection Problems. *Engineering Analysis with Boundary Elements,* Vol. 28, 2004, pp. 267–277.

Wyatt, B. S. Anode Systems for Cathodic Protection of Reinforced Concrete, *Cathodic Protection: Theory and Practice*, Chichester, UK, 1993, pp. 293–311.

Yan, J. F., S. N. R. Pakalapati, T. V. Nguyen, R. E. White, and R. B. Griffin. Mathematical Modeling of Cathodic Protection using the Boundary Element Method with a Nonlinear Polarization Curve. *Journal of the Electrochemical Society,* Vol. 139, No. 7, 1992, pp. 1932–1936.

Yunovich, M. Performance of High Potential Magnesium Anode: Factors Affecting Efficiency. CORROSION/2004, Paper No. 04044, 2004.

Zhang, X. G. *Corrosion and Electrochemistry of Zinc.* Plenum Press, New York, 1996, pp. 474.

Zornoza, E., J. Payá, and P. Garcés. Chloride-induced Corrosion of Steel Embedded in Mortars Containing Fly Ash and Spent Cracking Catalyst. *Corrosion Science,* Vol. 50, No. 6, 2008, pp. 1567–1575.

APPENDIX A:
GENERAL CONDITION OF NETL SAMPLE SLABS

Below are pictures and comments regarding the NETL zinc coated slabs. Every attempt was made to select a representative cross section of all the samples. The bottom line is that the majority of the samples do not have a bonded zinc coating.
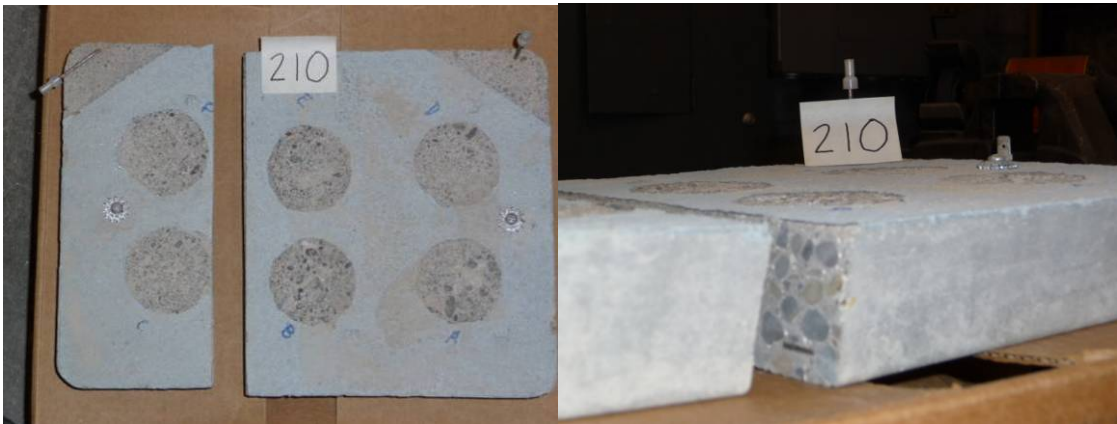
Slab 210: This slab is indicative of the samples that have better zinc bonding. Even though the zinc is more securely bonded to the surface, there are pockets where it has not. The zinc directly adjacent to the dolly location appears and sounds to be bonded. Some general properties of this sample are: Cl = 5 lbs/yard3 and Equivalent Electrochemical Age (@ 0.2 mA/ft2) = 0.37 years.

Slab 52: This slab is fully covered by zinc but the zinc is only bonded in a few spots around the edges. Running a solid object across the surface reveals quickly the extent to which the coating has debonded. Some general properties of this sample are: Cl = 2 lbs/yard3 and Equivalent Electrochemical Age (@ 0.2 mA/ft2) = 19 years.

Slab 228: As seen in the photo, the zinc has debonded across the cross sectional area. It does not appear that the zinc far away from the test dolly locations is bonded very well. If a solid object is run across the surface of the zinc it is obvious by sound that the zinc is not bonded to the surface. Some general properties of this sample are: Cl = 5 lbs/yard3 and Equivalent Electrochemical Age (@ 0.2 mA/ft2) = 22.38 years.

Slab1005: This slab is very indicative of the majority of the samples. The zinc coating has debonded within the vicinity of each of the dolly tests. On this sample there is a very thin section around the perimeter that appears and sounds to be bonded but the majority is not. Some general properties of this sample are: Cl = 10 lbs/yard3 and Equivalent Electrochemical Age (@ 0.2 mA/ft2) = 37.5 years.
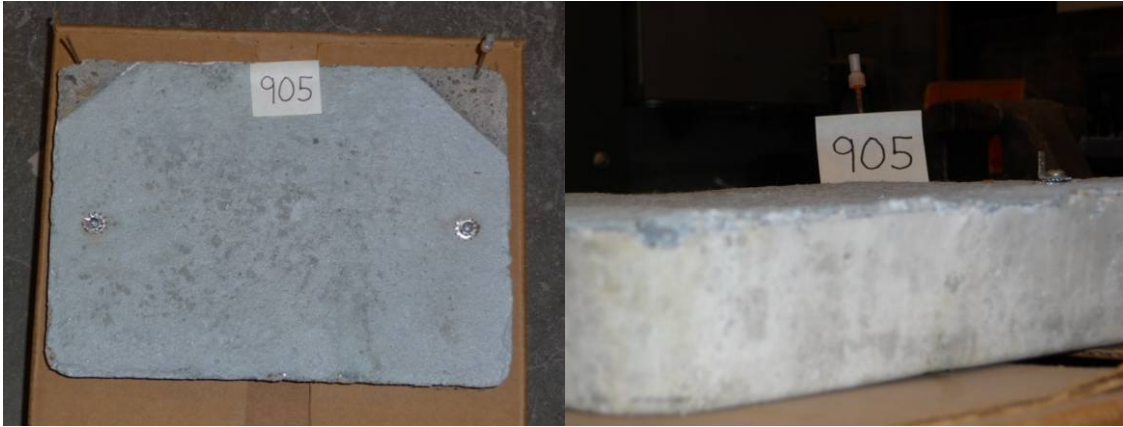
Slab 905: This sample is similar to slab 52 except that the debonded zinc has actually arched up from the concrete substrate. The edges are the only apparent spot of bonding. Some general properties of this sample are: Cl = 5 lbs/yard3 and Equivalent Electrochemical Age (@ 0.2 mA/ft2) = 45.4 years.

Slab 603: This slab was no longer zinc-coated. The aggregate is exposed as well as the surface is missing significant pockets of material as a result of bond testing. There is not much usable space to try out different techniques at a steady-state operation of the equipment. Some general properties of this sample are: Cl = 5 lbs/yard3 and Equivalent Electrochemical Age (@ 0.2 mA/ft2) = 108.8 years.

APPENDIX B:
STANDARD OPERATING PROCEDURE FOR GAS PERMEABILITY
TESTS

1. Use a concrete-wet saw to cut three 0.5" thick disks from a 4" concrete sample.

2. If using existing concrete slab sample cut a core using the coring-machine in MSU Bulk Lab then use concrete-wet saw to cut a 0.5" thick disk from the core.

3. Measure and record the thickness of each disk at 6 places around the disk.

4. Use 100% silicon dispensed via a caulking gun to seal disk to top of gas permeability cylinder. Dispense a bead of silicon around the inner edge of the cylinder then press the concrete disk centered evenly down on the silicon bead. Finish the seal with a small bead of silicon around the top edge of the disk and seal smooth with finger.
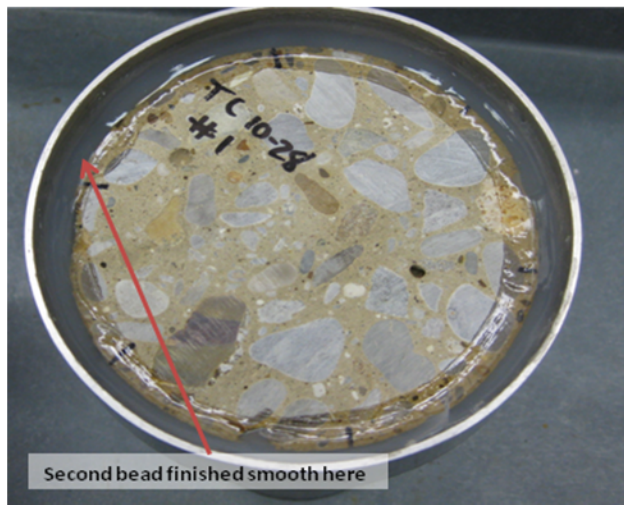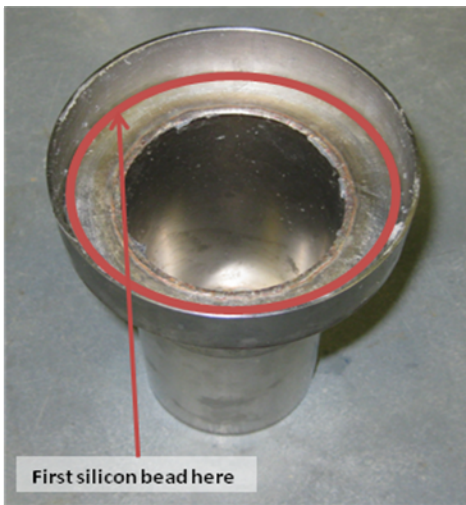
5. Seal all three concrete disks on the three gas permeability cylinders.

6. Place all three cylinders in oven @ 50°C overnight.

7. The next day remove the cylinders and pour in 175mL of methanol. Use a thin neck glass funnel inserted into the hole in the side of gas permeability cylinder to pour the methanol into the cylinder.

8. After the methonol in in the cylinder wrap para-film around the clyinder covering the hole in the side of the cylinder. Then wrap duct tape around the cylinder over the paprfilm. Do this for all three cylinders.

9. Weigh and record all three initial weights.

10. Place the cylinders into a water bath at 40°C. The level of the water bath should result in a water level reaching just below the duct tape wrapped around the clyinders.

11. Remove the cylinders momentarily from the water bath every ten minutes to re-weigh them and record the weight. A paper towel is used to dry the outside of the cylinder proir to weighing each time.

12. The test continues until a steady state mass loss is observed over a time period of at least eight measurements.

13. Upon completion of the test a razor blade is used to cut the disk from the cured silicon and the cured silicon from the cylinder. The methanol may not be poured down the sink but can be poured into a container with a lid and labeled for reuse.

APPENDIX C:
**STANDARD OPERATING PROCEDURE FOR DC RESISTIVITY TESTS**

1. Use a concrete-wet saw to cut two 1" by 1" by 1" cubes from concrete sample.


2. Choose two opposite sides of each cube are mark with an x. Measure and record the surface areas of the sides marked x and measure and record the height between the sides marked x at four places around the cube.

3. Use high-purity silver paint to completely paint the surfaces marked with an x. Then cut four 3" long pieces of silver solder. Bend one end of the silver solder to form a circle and use silver paint to place and hold the solder on the sample.
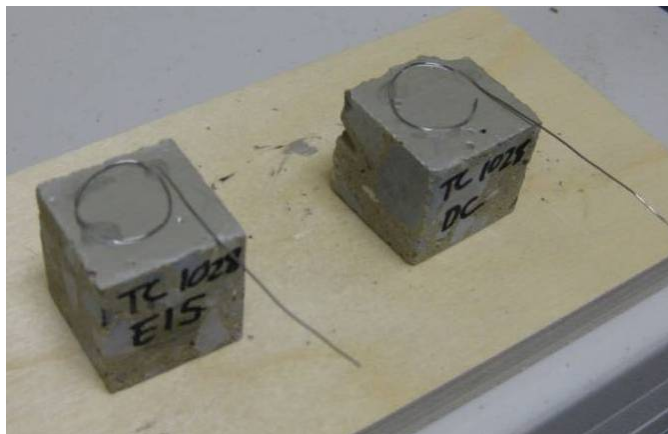

4. Cut four strips of adhesive carbon conductive tape 1.5" long by .5" wide. Stick the carbon tape over the solder.
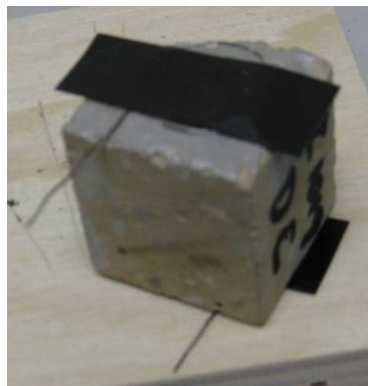
5. The cube being used for DC resistivity is then hooked up using alligator clips (one on each silver solder wire) to either side of a DC multi-meter. The multi-meter is then turned on to resistance (Ω) for 5 minutes. Record the DC resistance after 5 minutes, then turn off the multi-meter. Allow cube to set 10 minutes then turn on multi-meter to resistance for 5 minutes and measure and record again. Repeat this one more time.

APPENDIX D:
STANDARD OPERATING PROCEDURE FOR EIS TESTS

1. Use a concrete-wet saw to cut two 1" by 1" by 1" cubes from concrete sample.

2. Choose two opposite sides of each cube are mark with an x. Measure and record the surface areas of the sides marked x and measure and record the height between the sides marked x at four places around the cube.

3. Use high-purity silver paint to completely paint the surfaces marked with an x. Then cut four 3" long pieces of silver solder. Bend one end of the silver solder to form a circle and use silver paint to place and hold the solder on the sample.
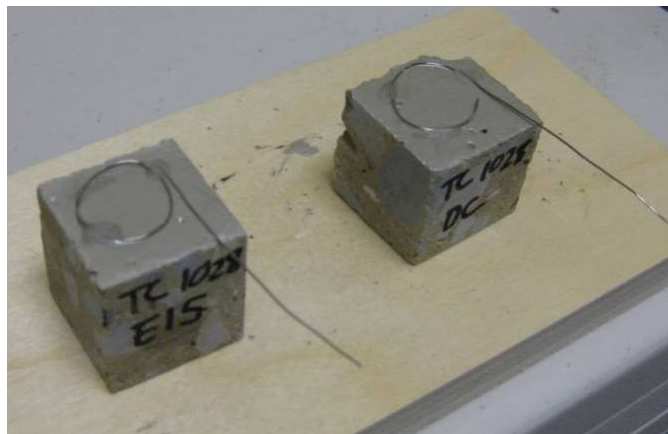
4. Cut 4 strips of adhesive carbon conductive tape 1.5" long by .5" wide. Stick the carbon tape over the solder.
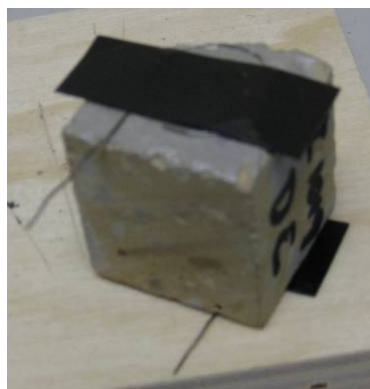
5. The cube being used for EIS testing is hooked up to the Gamry machine. One silver solder wire is hook to all blue and green leads. The other silver solder wire is hooked to all red and white leads. The black leads are hooked to each other but not to the sample in any way.

6. Open the Gamry Framework program. Select the Experiment, Electrochemical Impedance, and Potentiostatic EIS. Set-up program as shown below.
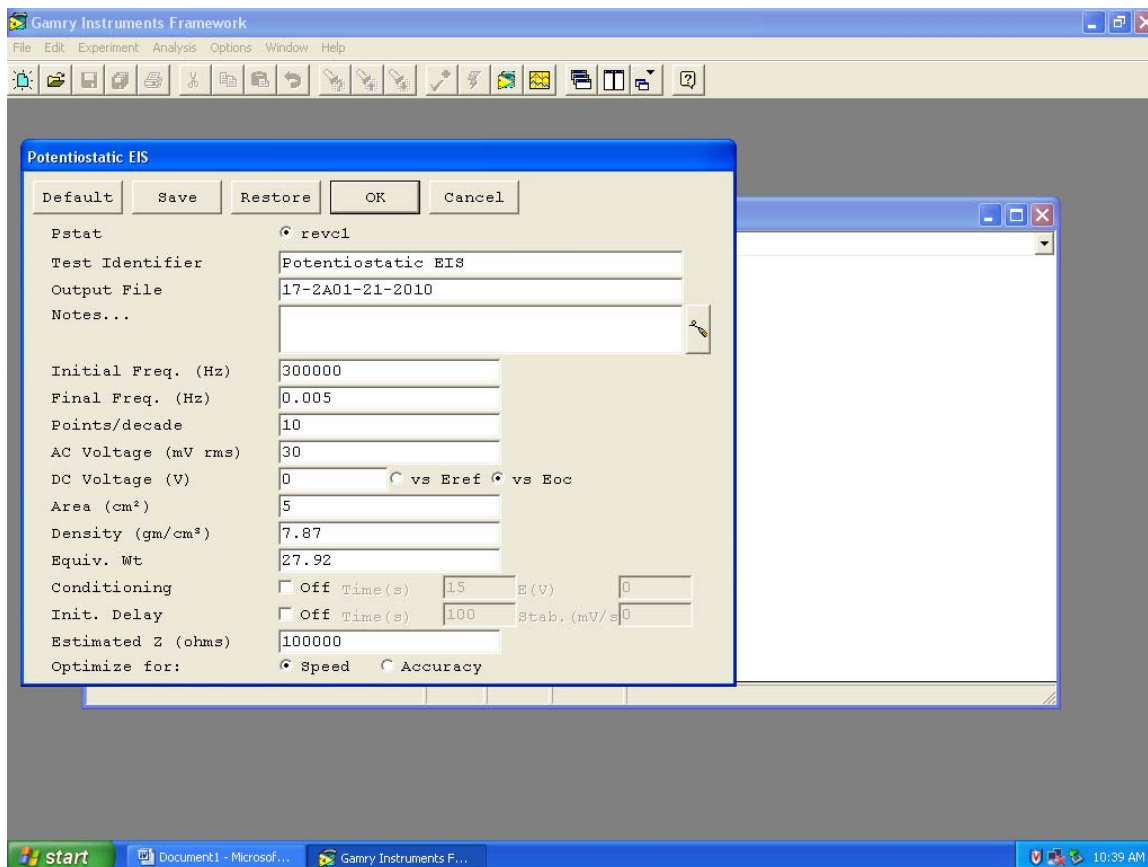
7. Select OK to start the experiment.

8. After test completes open the data using the E-Chem Analyst program. Click on the Nyquist tab to display a chart like the one below.
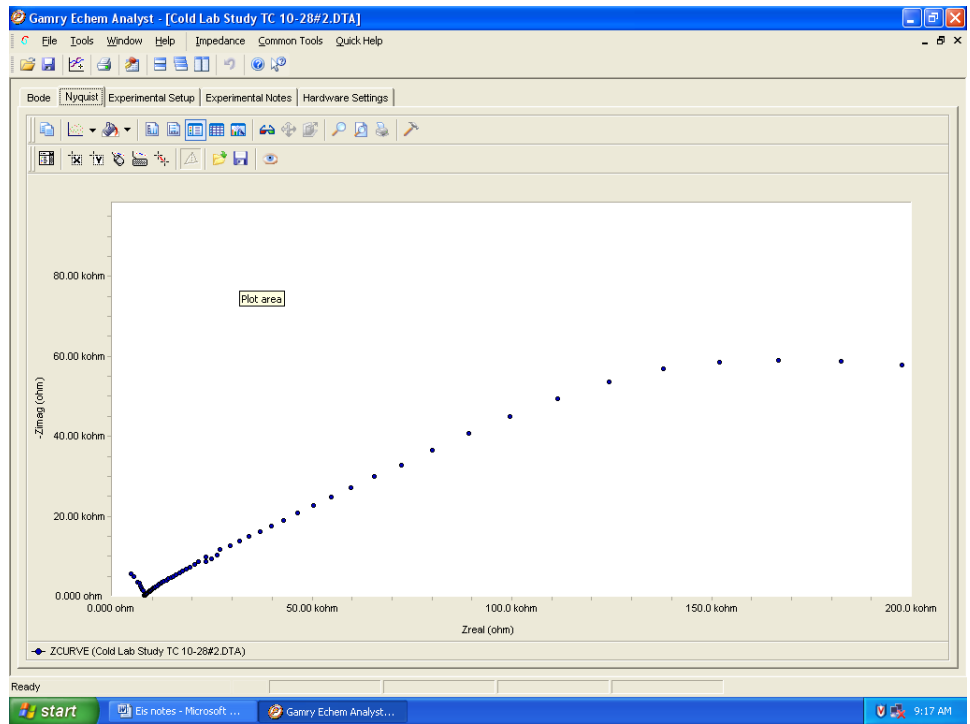
9. Select the Impedance tab and open the model editor. Construct a model like the one shown below.
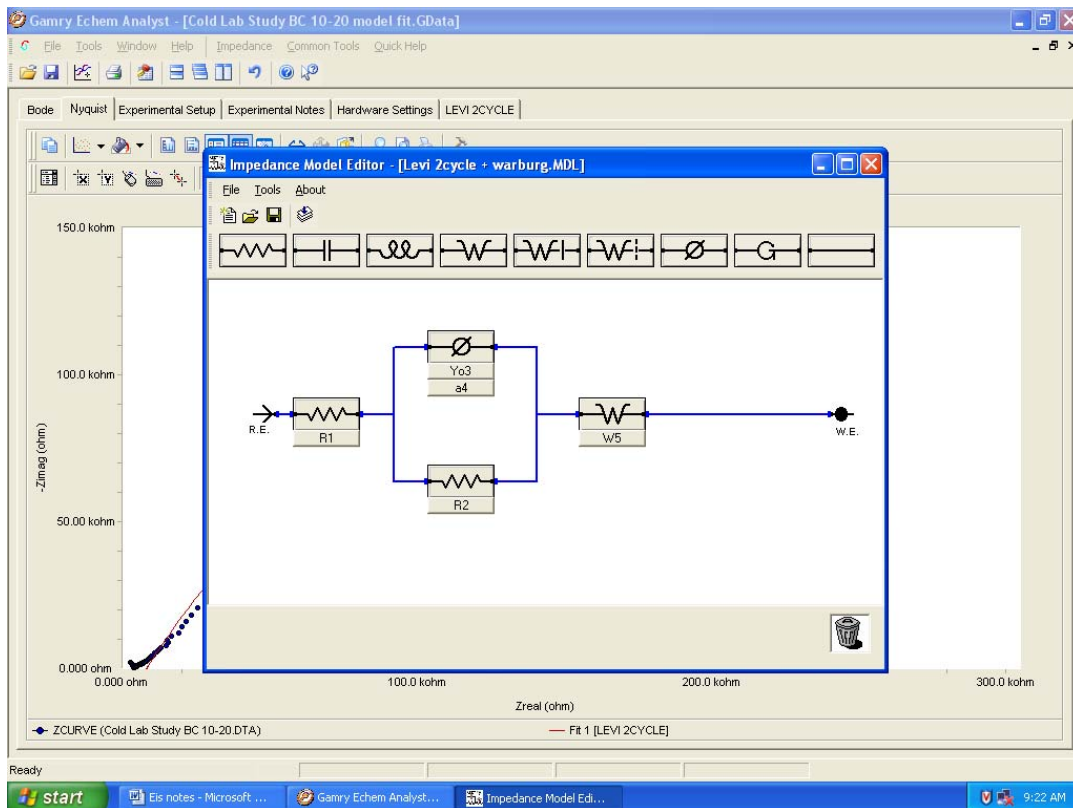
10. Save the model then return to the Nyquist plot and select the impedance tab and fit a model (simplex method). Vary the R1, R2, Y, A, and W values until the model closely fits the data on the Nyquist plot.
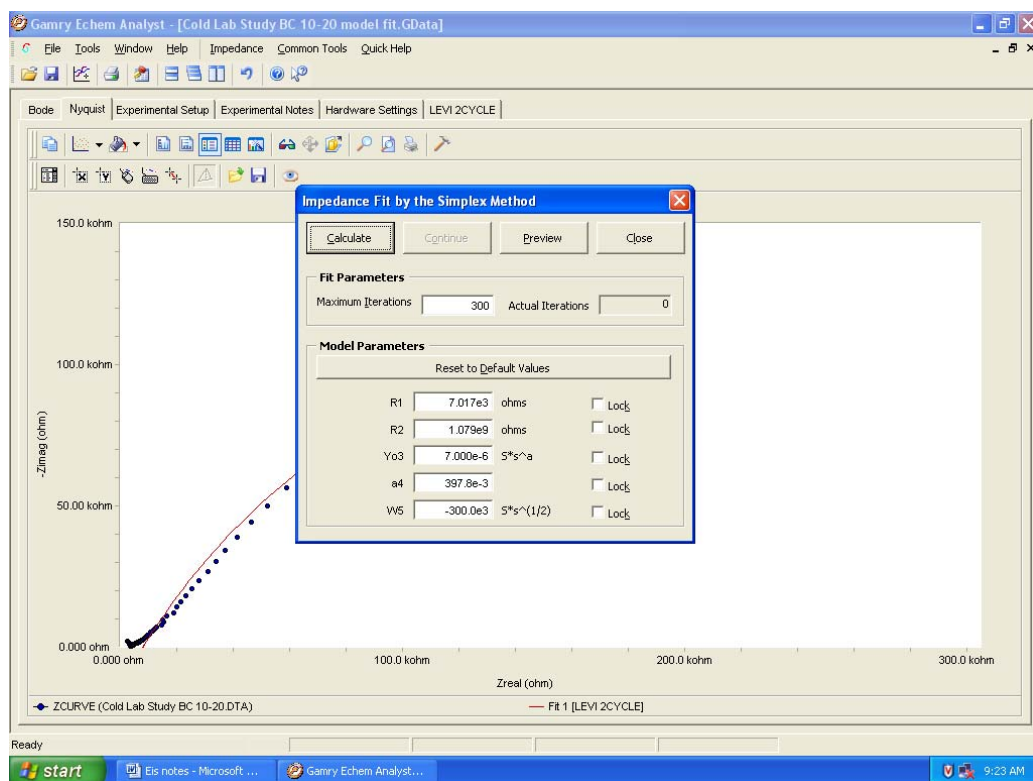
11. Click on the model tab which was named earlier when the model was saved. Record the data needed shown in the table highlighted below.

APPENDIX E:
ADDITIONAL OBSERVATIONS FROM SPRING 2010 OREGON FIELD
TRIP

System Controls

The figure below shows a section of the Yaquina Bay Bridge where the zinc coating is bubbled and debonding. One curious thing about this failure is the entire section was sprayed at the same time but only half of the surface is failing. The division between good zinc and bad zinc is the zone break, which is the vertical line on the wind brace. There are several sections on the Yaquina Bay Bridge that look like this. The arrows in the photo point to the zone breaks. The zones were established with tape when applying the arc spray. Once the spray operation was completed for the section, the tape was removed and a clear break in the zinc coating is achieved. According to the contractor, at some point the controllers for the system shut down temporarily. Apparently when the controllers turned back on or reset the amount of applied current was substantially higher than it should have been. This malfunctioning system was in operation for some time before the problem was identified and fixed. The general consensus of the contractors we interviewed was that the ICCP systems would benefit from increased investment and oversight (including real-time monitoring) to ensure best performance and to minimize the risk of mis-operation or malfunction. The next photo shows a scenario where ICCP system mis-operation or malfunction led to significant zone failure.

Large Rocks

One common comment from the spray contractors is that as more rock is exposed the bond strengths go down. Since the majority of the structure is coarse aggregates, understanding the bonding mechanism with rock or coarse aggregates is critical. The issue becomes more important if patch work or removal of old anodes is required as the removal process and surface profiling remove substantial amount of mortar. The next photo shows some of the rocks that were exposed on the McCullough Bay Bridge project during the profiling operation. The picture is from the top section of one of the piers. This section was only lightly sandblasted and blown

down, yet resulting in significant exposure of aggregates. If this were an anode removal operation, the exposure of aggregates would be much greater.
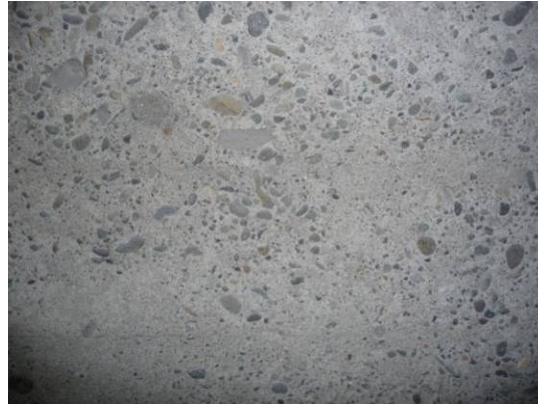
Furthermore, the contractor made a comment regarding bond testing that seemed to defeat the purpose. The current practice is that the inspectors look for reasonable spots to place the bond strength test pucks. Reasonable by his definition was a location that did not have large exposed rocks, extremely uneven areas, or patched surfaces. When the bond tests are conducted in this manner, the results are not inclusive of all conditions. The next photo shows a section on the McCullough Bay Bridge that was profiled and arc sprayed with zinc. Note the large and small rocks that have zinc directly on the surface. If bond tests were conducted in this section there is a high probability that the section would fail because of the rock concentration and the lack of bond to rock. The surface in the picture looks as though there are many pockets or holes; these are actually rocks just below the surface that had the mortar blasted from them during the profiling process. High concentrations of rock have the potential to be where the failure of the anode starts.

Patch Work

Significant effort and money is spent on fixing areas where the concrete surface has delaminated or where the coverage of bars is no longer acceptable. This step is the most time-consuming in the entire anode installation process. The end result of patching is a new concrete surface bonded

to an older concrete surface. The patch material (grout) has a maximum aggregate size much smaller than what is used in a typical concrete mix design. The largest size is approximately 0.25″ in diameter. Once the patch is sufficiently cured, the surface is profiled and then arc-sprayed with zinc. The roughness and exposed aggregate concentration of the prepared patch work is much more uniform than that of the base concrete material. The next figure shows a typical patch on the McCullough Bay Bridge project (*left*) and its close-up photo (*right*).

The next photo shows a patch area with TS-Zn anode applied. It appears that the current ODOT patching method works well and the bond to the substrate is adequate if installation specifications are closely followed. It is unclear why bond tests are not conducted on the patch areas especially if the patch is covering large sections of rebar close to the surface or coincides with large sections of the anode area. It is important to have the zinc anode bond uniformly to all surfaces to prevent weak or sub-standard areas where bond failure can initiate and propagate from.

Anode Removal

The work accomplished by the research team at the McCullough Bay Bridge project did not examine at the removal process for old anodes in great detail. Through conversations with personnel from Great Western Corporation and actual site inspections of other bridges along the coast with TS-Zn, we reached some initial conclusion regarding this process. The surface of the anode should be "chain dragged" to determine the extent of de-bonding. Once the debonded locations are identified, the old anode should be scraped from the surface using flat spade scrapers. Sections of the anode that could not be scraped off should be blown down to remove

any loose edges and the accumulated oxidation on the surface. Once the majority of the old anode has been scraped from the surface, the profiling process can begin. The next step is to apply the TS-Zn to the profiled surface.

An alternative removal method is to sand blast the entire anode from the surface. This method will also remove the majority if not all of the reaction layer. The advantage of this method is the surface will have a more uniform profile and a more uniform concentration of exposed aggregates.

APPENDIX F:
STANDARD OPERATING PROCEDURE FOR EVALUATING 2-D
MACRO-ROUGHNESS

1. Prepare a Contour Gauge, like the one shown below, such that 2 inches of pins are isolated from the others.

   .

2. Press the contour gauge evenly across one diameter of a bond tested site.

3. Using the contour produced, lay the gauge on grid paper for measurement as shown below with the highest pin on a horizontal line for simplicity.
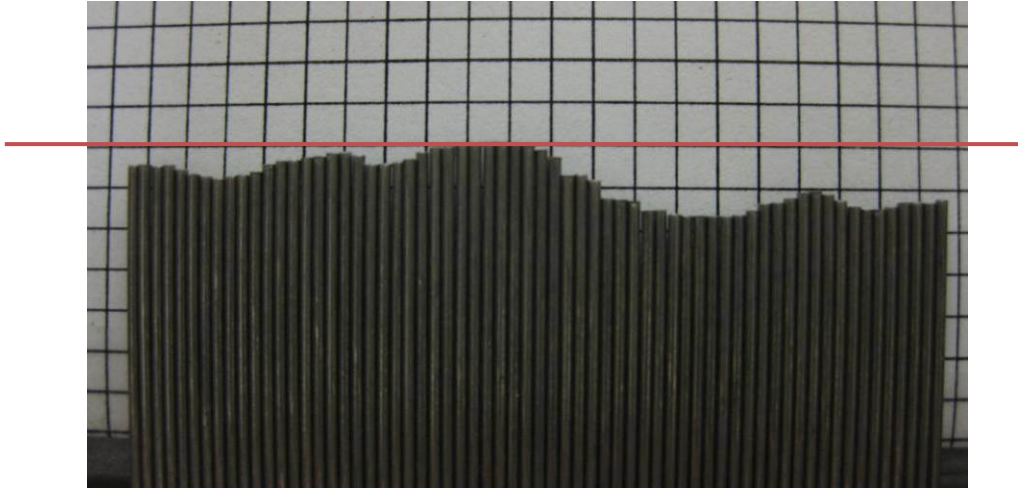
4. Take a picture of the gauge laid out on the grid paper.

5. Determine the "roughness area" by finding how much area is between the horizontal line created in step three and the contour pins shown below by the green area.
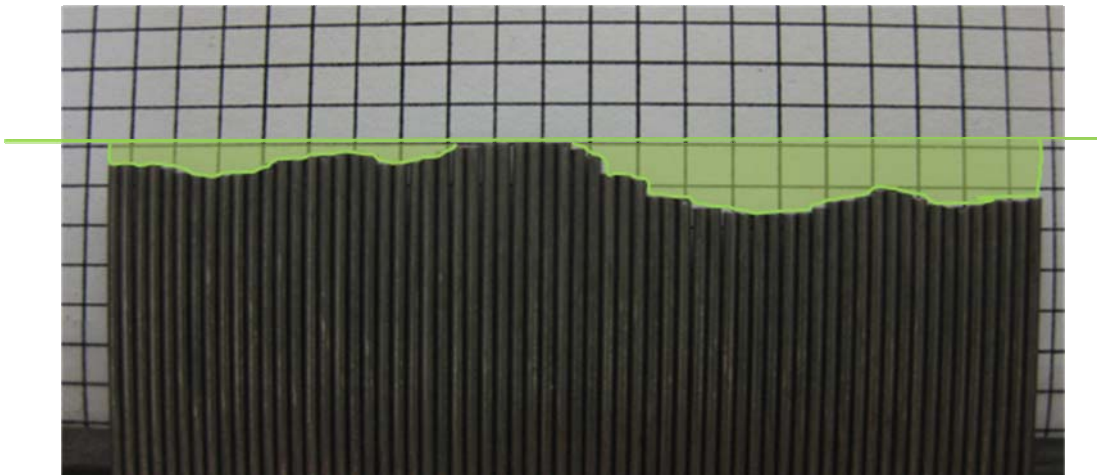
6. Use the image editing program paint.net (or Photoshop or similar program) to precisely measure virtual roughness area. Open paint.net and load the picture of the contour gauge properly oriented on the paper. Use the "lasso select" tool inside paint.net starting in the upper-left most corner of the soon to be selected virtual roughness area. By holding down the left mouse button while using the lasso select tool the area can be traced carefully.

7. After the area is selected the status bar below the image will display the area of the selection in pixels. Change this to display in square inches using the units menu.

Change from Pixels to Inches

Area: 131,829 pixels square

Area: 4.07 inches square
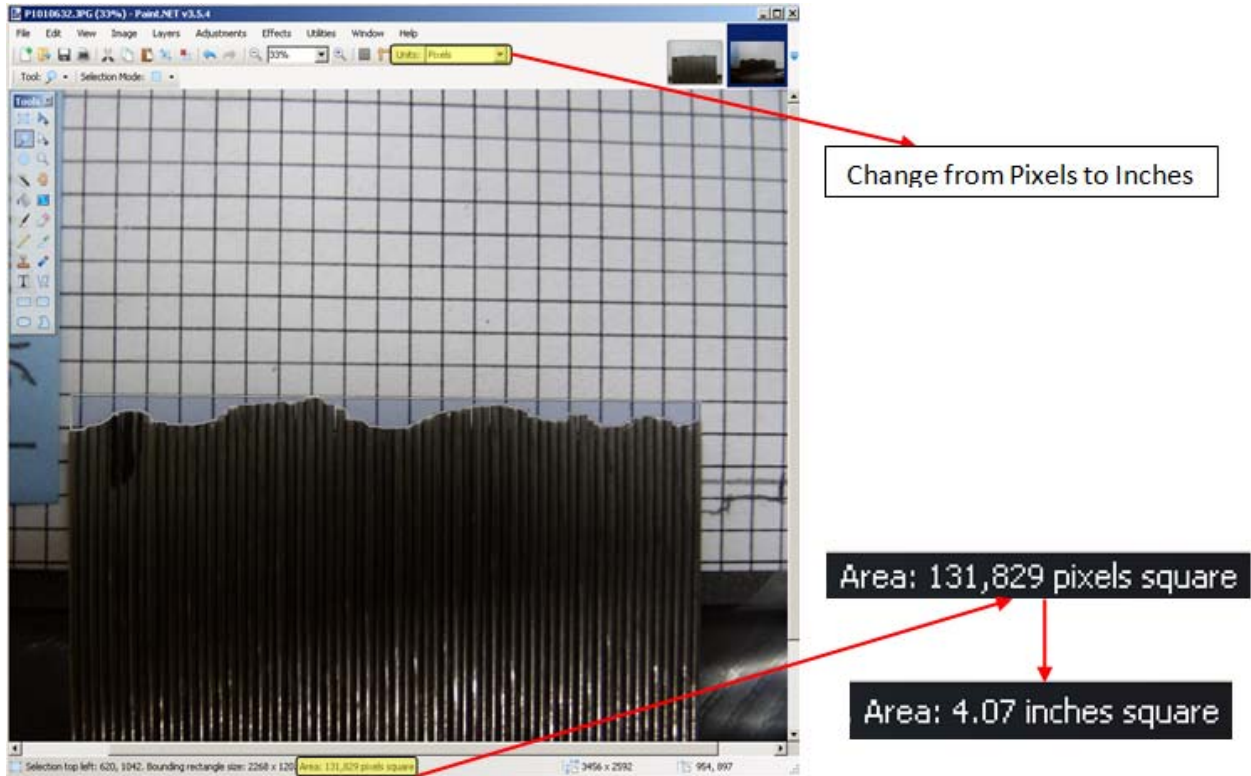
8. Normalize the virtual area from paint.net to actual area using the grid paper size.

9. Use the rectangle select tool inside paint.net to determine the average virtual area of a grid box on the image. Do this by selecting three different rectangles on the image and note their virtual areas. Then use the average as the recorded value.
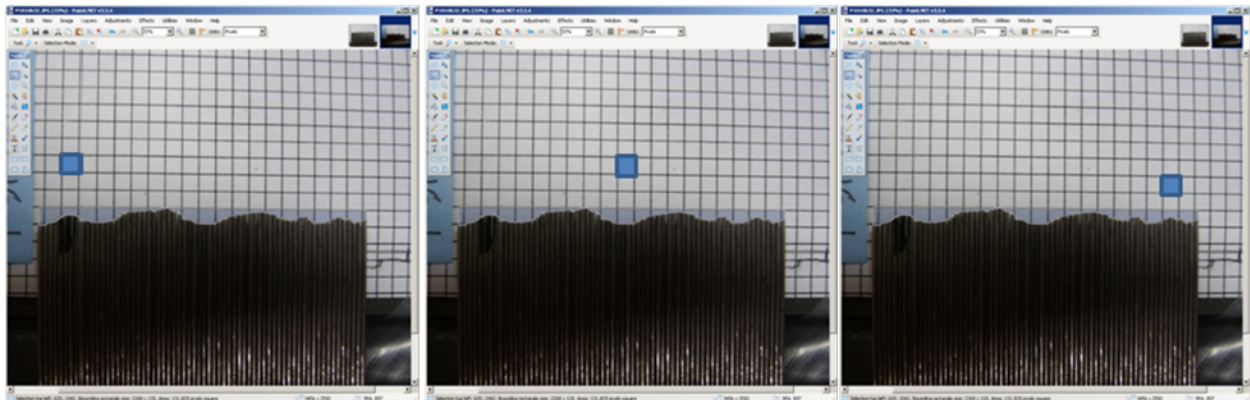
10. The actual roughness area is then = (virtual grid box area/actual grid box area) * (virtual roughness area).

11. Repeat this process for three different diameters on a bond-tested site.

12. Determine the roughness classification on scale defined below.

Roughness Area (actual square inches)

.40   .73   1.06   1.40

1   2   3   4   5

Roughness Rating
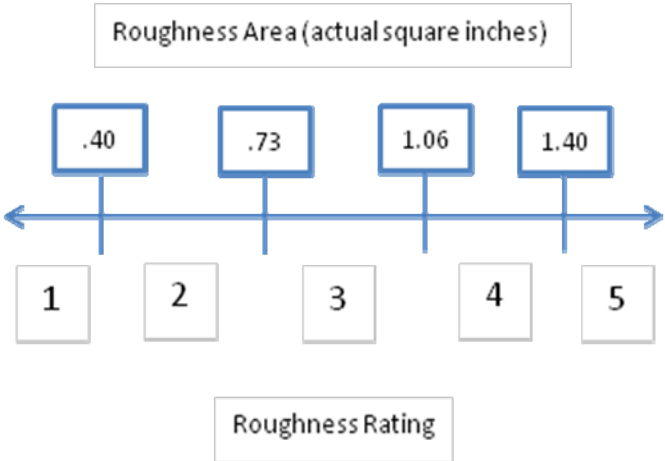
**APPENDIX G:**
STANDARD OPERATING PROCEDURE FOR PERCENT EXPOSED
AGGREGATES

1. Prepare a phenolphthalein solution of 1 gram phenolphthalein, 50 mL de-ionized (DI) water and enough alcohol to bring solution to 100 mL

2. Using a small pipette spread enough phenolphthalein solution on the bond tested area to wet the entire area. (usually 0.5 mL)

3. When concrete surface turns pink/purple take a picture of the surface.

4. If phenolphthalein solution fails to turn concrete paste pink, prepare a lime slurry with 30 g lime powder mixed with 200 mL DI water.

5. Use a paint brush to wet the concrete surface with the lime slurry.

6. Let the concrete surface dry for 3 minutes then reapply the phenolphthalein solution.

7. Take picture when concrete surface turns pink.

8. To determine what percent of the surface is paste vs. rock, use paint.net, Photoshop or similar image editing software.

9. Open sample picture in paint.net and change units to inches.
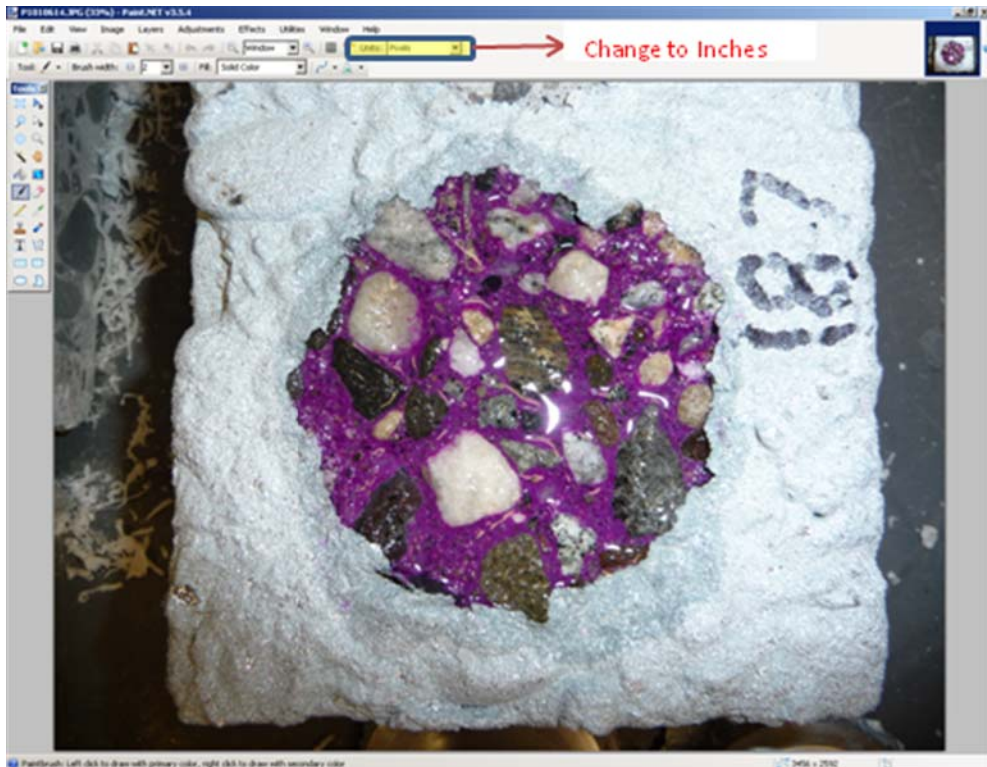
10. Use the ellipse selection tool to select the bond tested area and modify the ellipse to best cover the area with the move tool. Record the area of the ellipse.
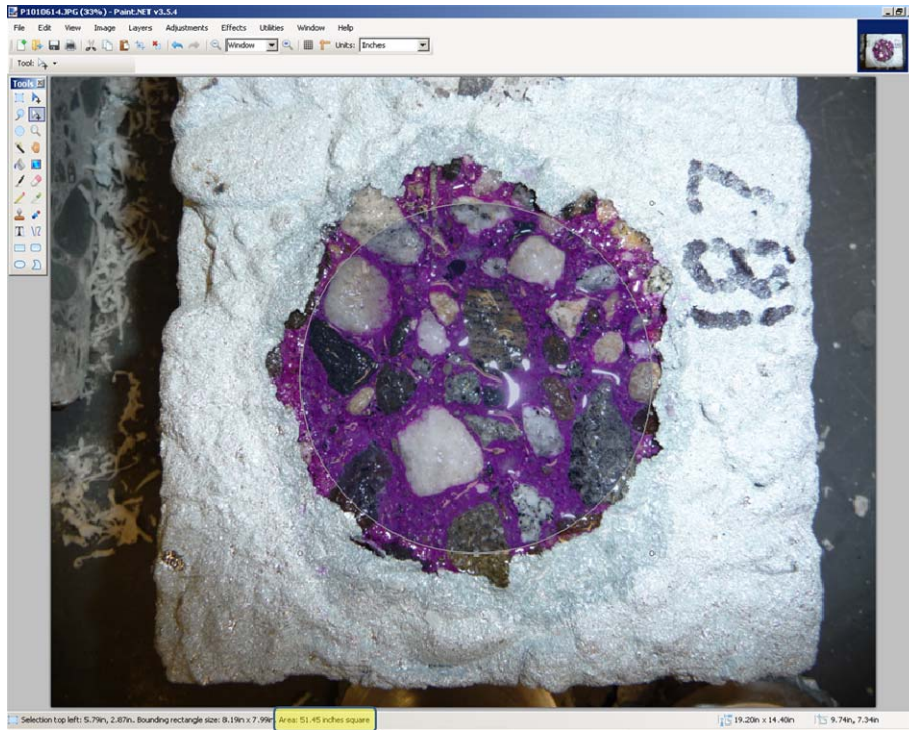
11. Select the menu item "image" then select crop to selection.
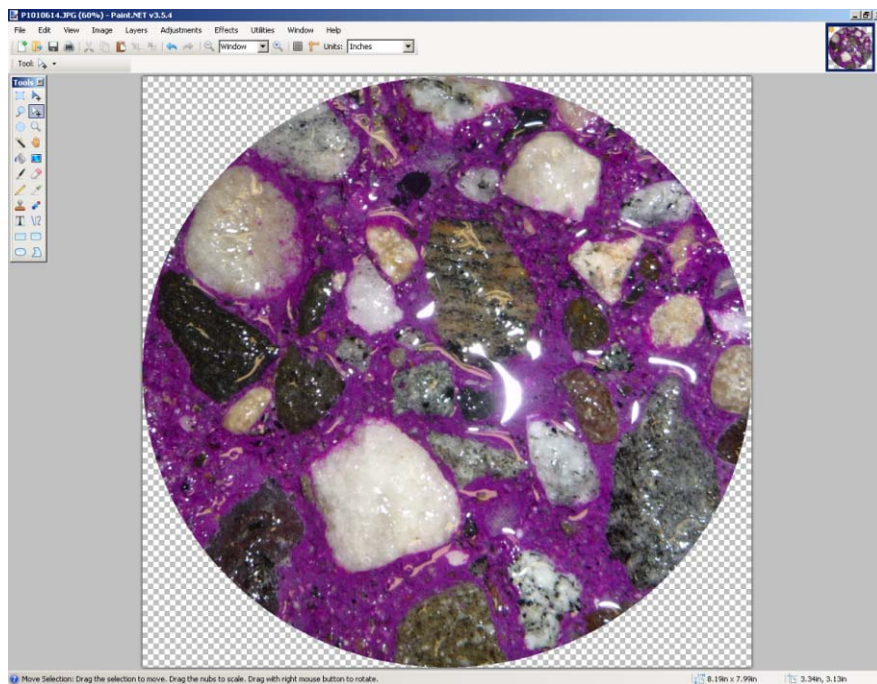
12. Select menu item "adjustments" then select hue/saturation. Adjust the saturation to between 150 and 200 to create clear distinction between rocks and paste.
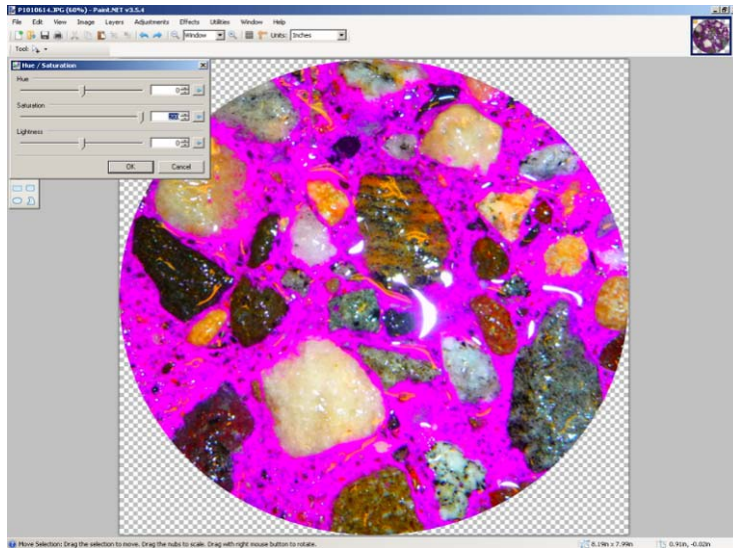
13. Use the magic wand tool. Change the flood mode to global. Select the pink color that best represents the cement paste. Record the cement paste area. (note: the tolerance setting can be adjusted to a level that allows for the best selection of cement paste area)
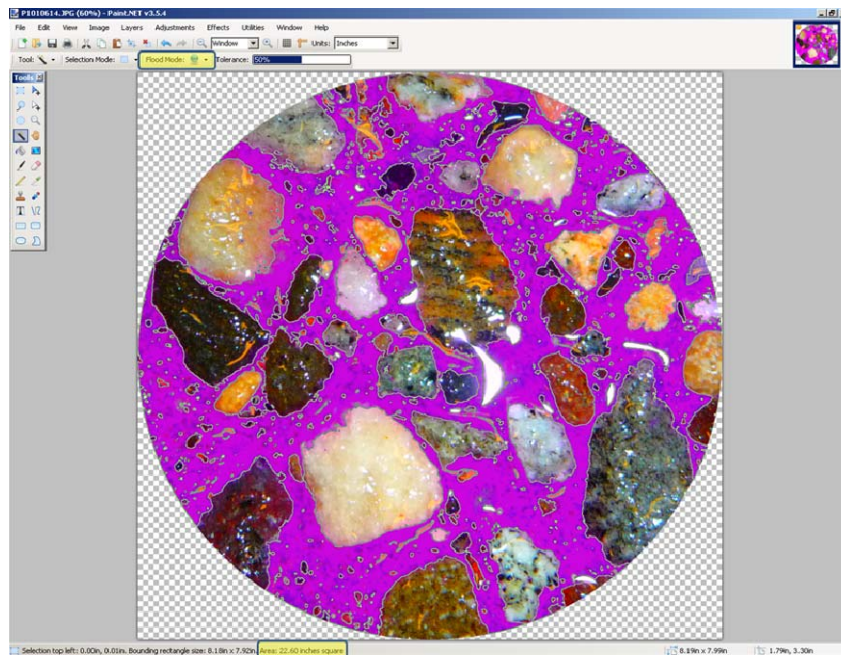
14. Now the percent of surface that is cement paste is = (paste area)/(ellipse area) *100%

15. The percent of the surface that is rock (i.e. exposed aggregates) is then 100% - percent paste.

16. This percent rock can then be rated on the following scale.

% Rock

13	22	31	40

1	2	3	4	5

% Rock Rating
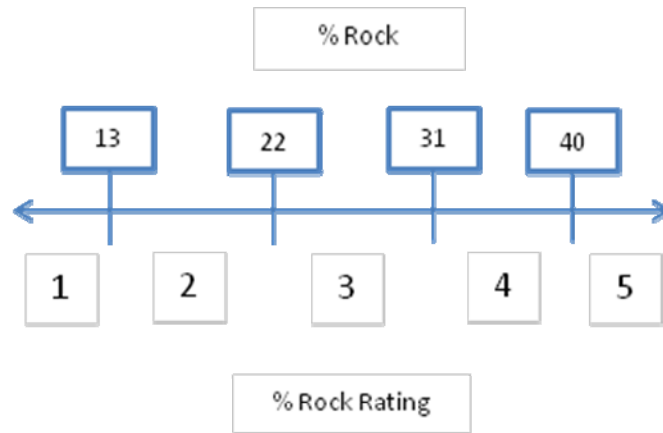
APPENDIX H:
STANDARD OPERATING PROCEDURE FOR EVALUATING SURFACE
MICRO-ROUGHNESS

1. Use the Time Co. Hand-held Roughness Tester Model TR200 or similar meter.

2. Insert stylus into underside of tester.

3. Use settings: LTH: 0.8*5mm, STD: ISO, RAN: ±40μm, FIL: RC. Arrange meter so that it sits level on the sample with the stylus on a section of cement paste.

4. Press the rectangular play button on the tester to begin the test.

5. Record the results from the tester's digital screen.

6. Repeat this process three times for each bond test site. Test different paste sections each time and record the average micro-roughness.

APPENDIX I:
STANDARD OPERATING PROCEDURE FOR EVALUATING RMS
**MACRO-ROUGHNESS**

1. Prepare a Contour Gauge such that 2 inches of pins are isolated from the others.

2. Press the contour gauge evenly across one diameter of a bond tested site.

3. Using the contour produced lay the gauge on grid paper for measurement.

4. Take a picture of the gauge laid out on the grid paper.

5. Using paint.net, or a similar image editing software, draw a horizontal line at the "mean surface." The mean surface is the horizontal line midway between the highest and lowest points on the surface.
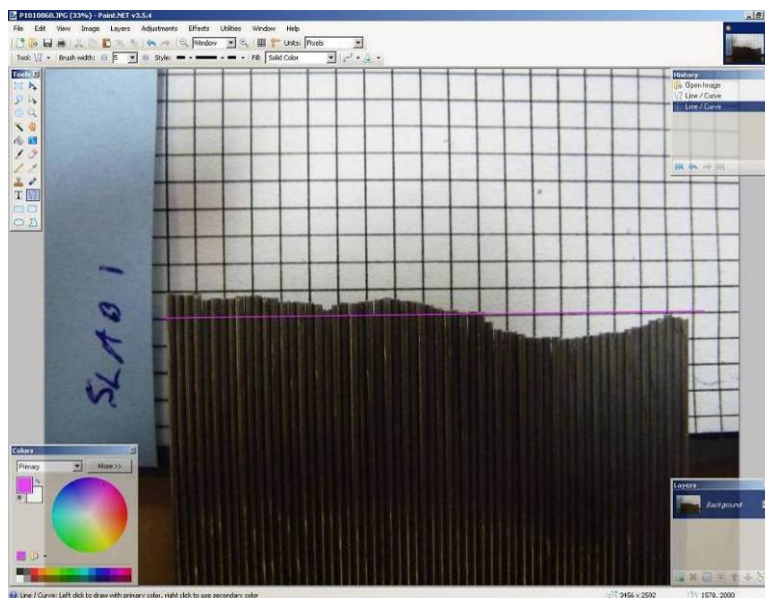
6. Now the distance between the mean surface line and the contour is measured at 20 places (each vertical box line) across the surface and recorded.
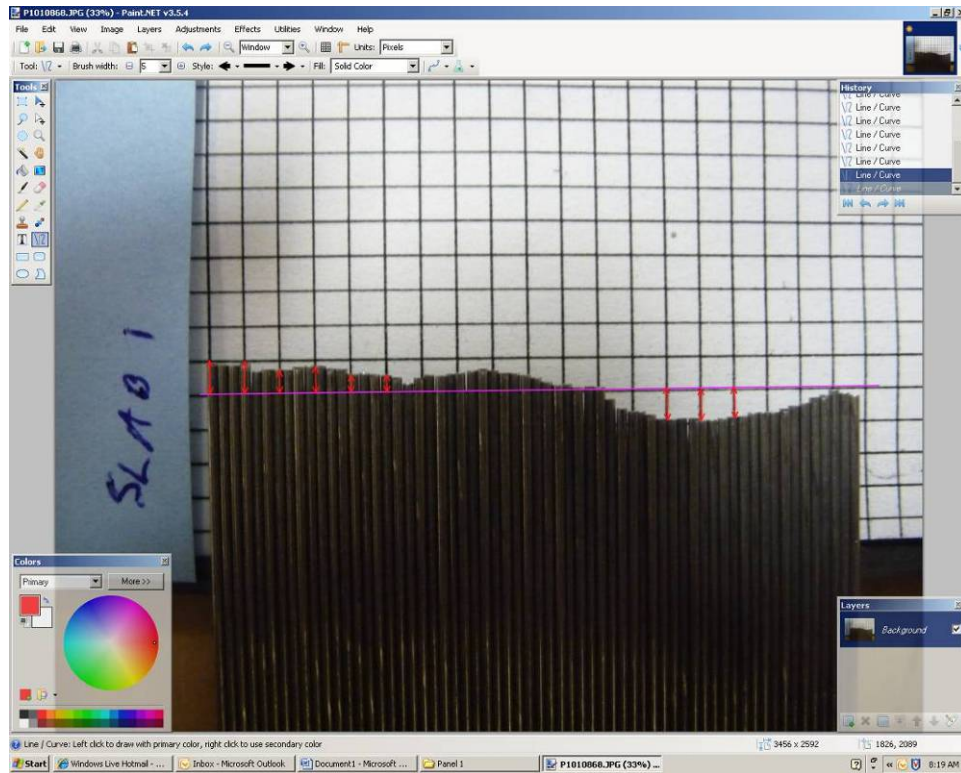
7. The root mean square (RMS) Roughness (Rq) is then found by squaring each distance measure (yi) from above, then adding all the squared values, dividing by 20 (the number of measurements), and taking the square root of that number.

$$R_q = \sqrt{\frac{1}{n} \sum_{i=1}^{n} y_i^2}$$

APPENDIX J:
ADDITIONAL OBSERVATIONS FROM FALL 2010 OREGON FIELD
TRIP

Sandblasting

Sand blasting and the resulting profile is the most important aspect to installing the TS-Zn anode. The process currently being used at the McCullough Bay bridge project involves blasting the surface with sand to remove any loose material, survey surface for any surface metal, isolate surface metal from contact with anode, patching any cracks or areas that rebar has been exposed, blow the surface down with clean compressed air, apply anode. The assumption is that all the concrete will behave the same but in practice this is not the case. The bridge is comprised of hundreds if not thousands of individual batches of concrete each having slightly different properties. After the natural aging and electrochemical aging by ICCP, the outer skin of the concrete that the anode attaches too has been transformed into a material with its own unique properties. When the entire bridge is blasted with a #8 nozzle at high pressure and sand volume, the majority of the old anode will be removed but the surface profiling will not necessarily have a roughness in the desired range. This is due in part to the underlying concrete and how the surface was profiled before the old anode was applied. Either way the volume of sand needed to remove the anode profiles the surface on a macroscopic scale but does not provide an even distribution of micro-anchor spots across the surface. One possible solution would be to remove the old anode first with high pressure and high sand volume then re-blast the surface with the smaller nozzle and lower sand volume to achieve the micro-texture of the mortar fraction to ensure bonding.

Anode Installation

This process is physical in nature due to the equipment used to deposit the molten zinc on the surface. In a laboratory it is easy to maintain specified standoff distances and angles but in the field inside the enclosure is a different matter. The process of building millage on the surface requires multiple passes in orthogonal directions. It is important to maintain a minimum standoff distance during the passes so the underlying zinc is not thermally shocked and any surface oxidation is minimized. One thing that was not tried but could lead to a better base bond would be to apply the first two passes with the gun face very close to the surface. The idea being that if the anchor spots are not filled with molten zinc on the first pass they never will be filled because of the spread out of the subsequent splats from additional passes. If the gun face was closer to the surface and the travel speed slightly decreased, the opportunity to fill the micro-anchors would be much greater than if the first two passes were fast across the surface.

It is hypothesized that part of forming a sound bond is partially achieved by activating the impressed current system and starting the electrons flow as quickly as possible (after each zone is zinced) to establish the new reaction layer and pathways.